NOT FOR PUBLICATION

NEANDC(J)-164/U
INDC(JPN)-153/U

PROGRESS REPORT

(July 1990 to June 1991 inclusive)

AUGUST 1991

Editor

S. KIKUCHI

Japanese Nuclear Data Committee

Japan Atomic Energy Research Institute

Tokai Research Establishment

Tokai-mura, Ibaraki-ken, Japan

Editor's Note

This is a collection of reports which have been submitted to the Japanese Nuclear Data Committee at the committee's request. The request was addressed to the following individuals who might represent or be in touch with groups doing researches related to the nuclear data of interest to the development of the nuclear energy program.

Although the editor tried not to miss any appropriate addressees, there may have been some oversight. Meanwhile, contribution of a report rested with discretion of its author. The coverage of this document, therefore, may not be uniform over the related field or research.

In this progress report, each individual report is generally reproduced as it was received by the JNDC secretariat, and editor also let pass some simple obvious errors in the manuscripts if any.

This edition covers a period of July 1, 1990 to June 30, 1991. The information herein contained is of a nature of "Private Communication". <u>Data contained in this report should not be quoted without the author's permission.</u>

TABLE OF CONTENTS

D. Nuclear Data Center, Department of Physics and Working Groups of Japanese Nuclear Data Committee

ELEMENT S	A	QUANTITY	ENERGY MIN	MAX	LAB	TYPE	DOCUMENTATION REF VOL PAGE	DATE	COMMENTS
SI		(N,GAMMA)	1.0+4	6.0+5	TIT	EXPT-PROG	NEANDC(J)-164U	AUG 91	IGASHIRA+.P131.AT 91JUELICH CONF
SI		NONELA GAMMA	7.8+6	1.3+7	JAE	EXPT-PROG	NEANDC(J)-164U	AUG 91	HASEGAWA+.P9.PRESENTED AT 91JUELICH
SI		NUCL PROD	2.5+6	4.0+7	TOH	EXPT-PROG	NEANDC(J)-164U	AUG 91	UWAMINO+P143.AL28,AL29,MG27 PROD,NDG
S	32	(N,GAMMA)	2.0+5		TIT	EXPT-PROG	NEANDC(J)-164U	AUG 91	KITAZAWA+.P129.SUBMITTED TO NP/A
CA		(N,GAMMA)	1.0+4	6.0+5	TIT	EXPT-PROG	NEANDC(J)-164U	AUG 91	IGASHIRA+.P131.AT 91JUELICH CONF
CA		NUCL PROD	2.3+6	4.0+7	TOH	EXPT-PROG	NEANDC(J)-164U	AUG 91	UWAMINO+.P143.K42,K43 PROD,ACT S,NDG
V	51	(N,P)	1.7+6	4.0+7	TOH	EXPT-PROG	NEANDC(J)-164U	AUG 91	UWAMINO+.P143.ACT SIG,NDG
V	51	(N,ALPHA)	2.1+6	4.0+7	TOH	EXPT-PROG	NEANDC(J)-164U	AUG 91	UWAMINO+.P143.ACT SIG IN FIG
V	51	NUCL PROD	0.0+0	4.0+7	TOH	EXPT-PROG	NEANDC(J)-164U	AUG 91	UWAMINO+.P143.SC46,SC47 PROD SIG,FIG
CR		(N,GAMMA)	1.0+4	6.0+5	TIT	EXPT-PROG	NEANDC(J)-164U	AUG 91	IGASHIRA+.P131.AT 91JUELICH CONF
CR		NUCL PROD	2.2+6	4.0+7	TOH	EXPT-PROG	NEANDC(J)-164U	AUG 91	UWAMINO+.P143.V52,V53 PROD,ACT S,NDG
CR	50	(N,2N)	1.3+7	4.0+7	TOH	EXPT-PROG	NEANDC(J)-164U	AUG 91	UWAMINO+.P143.ACT SIG,NDG
CR	50	(N,XN) X>2	2.4+7	4.0+7	TOH	EXPT-PROG	NEANDC(J)-164U	AUG 91	UWAMINO+.P143.X=3,ACT SIG,NDG
MN	55	(N,2N)	FISS		KNK	EXPT-PROG	NEANDC(J)-164U	AUG 91	HORIBE+.P34.PRESENTED AT 91JUELICH
MN	55	(N,2N)	1.0+7	4.0+7	TOH	EXPT-PROG	NEANDC(J)-164U	AUG 91	UWAMINO+.P143.ACT SIG,NDG
MN	55	(N,XN) X>2	3.2+7	4.0+7	TOH	EXPT-PROG	NEANDC(J)-164U	AUG 91	UWAMINO+.P143.X=4,ACT SIG,NDG
MN	55	NUCL PROD	9.2+6	4.0+7	TOH	EXPT-PROG	NEANDC(J)-164U	AUG 91	UWAMINO+.P143.(N,PA)TI51,ACT SIG,NDG
FE		NONELA GAMMA	7.8+6	1.3+7	JAE	EXPT-PROG	NEANDC(J)-164U	AUG 91	HASEGAWA+.P9.PRESENTED AT 91JUELICH
FE		N EMISSION	1.4+7		YOK	EXPT-PROG	NEANDC(J)-164U	AUG 91	SHIRATO+.P91.DA/DE IN FIG
CO		(N,GAMMA)	1.0+4	6.0+5	TIT	EXPT-PROG	NEANDC(J)-164U	AUG 91	IGASHIRA+.P131.AT 91JUELICH CONF

ELEMENT S	A	QUANTITY	ENERGY MIN	MAX	LAB	TYPE	DOCUMENTATION REF VOL PAGE	DATE	COMMENTS
NI		NONELA GAMMA	7.8+6	1.3+7	JAE	EXPT-PROG	NEANDC(J)-164U	AUG 91	HASEGAWA+.P9.PRESENTED AT 91JUELICH
NI	58	(N,2N)	FISS		KNK	EXPT-PROG	NEANDC(J)-164U	AUG 91	HORIBE+.P34.PRESENTED AT 91JUELICH
NI	58	(N,NP)	FISS		KNK	EXPT-PROG	NEANDC(J)-164U	AUG 91	HORIBE+.P34.PRESENTED AT 91JUELICH
NI	60	DIFF ELASTIC	1.9+7		JAE	EXPT-PROG	NEANDC(J)-164U	AUG 91	YAMANOUTI+.P11.AT 91JUELICH CONF
NI	60	DIFF INELAST	1.9+7		JAE	EXPT-PROG	NEANDC(J)-164U	AUG 91	YAMANOUTI+.P11.AT 91JUELICH CONF
CU		NONELA GAMMA	7.8+6	1.3+7	JAE	EXPT-PROG	NEANDC(J)-164U	AUG 91	HASEGAWA+.P9.PRESENTED AT 91JUELICH
CU		NUCL PROD	1.0+5	4.0+7	TOH	EXPT-PROG	NEANDC(J)-164U	AUG 91	UWAMINO+.P143.CO62M PROD,ACT SIG,NDG
CU	63	(N,2N)	1.1+7	4.0+7	TOH	EXPT-PROG	NEANDC(J)-164U	AUG 91	UWAMINO+.P143.ACT SIG,NDG
CU	63	(N,XN) X>2	2.0+7	4.0+7	TOH	EXPT-PROG	NEANDC(J)-164U	AUG 91	UWAMINO+.P143.X=3,ACT SIG,NDG
CU	65	(N,P)	1.4+6	4.0+7	TOH	EXPT-PROG	NEANDC(J)-164U	AUG 91	UWAMINO+.P143.ACT SIG,NDG
ZN		NUCL PROD	0.0+0	4.0+7	TOH	EXPT-PROG	NEANDC(J)-164U	AUG 91	UWAMINO+.P143.NI65,CU64,CU66,68M,NDG
ZN	64	(N,2N)	1.2+7	4.0+7	TOH	EXPT-PROG	NEANDC(J)-164U	AUG 91	UWAMINO+.P143.ACT SIG,NDG
ZN	64	(N,XN) X>2	2.1+7	4.0+7	TOH	EXPT-PROG	NEANDC(J)-164U	AUG 91	UWAMINO+.P143.X=3,ACT SIG,NDG
ZN	64	(N,T)	1.0+7	4.0+7	TOH	EXPT-PROG	NEANDC(J)-164U	AUG 91	UWAMINO+.P143.ACT SIG,NDG
SR	90	(N,GAMMA)	2.5-2		JAE	EXPT-PROG	NEANDC(J)-164U	AUG 91	HARA+.P10.ACT SIG=15.3+-1.3MB
ZR		(N,GAMMA)	1.0+4	6.0+5	TIT	EXPT-PROG	NEANDC(J)-164U	AUG 91	IGASHIRA+.P131.AT 91JUELICH CONF
AG	107	EVALUATION	1.0-5	2.0+7	JAE	EVAL-PROG	NEANDC(J)-164U	AUG 91	LIU+.P23.PUBLISHED AS JAERI-M 91-011
AG	109	EVALUATION	1.0-5	2.0+7	JAE	EVAL-PROG	NEANDC(J)-164U	AUG 91	LIU+.P23.PUBLISHED AS JAERI-M 91-011
AG	0	EVALUATION	1.0-5	2.0+7	JAE	EVAL-PROG	NEANDC(J)-164U	AUG 91	LIU+.P23.PUBLISHED AS JAERI-M 91-011
SB		(N,GAMMA)	1.0-2	1.0+0	KTO	EXPT-PROG	NEANDC(J)-164U	AUG 91	KOBAYASHI+.P46.AT 91JUELICH CONF

ELEMENT S	A	QUANTITY	ENERGY MIN	MAX	LAB	TYPE	DOCUMENTATION REF VOL PAGE	DATE	COMMENTS
SB		(N,GAMMA)	1.0-2	1.0+0	KTO	EXPT-PROG	NEANDC(J)-164U	AUG 91	KOBAYASHI+.P47.PUBL IN JAERI-M91-032
GD	0	RESON PARAMS	0.0+0	1.0+4	JAE	EXPT-PROG	NEANDC(J)-164U	AUG 91	OHKUBO.P12.PUBL AS JAERI-M 90-213
GD	0	STRNTH FNCTN	0.0+0	1.0+4	JAE	EXPT-PROG	NEANDC(J)-164U	AUG 91	OHKUBO.P12.SO=(1.2+-0.2)E-4
AU	197	(N,GAMMA)	1.0-2	1.0+0	KTO	EXPT-PROG	NEANDC(J)-164U	AUG 91	KOBAYASHI+.P47.PUBL IN JAERI-M91-032
AU	197	(N,GAMMA)	1.0-2	1.0+0	KTO	EXPT-PROG	NEANDC(J)-164U	AUG 91	KOBAYASHI+.P46.AT 91JUELICH CONF
AU	197	(N,2N)	8.1+6	4.0+7	TOH	EXPT-PROG	NEANDC(J)-164U	AUG 91	UWAMINO+.P143.ACT SIG IN FIG
AU	197	(N,XN) X>2	2.3+7	4.0+7	TOH	EXPT-PROG	NEANDC(J)-164U	AUG 91	UWAMINO+.P143.X=4.ACT SIG IN FIG
PB		NONELA GAMMA	7.8+6	1.3+7	JAE	EXPT-PROG	NEANDC(J)-164U	AUG 91	HASEGAWA+.P9.PRESENTED AT 91JUELICH
PB	204	EVALUATION	1.0-5	1.0+9	JAE	EVAL-PROG	NEANDC(J)-164U	AUG 91	FUKAHORI+.P24.EVAP+PREEQ CAL,NDG
PB	206	EVALUATION	1.0-5	1.0+9	JAE	EVAL-PROG	NEANDC(J)-164U	AUG 91	FUKAHORI+.P24.EVAP+PREEQ CAL,NDG
PB	207	EVALUATION	1.0-5	1.0+9	JAE	EVAL-PROG	NEANDC(J)-164U	AUG 91	FUKAHORI+.P24.EVAP+PREEQ CAL,NDG
PB	208	EVALUATION	1.0-5	1.0+9	JAE	EVAL-PROG	NEANDC(J)-164U	AUG 91	FUKAHORI+.P24.EVAP+PREEQ CAL,NDG
PB	0	EVALUATION	1.0-5	1.0+9	JAE	EVAL-PROG	NEANDC(J)-164U	AUG 91	FUKAHORI+.P24.EVAP+PREEQ CAL,NDG
BI	209	EVALUATION	1.0-5	1.0+9	JAE	EVAL-PROG	NEANDC(J)-164U	AUG 91	FUKAHORI+.P24.EVAP+PREEQ CAL,NDG
BI	209	NONELA GAMMA	7.8+6	1.3+7	JAE	EXPT-PROG	NEANDC(J)-164U	AUG 91	HASEGAWA+.P9.PRESENTED AT 91JUELICH
TH	232	N EMISSION	1.8+7		TOH	EXPT-PROG	NEANDC(J)-164U	AUG 91	BABA+.P109.PUBL AS JAERI-M 91-059
U	235	SPECT FISS N	NDG		KNK	THEO-PROG	NEANDC(J)-164U	AUG 91	OHSAWA.P33.IN JAERI-M 91-032,383
U	238	(N,GAMMA)	NDG		JAE	EVAL-PROG	NEANDC(J)-164U	AUG 91	KANDA+.P26.PRESENTED AT 91JUELICH
U	238	(N,GAMMA)	2.4+4	1.5+5	KTO	EXPT-PROG	NEANDC(J)-164U	AUG 91	KOBAYASHI+.P46.AT 91JUELICH CONF
U	238	N EMISSION	1.8+7		TOH	EXPT-PROG	NEANDC(J)-164U	AUG 91	BABA+.P109.PUBL AS JAERI-M 91-059

CONTENTS OF JAPANESE PROGRESS REPORT NEANDC(J)-164/U

ELEMENT S A	QUANTITY	ENERGY MIN	ENERGY MAX	LAB	TYPE	DOCUMENTATION REF VOL PAGE	DATE	COMMENTS
PU 239	SPECT FISS N	NDG		KNK	THEO-PROG	NEANDC(J)-164U	AUG 91	OHSAWA.P33.IN JAERI-M 91-032,383
CF 252	SPECT FISS N	NDG		KNK	THEO-PROG	NEANDC(J)-164U	AUG 91	OHSAWA.P33.IN JAERI-M 91-032,383
MANY	EVALUATION	1.0-5	2.0+7	JAE	COMP-PROG	NEANDC(J)-164U	AUG 91	NAKAZAWA+.P16.61 DOSIMETRY REACTIONS
MANY	EVALUATION	1.0-5	2.0+7	JAE	EVAL-PROG	NEANDC(J)-164U	AUG 91	NAKAGAWA+.P13.172 FP,AT 91JUELICH
MANY	(N,2N)	1.3+7	1.5+7	NAG	EXPT-PROG	NEANDC(J)-164U	AUG 91	KAWADE+.P82.ACT SIG,AT 91JUELICH
MANY	N EMISSION	1.0-5	2.0+7	JAE	EVAL-PROG	NEANDC(J)-164U	AUG 91	YU+.P15.FOR JENDL-3 FUSION FILE,NDG
MANY	(N,P)	1.3+7	1.5+7	NAG	EXPT-PROG	NEANDC(J)-164U	AUG 91	KAWADE+.P82.ACT SIG,AT 91JUELICH
MANY	(N,NP)	1.3+7	1.5+7	NAG	EXPT-PROG	NEANDC(J)-164U	AUG 91	KAWADE+.P82.ACT SIG,AT 91JUELICH
MANY	(N,T)	1.3+7	1.5+7	NAG	EXPT-PROG	NEANDC(J)-164U	AUG 91	KAWADE+.P82.ACT SIG,AT 91JUELICH
MANY	(N,ALPHA)	1.3+7	1.5+7	NAG	EXPT-PROG	NEANDC(J)-164U	AUG 91	KAWADE+.P82.ACT SIG,AT 91JUELICH

The content table in the CINDA format was compiled by the JNDC CINDA Group;

S. Chiba (JAERI), M. Kawai (Toshiba), H. Kitazawa (Tokyo Inst. of Tech.), H. Matsunobu (Sumitomo Atomic Energy Industries), T. Nakagawa (JAERI), R. Nakasima (Hosei Univ.), M. Sakamoto (JAERI)

I. Electrotechnical Laboratory

A. Quantum Radiation Division

I-A-1 The Effect of Angular Straggling of Deuterons on Energy Distribution of Reference 2413 keV Neutron Field Produced by D(d,n)^{3}He Reaction

K. Kudo, N. Takeda, Matiullah*, H. Tanoue and A. Fukuda

Production of monoenergetic neutrons with least possible spread is highly desirable for accurate determination of experimental neutron cross section data and calibration of neutron spectrometers especially those used in fusion diagnostics concerning the DD and DT plasma. In this context, in one of our earlier paper, we reported a technique[1] for production of the reference monoenergetic neutron field of 2413 keV using a D(d,n)^{3}He reaction. Therein, it was concluded that those neutrons which are emitted at a judiciously chosen angle of 100° have energy of 2413 keV regardless of the target thickness, its age and the incident deuteron beam energy. The neutron energy spectra were calculated on the basis of the relativistic kinematics of a two-body reaction taking in to account both the angular differential cross section for the D(d,n)^{3}He reaction and the stopping power for deuterons in a homogeneously distributed Ti-D target. However, the angular straggling of the deuterons in the target was ignored for the sake of simplicity. It would be very informative to determine the effect of the angular straggling of incident deuterons in a target material which may results in an energy spread of the neutrons emitted at a reference angle of 100° . The angular straggling mainly occurs due to multiple small-angle scattering during the process of the slowing down of deuterons in a Ti-D target. In addition to the angular straggling of deuterons, solid angle subtended by the detector with neutron source (target) also

---

* Guest researcher from: Center for Nuclear Studies, P.O. Nilore, Islamabad, Pakistan

causes the energy spread of the emitted neutrons and is dependent upon the experimental set-up. The effect of these factors on the distribution of the neutrons emitted at 100° can be determined, assuming a Gaussian shaped angular distribution for projectile deuterons[(2),(3)]. The mean squared scattering angle $<\theta^2>$ would then be equal to the variance σ^2 of the Gaussian distribution, represented by the following formula,

$$\langle\vartheta^2\rangle = 0.0785 \frac{Z_p^2}{\langle E_p\rangle^2} \frac{Z_t^2 \rho_t \Delta x_t}{A_t} \times \ln\left(3.675 \times 10^4 \frac{\langle E_p\rangle}{Z_p Z_t^{4/3}}\right),$$

with a mean deuteron energy $<E_d>$ in the target thickness of $\rho_t \Delta X_t$ and with the mass number A and the atomic number Z for deuterons (index p) and target materials (index t).

The neutron energy distributions for a thick Ti-D target (by thick target we mean here that all the deuterons are stopped in the target material) have been calculated by means of semi-analytical formulae of relativistic kinematics of a two-body reaction. As mentioned above, the angular straggling of deuterons was assumed to be a Gaussian like distribution. The polar angle was divided into 90 grids in calculations whilst the azimuthal angle was divided into 30 grids. The angle made between the angularly straggled deuteron vector and neutron vector generated by a $D(d,n)^3He$ reaction was calculated in order to determine the emitted neutron energy. Moreover, the *solid angle subtended by* the *neutron detector* with the *target* was considered as an angle spread around the fixed angle of 100° with respect to the direction of initial deuteron beam incident on the Ti-D target.

The calculated neutron energy distributions are shown in Fig. 1 at the reference neutron emission angle of 100° with respect to the incident deuteron beam direction of energy 260 keV for a 0.9 mg/cm^2 thick Ti-D target. The solid and dotted curves correspond to the neutron spectra taking into account the angular straggling of deuterons at 100° with the angle spread of ± 0° and ± 1° respectively. The double dotted curve represents the spectrum neglecting the angular straggling of deuterons with no angle-spread around 100° . The mean energy of the emitted neutrons, calculated under the above conditions, is distributed within (2413± 2) keV. However, the energy spread caused by the angular straggling of deuterons becomes larger at full width at less than 1/20 maximum. The inclusion of solid angle spread (subtended by the detector with the Ti-D target) to the emission angle affects the energy spread at full width at about 1/10 maximum in the case of (100± 1)°

We also investigated the effect of the above undesired energy spread on the pulse height distributions of a ^{3}He proportional counter. For these investigations, the neutron energy distributions shown in Fig. 1 were used as an input data in the Monte Carlo code NRESP[(4),(5)] for the pulse height calculations. The calculated pulse height spectra were folded with the energy resolution of about 3 % at the peak region of the

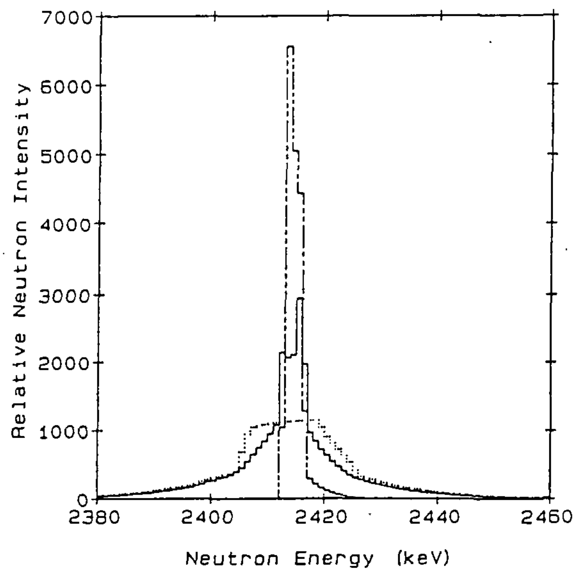

Fig. 1: Calculated neutron energy spectra. Solid curve shows only angular straggling. Dotted curve corresponds to both straggling and angular spread. The double dotted curve ignores both straggling and spread.

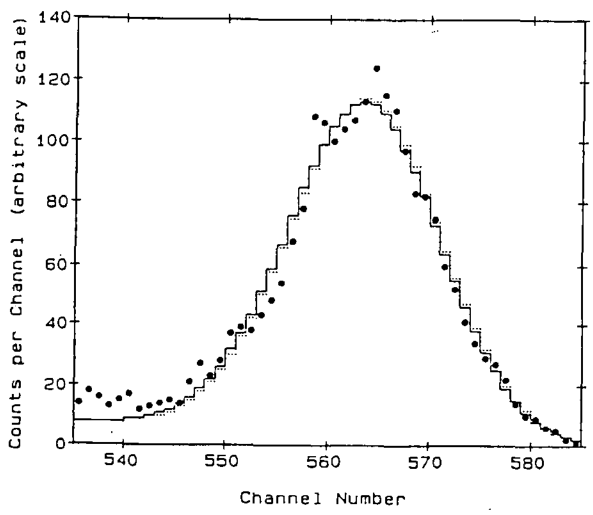

Fig. 2: Pulse height spectra from a ^{3}He proportional counter. Solid and dotted curves correspond to the spectra with and without angular straggling respectively. Blacked circles show experimental values.

spectrum originated from the $^{3}He(n,p)T$ reaction and fitted to the experimental spectrum. The results obtained are presented in Figure 2. The solid and dotted curves represent the calculated spectra with and without taking into account the angular straggling respectively. The experimentally observed spectrum is shown by blacked circles in the figure. No significant difference can be seen among the calculated and experimental spectra, shown in the above figure. This is very advantageous for the reference neutron field as it would be used for calibration of the precise neutron spectrometers which are used in fusion diagnostics.

To summarize, in the foregoing, we have described our work concerning the angular straggling effect of the incident deuterons in a Ti-D target on the emitted neutron energy distribution at a reference angle of 100° . Our results indicated that the angular straggling of deuterons in a target material is responsible for the energy spread of the emitted neutrons. This energy spread is slightly larger than that when the angular straggling of deuterons is ignored. However, the energy spread caused by the angular straggling effect does not significantly change the actual pulse height spectrum of a ^{3}He proportional counter which has the energy resolution of 3% at the peak region induced by a $^{3}He(n,p)T$ reaction. This reference energy field of 2413 keV would mainly be used for the calibration of precise spectrometers which are required to yield an energy response with ± 0.5% in a DD neutron energy range with an energy resolution uncertainty of less than 2 %.

References:

(1) K. Kudo, N. Takeda, Matiullah and A. Fukuda, In:Conf.Proc. on Nucl. Data for Sci. & Eng., held in Juelich, FRG(1991).

(2) A. Pavlik and G. Winkler, INDC(AUS)-011/LI, IAEA (1986).

(3) H. Klein, H.J. Brede and B.R. L.Siebert, Nucl. Instrum. Meth. 193 (1982) 635.

(4) G. Dietze and H. Klein, PTB report ND-22 (1982).

(5) K. Kudo and T. Kinoshita, Nucl. Eng. & Design/Fusion 10 (1989)145.

II. Japan Atomic Energy Research Institute

A. Accelerator Engineering Laboratory

Department of Reactor Engineering

II-A-1 Gamma-ray Production Cross Section Measurements of Some Structural Materials Between 7.8 and 13.0 MeV

Kazuo Hasegawa, Motoharu Mizumoto, Satoshi Chiba, Masayoshi Sugimoto, Yoshimaro Yamanouti, Masayuki Igashira* and Hideo Kitazawa*

A paper on this subject was presented at the International Conference on Nuclear Data for Science and Technology, May 13-17, 1991, Jülich, with the following abstract:

Gamma-ray production cross sections have been measured for Al, Si, Fe, Ni, Cu, Pb and Bi at incident neutron energies from 7.8 to 13.0 MeV using monoenergetic neutron sources. Neutrons were produced at the JAERI Tandem accelerator by the $^{2}H(d,n)^{3}He$ reaction for 7.8 and 10.0 MeV and $^{1}H(^{11}B,n)^{11}C$ reaction for 11.5 and 13.0 MeV. Emitted gamma-rays were measured with a 7.6 cm dia. x 15.2 cm long NaI(Tl) detector surrounded by a 25.4 cm dia. x 25.4 cm long annular NaI(Tl) detector operated in an anti-coincidence mode. Time-of-flight technique was used to reduce backgrounds. To obtain gamma-ray energy spectra, measured pulse height data were unfolded by the FERDOR code. Several correction factors were calculated by the Monte Carlo method such as angular distribution of source neutrons, neutron multiple scattering, outgoing gamma-ray attenuation and Compton scattering in the sample. Differential cross sections are given as a function of gamma-ray energy over the region from 0.7 to 12 MeV. Discrete gamma-ray and total gamma-ray production cross sections are also presented.

---

* Tokyo Institute of Technology

II-C-2 **Neutron Transmission Measurements on Gallium in the Resonance Region**

Makio Ohkubo

A paper on this subject was published in JAERI-M 90-213 with the following abstract:

Neutron transmission measurements were made on natural gallium using a TOF spectrometer of the Japan Atomic Energy Research Institute linear accelerator. Neutron resonance parameters are obtained for 54 levels in the energy region extended up to 10.4 keV. The average level spacing $\bar{D}$ and the s-wave strength function S_0 are deduced to be:

$$\bar{D} = 185 \pm 12 \text{ eV},$$

$$S_0 = (1.2 \pm 0.2) \times 10^{-4} \text{ below } 10.4 \text{ keV}.$$

D. Nuclear Data Center, Department of Physics and Working Groups of Japanese Nuclear Data Committee

II-D-1 JENDL-3 FP Nuclear Data Library

JNDC FP Nuclear Data Working Group

T. Nakagawa, M. Kawai[1)], S. Iijima[1)], H. Matsunobu[2)], T. Watanabe[3)], Y. Nakajima, T. Sugi, M. Sasaki[4)], A. Zukeran[5)], K. Kaneko[6)] and H. Takano

A paper on this subject was presented at Int. Conf. on Nuclear Data for Science and Technology, May 13 - 17, 1991, at Jülich with the following abstract:

Evaluation of neutron nuclear data for 172 nuclides given in Table 1 has been made for JENDL-3. Evaluated quantities are the total, elastic and inelastic scattering, capture and threshold reaction cross sections, the angular and energy distributions of secondary neutrons in the incident neutron energy range from 10^{-5} eV to 20 MeV. The evaluation was made on

---

1) Toshiba Corporation, Kawasaki-ku, Kawasaki 210

2) Sumitomo Atomic Energy Industries, Ltd., Chiyoda-ku, Tokyo 101

3) Kawasaki Heavy Industries, Ltd., Koto-ku, Tokyo 136

4) Mitsubishi Atomic Power Industries, Inc., Minato-ku, Tokyo 105

5) Hitachi, Ltd., Hitachi-shi, Ibaraki-ken 316

6) The Japan Research Institute, Ltd., Monato-ku, Tokyo 107

the basis of theoretical calculations with optical, statistical, pre-equilibrium and multi-step evaporation models as well as available experimental data. Below 100 keV, resolved and unresolved resonance parameters were evaluated. The benchmark tests performed by comparing with experimental data at STEK, EBR-II and CFRMF have confirmed the reliability of the present evaluation.

Table 1 Nuclides in JENDL-3 FP Nuclear Data Library

As-75, Se-74, 76, 77, 78, 79, 80, 82, Br-79, 81, Kr-78, 80, 82, 83, 84, 85, 86, Rb-85, 87, Sr-86, 87, 88, 89, 90, Y-89, 91, Zr-90, 91, 92, 93, 94, 95, 96, Nb-93, 94, 95, Mo-92, 94, 95, 96, 97, 98, 99, 100, Tc-99, Ru-96, 98, 99, 100, 101, 102, 103, 104, 106, Rh-103, 105, Pd-102, 104, 105, 106, 107, 108, 110, Ag-107, 109, 110m, Cd-106, 108, 110, 111, 112, 113, 114, 116, In-113, 115, Sn-112, 114, 115, 116, 117, 118, 119, 120, 122, 123, 124, 126, Sb-121, 123, 124, 125, Te-120, 122, 123, 124, 125, 126, 127m, 128, 129m, 130, I-127, 129, 131, Xe-124, 126, 128, 129, 130, 131, 132, 133, 134, 135, 136, Cs-133, 134, 135, 136, 137, Ba-130, 132, 134, 135, 136, 137, 138, 140, La-138, 139, Ce-140, 141, 142, 144, Pr-141, 143, Nd-142, 143, 144, 145, 146, 147, 148, 150, Pm-147, 148, 148m, 149, Sm-144, 147, 148, 149, 150, 151, 152, 153, 154, Eu-151, 152, 153, 154, 155, 156, Gd-152, 154, 155, 156, 157, 158, 160, Tb-159

II-D-2

Evaluation of JENDL-3 Fusion File

Baosheng YU* and Satoshi CHIBA

In order to provide good accuracy data on the double differential spectra of secondary neutrons and charged particles, a special purpose file, called JENDL-3 Fusion File, is being prepared. Instead of the ENDF-5, this file has a format of the ENDF-6. The spectral data on charged particles are stored in this file because they are required in calculations of the PKA (Primary Knock-on Atom) spectra[1].

According to our previous work[2], the DDXs of secondary neutrons are expressed by the Kumabe's[3] or Kalbach's[4] systematics, depending on the target nucleus. The DDXs of secondary charged particles are given by the Kalbach's systematics. The composite energy differential cross sections (EDXs) and the precompound fraction (f_{MSD}) required in these systematics were calculated by the SINCROS-II code system[5]. The JENDL-3 Fusion File will contain 20 elements together with their prominent stable isotopes that have significant importance in fusion neutronics, ranging from ^{27}Al to ^{209}Bi.

References

1) M. Kawai and T. Fukahori, private communication.

2) B. Yu, S. Chiba and T. Fukahori, to be published.

3) I. Kumabe, Y. Watanabe, Y. Nohtomi and M. Hanada, Nucl. Sci. Eng. 104, 280(1990).

4) C. Kalbach, Phys. Rev. C37, 2350(1988).

5) N. Yamamuro, JAERI-M 90-006(1990).

---

* Visiting scientist from China Institute of Atomic Energy, Beijing, People's Republic of China, under STA scientist exchange program.

II-D-3

JENDL Dosimetry File

Masaharu NAKAZAWA[1)], Katsuhei KOBAYASHI[2)], Shin IWASAKI[3)], Tetsuo IGUCHI[1)], Kiyoshi SAKURAI, Yujiro IKEDA, Tsuneo NAKAGAWA

A paper on this subject will be published as JAERI report with the following abstract:

The JENDL Dosimetry File based on JENDL-3 was compiled and integral tests of cross section data were performed by Dosimetry Integral Test Working Group of Japanese Nuclear Data Committee. Data stored in the JENDL Dosimetry File are the cross sections and their covariance data for 61 reactions. The cross sections were mainly taken from JENDL-3 and the covariances from IRDF-85. For some reactions, data were adopted from other evaluated data files. The data are given in the neutron energy region below 20 MeV in point-wise and group-wise files in the ENDF-5 format. In order to confirm reliability of the data, several integral tests were carried out; comparison with IRDF-85 and average cross sections measured in fission neutron fields, fast reactor spectra, DT neutron fields and Li(d,n) neutron fields. As a result, it has been found that the JENDL Dosimetry File gives better results than IRDF-85 but there are some problems to be improved in future. The contents of the JENDL Dosimetry File and the results of the integral tests are described in this report. All of the dosimetry cross sections are shown in a graphical form.

---

1) University of Tokyo, Faculty of Engineering

2) Kyoto University, Research Reactor Institute

3) Tohoku University, Faculty of Engineering

II-D-4

Evaluation of Neutron Cross Sections of Hydrogen up to 10 GeV

Satoshi CHIBA

The neutron total, elastic scattering and capture cross sections of hydrogen were evaluated from 20 MeV to 10 GeV. The total and elastic scattering cross sections were evaluated by a comprehensive least-squares method by taking account of the experimental information stored in NESTOR-2[1]. This work was first motivated by a request from the ESNIT group[2] up to 50 MeV, but was later extended by the author up to 10 GeV to give a standard cross section data set with full covariance information. No attempt was made to evaluate these cross sections by using the phase-shift method, in which good quality p-p scattering data constrain the parameters through the assumption of the charge independence. However, as long as the total cross section is concerned, it must be recognized that quality of the up-to-date neutron data surpasses that of charged particle scattering data.

The total cross section was evaluated by the generalized least-squares method using the NDES/GMA system[3]. The resultant cross section and error-correlation matrix are shown in **Figs. 1** and **2**. Legendre coefficients of the elastic scattering were determined by the least-squared method up to ℓ=10. Some of them are shown in **Fig. 3**. The capture cross section was calculated by a formula given by Horsley[4] which was obtained by the principle of the detailed balance, by using a formula of Feshbach and Schwinger[5] for the D(γ,n)p reaction. The pion production cross section have to be evaluated in the future.

References

1) T. Nakagawa, *"NESTOR-2"*, private communication.

2) S. Ohno and K. Noda, private communication.

3) S. Chiba, *"NDES/GMA"*, unpublished memo.

4) A. Horsley, Nuclear Data, 2, 243(1966).

5) H. Feshbach and J. Schwinger, Phys. Rev. 84, 194(1951).

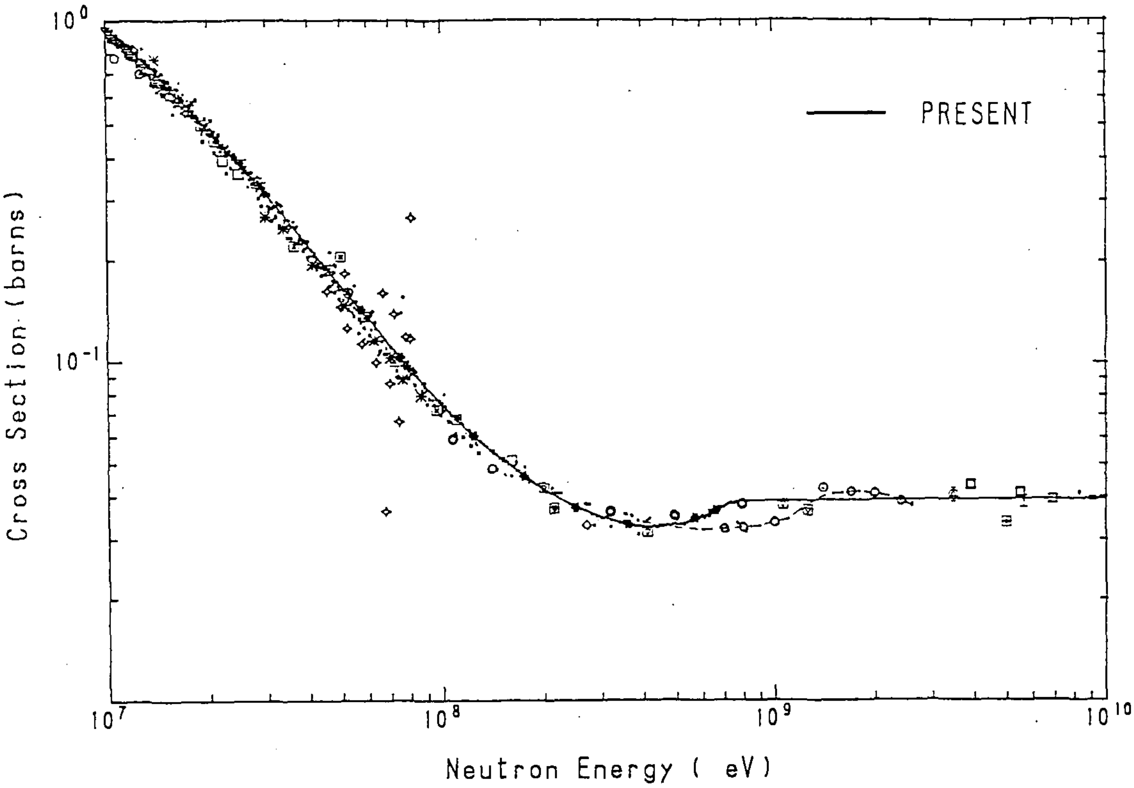

Fig. 1 Total cross section of hydrogen

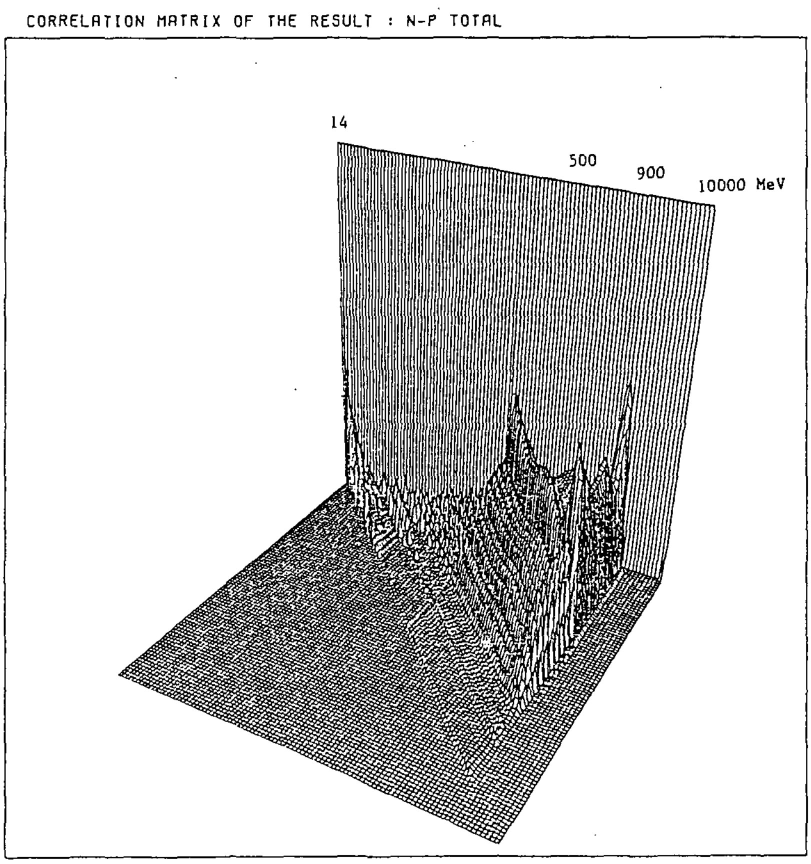

Fig. 2 Error correlation matrix of the evaluated hydrogen total cross section.

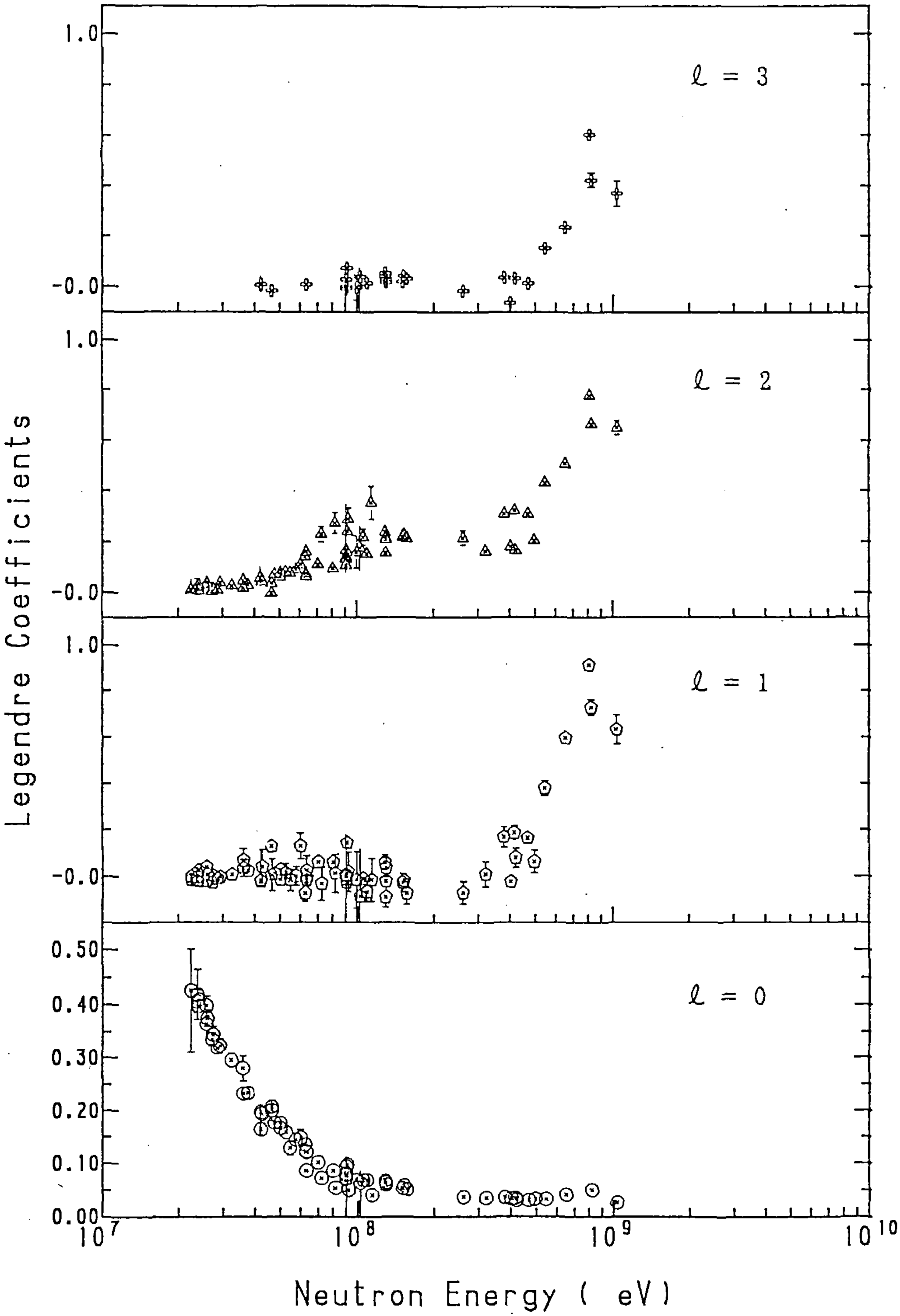

Fig. 3 Legendre coefficients of the elastic n–p scattering obtained from the least-squares method. The notation of the ENDF-6 is taken; the ℓ=0 component is given in barns, while other partial waves have no dimension.

II-D-5 Reevaluation of the DDX Data of ^{14}N in JENDL-3

Y. KANDA*, T. MURATA**, Y. NAKAJIMA*** and T. ASAMI****

The detailed comparison of the neutron emission DDX (Double Differential Cross-section) data of ^{14}N in JENDL-3 with the experimental data of Tohoku University[1,2] and Osaka University[3] to examine the defects for the ^{14}N data of JENDL-3 (MAT=3071). The data reevaluation was made based on this examination. The main parts of the reevaluation are as follows:

a) The cross-section data for the 7th- and 8th-levels of the inelastic scattering were adjusted to fit to the experimental ones.

b) All the inelastic scattering data were given for discrete levels instead of the neutron continuum, and twenty-six discrete levels were newly added in the evaluation.

c) The angular distributions for the continuum, neutrons from the reactions of (n,2n), (n,n'p), (n,n'd) and so on were assumed to be isotopic in the center of mass system instead of in the laboratory system.

The reevaluated data for the neutron emission DDX at around 14 MeV-neutrons are in good agreement with the experimental ones generally, and the data were improved remarkably, as shown in Fig.1.

This work was done as a part of the activities of the JNDC working

---

* Department of Energy Conversion Engineering, Kyushu University

** Nuclear Engineering Laboratory, Toshiba Corporation

*** Nuclear Data Center, Japan Atomic Energy Research Institute

**** Nuclear Energy Data Center

group on fusion nuclear data.

A paper on this subject has been presented at the 1990 Symposium on Nuclear Data, Tokai, Nov. 29 and 30 1990[4].

References

1) Baba, M.: '85Santa Fe Vol.1, 223 (1985).

2) Baba, M.: Rad. Eff. 92, 223 (1986).

3) Takahashi, A.: OKTAV-A-87-01 (1987).

4) Igashira, M. and Nakagawa, T.(Ed.): JAERI-M 91-032 (1991), p.376.

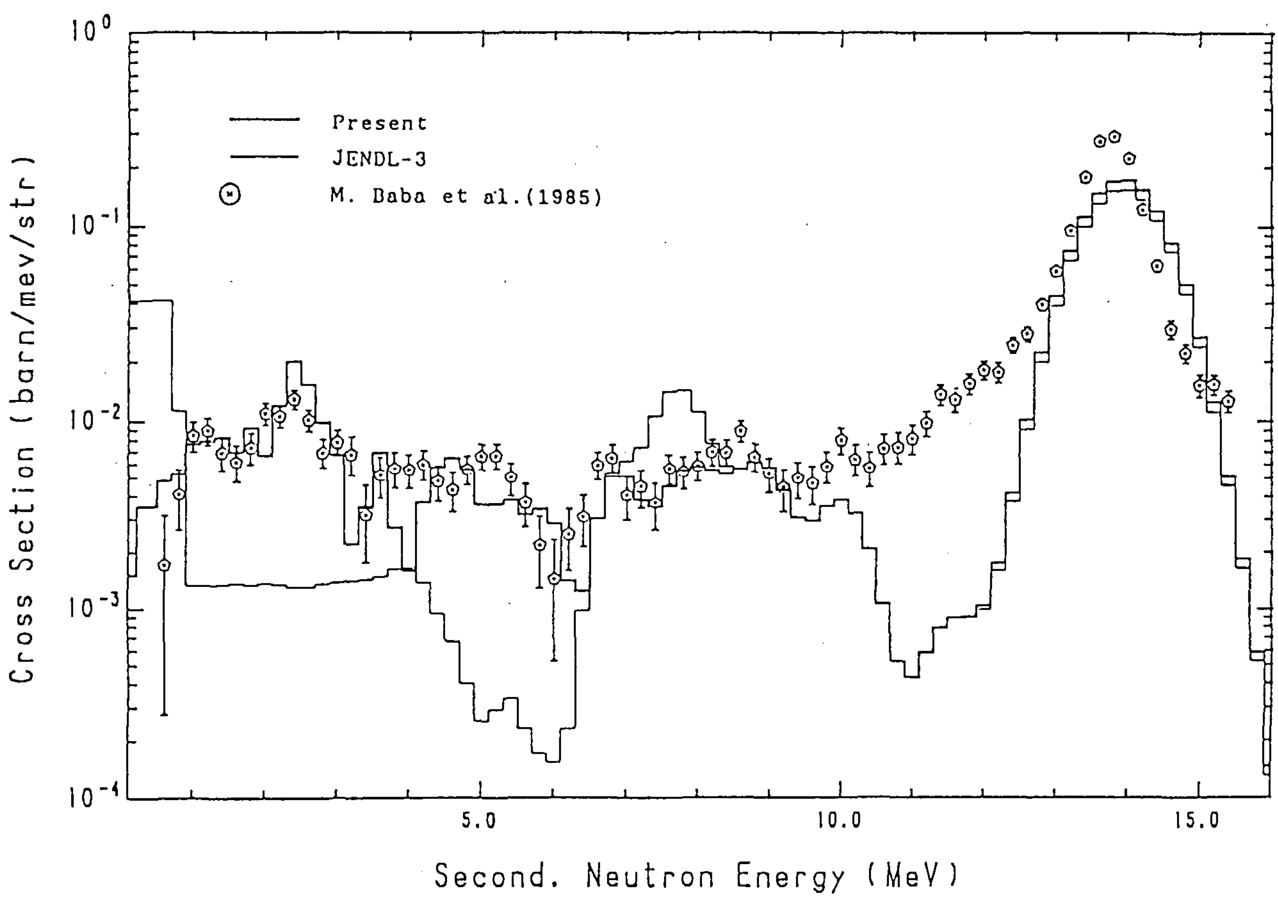

Fig. 1 The double differential cross sections of ^{14}N for the neutrons emitted at the laboratory angle of 30 deg., induced by the 14.2-MeV neutrons. The reevaluated data are compared with the JENDL-3 data and the experimental ones of Tohoku University[3].

II-D-6

Evaluation of Neutron Nuclear Data of Natural Silver and Its Isotopes

LIU Ting-jin*, Keiichi SHIBATA and Tsuneo NAKAGAWA

A paper on this subject was published as JAERI-M 91-011 (1991) with the following abstract:

Neutron nuclear data of natural silver and its isotopes (^{107}Ag and ^{109}Ag) have been evaluated in the energy range from 10^{-5} eV to 20 MeV. Evaluated quantities are the total, elastic and inelastic scattering, capture, (n,2n), (n,3n), (n,p), (n,α), (n,np), (n,nα) reaction and gamma-ray production cross sections, the resonance parameters and the angular and energy distributions of emitted neutrons and gamma-rays. The evaluation is based on available experimental data and theoretical calculations. The experimental data were carefully examined and selected. Multi-step Hauser-Feshbach calculation played an important role in the determination of the reaction cross sections. The precompoud process was taken into account above 5 MeV, in addition to the compound one. The evaluated data have been compiled into JENDL-3 in the ENDF-5 format.

---

* Institute of Atomic Energy, Beijing, The People's Republic of China

II-D-7

Evaluation of Nuclear Data in the Medium Energy Region for $^{204,206,207,208,nat}Pb$ and ^{209}Bi

T. Fukahori and S. Pearlstein*

Nuclear data in the medium energy region are necessary to many applications, for example, design of spallation neutron sources. However, they have never been prepared, except those of iron[1]. In this paper, an evaluation of neutron and proton induced nuclear data for $^{204,206,207,208,nat}Pb$ and ^{209}Bi in the energy region from 10^{-5} eV to 1 GeV has been performed using mainly ALICE-F and nuclear systematics[2] embedded in PEND6F which is a compilation code to the ENDF-6 format. The code ALICE[3], using evaporation and preequilibrium theories, was modified to ALICE-P by Pearlstein[1], and in the present study the 1989 version of ALICE[4] was modified to ALICE-F. The modifications consist mainly of changes in optical model parameters, the calculation of inverse cross sections, and mass calculation part.

The total (for neutrons), elastic scattering and reaction cross sections were calculated by the optical model with parameters stored in ALICE-F[1]. The angular distributions of elastically scattered particles were based on a diffraction model[5] amended for relativistic effects and empirical fits to high energy data. For fission cross section, experimental data of several isotopes near lead in the energy range from 50 MeV to 9 GeV were reviewed, and a systematics was derived and stored in the code PEND6F. Figure 1 shows the evaluated result for the ^{208}Pb (p,f) cross section.

---

* National Nuclear Data Center, Brookhaven National Laboratory,
Building 197D, Upton, New York 11973, U.S.A.

References:

1) S. Pearlstein, J. Astrophys., 346 (1989) 1049

2) S. Pearlstein, Nucl. Sci. Eng., 95 (1987) 116

3) M. Blann, CODE ALICE/85/300, UCID-20169 (1985)

4) M. Blann, CODE ALICE/89, private communication (1989)

5) S. Pearlstein, Nucl. Sci. Eng., 49 (1972) 162

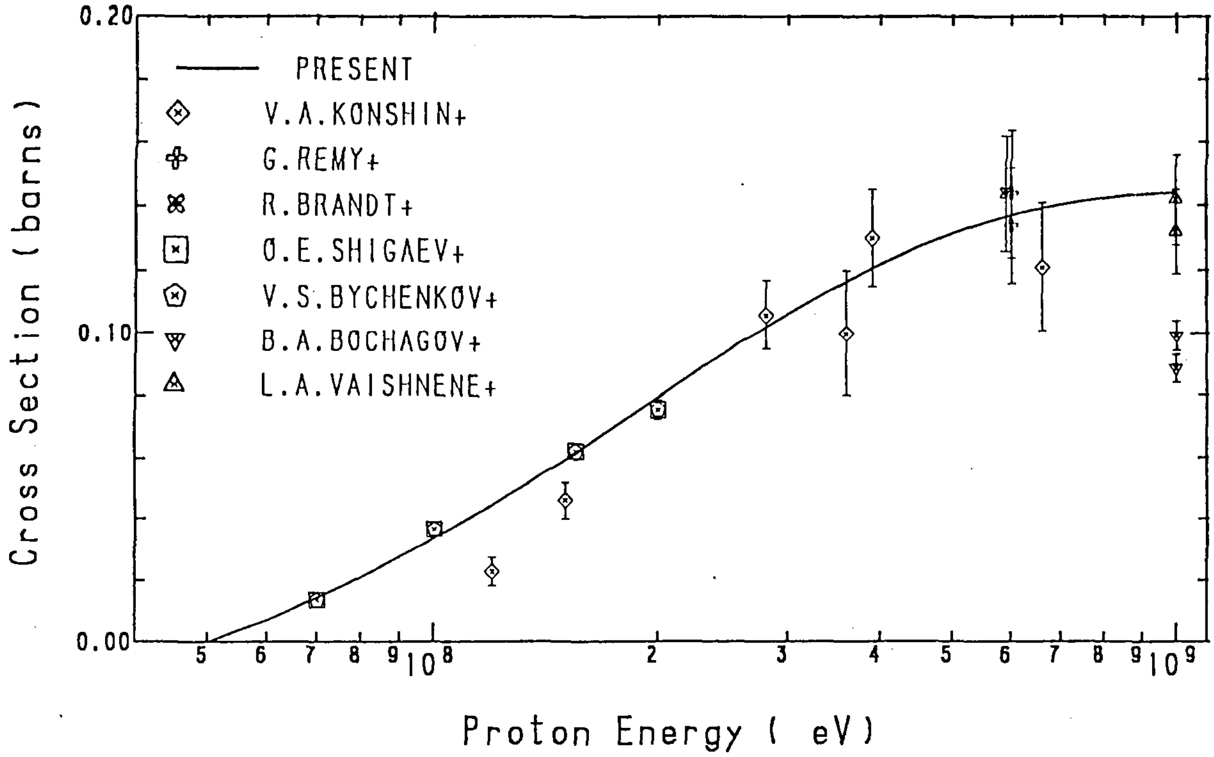

Fig. 1 Evaluated result for ^{208}Pb (p,f) cross section.

II-D-8 A REPORT ON EVALUATED $^{238}U(n,\gamma)$ CROSS SECTION

Y.Kanda*, Y.Kikuchi, Y.Nakajima, M.G.Sowerby**, M.C.Moxon**,

F.H.Fröhner***, W.P.Poenitz**** and L.W.Weston*****

A paper on this subject will be presented in the Proceedings of the International Conference on Nuclear Data for Science and Thechnology (13–17, May, 1991 at Jülich, Federal Republic of Germany), with the following abstract :

A longstanding and difficult problem in nuclear data evaluation has been that ^{238}U capture cross sections in the unresolved resonance region evaluated on the basis of available experiments are larger than the ones expected from the reactor physics analysis. However, the new versions of the major files, ENDF/B-VI, JEF-2 and JENDL-3 have now adopted lower values than the respective previous versions. To be convinced that these new evaluations are correct, a subgroup in the NEACRP/NEANDC Working Group on Internaional Evaluation Cooperation has studied the problem.

New resonance parameters deduced from capture and transmission data by the shape analysis method can be used to renormalise early capture cross section experiments. The average capture cross sections calculated from these then has high weight in a simultaneous evaluations which leads to lower evaluated capture values. Theoretical model fitting to available experiments gives similar values. Two recent measurement agree with the lower ones. Therefore, the subgroup concludes that the lower capture cross sections of ^{238}U recomended in ENDF/B-VI, JEF-2 and JENDL-3 are reasonable.

---

* Kyushu University, Kasuga, Fukuoka, 816, Japan

** Atomic Energy Research Establishment, Harwell, Oxon, OX11 ORA, U.K.

*** Kernforschungzentrum Karlsruhe, Karlsruhe, F.R.Germany

**** Argonne National Laboratory-West, Idaho Falls, ID 83403-2528, U.S.A.

***** Oak Ridge National Laboratory, Oak Ridge, TN 37830, U.S.A.

II-D-9

Measurement of the Thick-Target (p,n) Neutron Spectra from Accelerator Structural Materials at 10 MeV

Satoshi CHIBA, Kazuo HASEGAWA, Tokio FUKAHORI, Masayoshi SUGIMOTO, Hiroshi NAKASHIMA and Motoharu MIZUMOTO

In order to provide detailed data for shielding calculations of BTA (Basic Technology Accelerator, 10 MeV, 10 mA proton LINAC) that will be used for the mock-up test of the injector of ETA (Engineering Test Accelerator, 1.5 GeV, 10 mA proton LINAC)[1], the thick target (p,n) neutron spectra from several accelerator structural materials were measured at proton energy of 10 MeV.

The experiment was done at the JAERI tandem accelerator. The protons were produced from the in-terminal duo-plasmatron ion source. They were then chopped and bunched into a pulsed beam of 1 MHz repetition and 1 ns duration in FWHM in order to determin the neutron energy by the Time-of-Flight (TOF) method. The average beam current was typically 100 nA at the target. The targets, C, Al, Fe, Cr, Ni, Cu, Ti and Pb, have chemical purities better than 99.2%, and were fabricated into disks of 2 cm in diameter and 1 mm in thickness, which were thick enough to stop 10-MeV protons completely even in C. A target made of SUS304, 2mm in thickness, was also prepared separately. The neutrons were detected by an NE213 scintillator between 0 and 140 degrees. The data were recorded onto an optical magnetic disk through a PC-based data acquisition system. The data were later analyzed offline. Several PASCAL programs were written for this purpose. After the correction for backgrounds, dead time (both of TAC and ADC) and detection efficiency were made, the TOF spectra were converted into the energy spectra. They were then corrected for the effects of the in-scattering and attenuation in the target assembly, of which the correction factors were calculated by the MCNP program[2]. The data were extrapolated to obtain the total yield by assuming the evaporation spectrum below 1 MeV, where the measured data become uncertain due to ambiguities in the detection efficiency. The data were finally compiled in an EXFOR-like format, with information on the random and correlated error components in 50-keV intervals.

In **Figs. 1** and **2**, the results for carbon and aluminum at 0 deg. are shown. In these light elements, discrete level structures in the compound nuclei, especially of the isobaric-analog state resonance, are prominent. It should be noted that all of the neutrons from the carbon target come from ^{13}C that is only 1% abundant.

The data obtained in the present work are available upon request.

References

1) M. Mizumoto et al., *"DEVELOPMENT PLAN OF BASIC TECHNOLOGY FOR A HIGH INTENSITY PROTON LINEAR ACCELERATOR"*, Proc. of The 2nd International Symposium on ADVANCED NUCLEAR ENERGY RESEARCH - Evolution by Accelerators -, Jan. 24-26, 1990 at Mito Plaza Hotel, Mito, Ibaraki, Japan.
2) J. F. Briesmeister (Ed.), *"MCNP - A General Monte Carlo Code for Neutron and Photon Transport, Version 3A"*, LA-7396-M, Rev. 2 (1986).

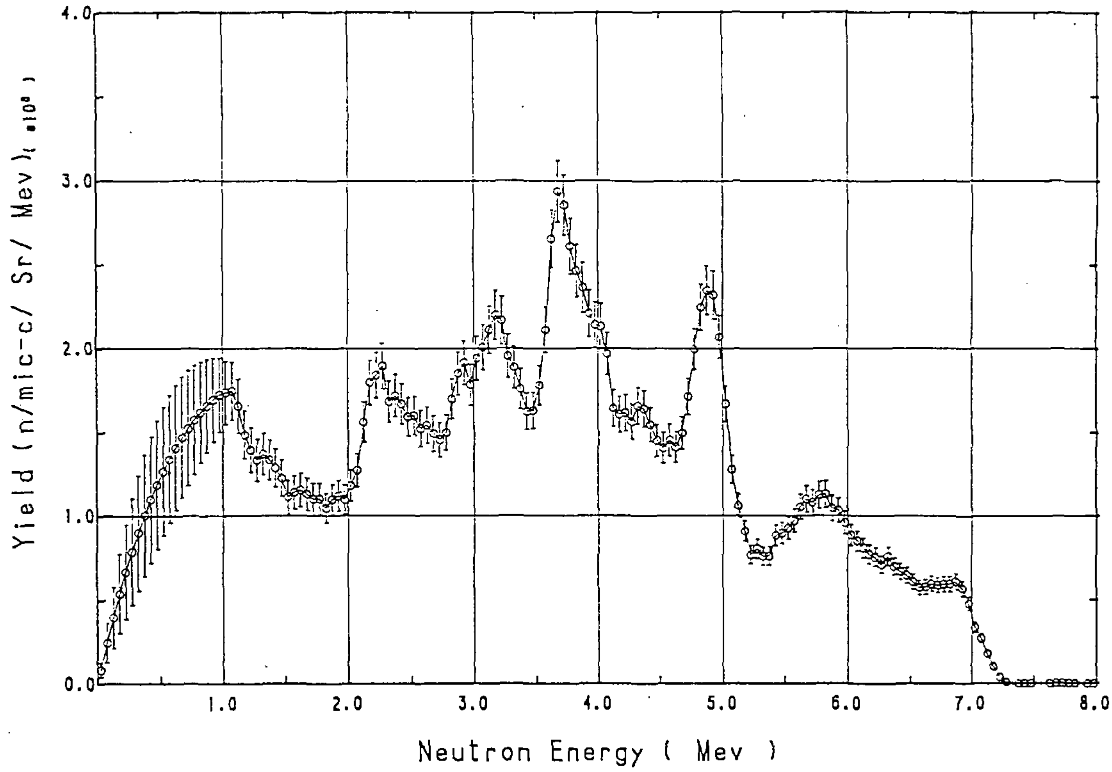

Fig. 1 Thick target (p,n) neutron spectrum from carbon measured at 0 deg. with 10-MeV protons

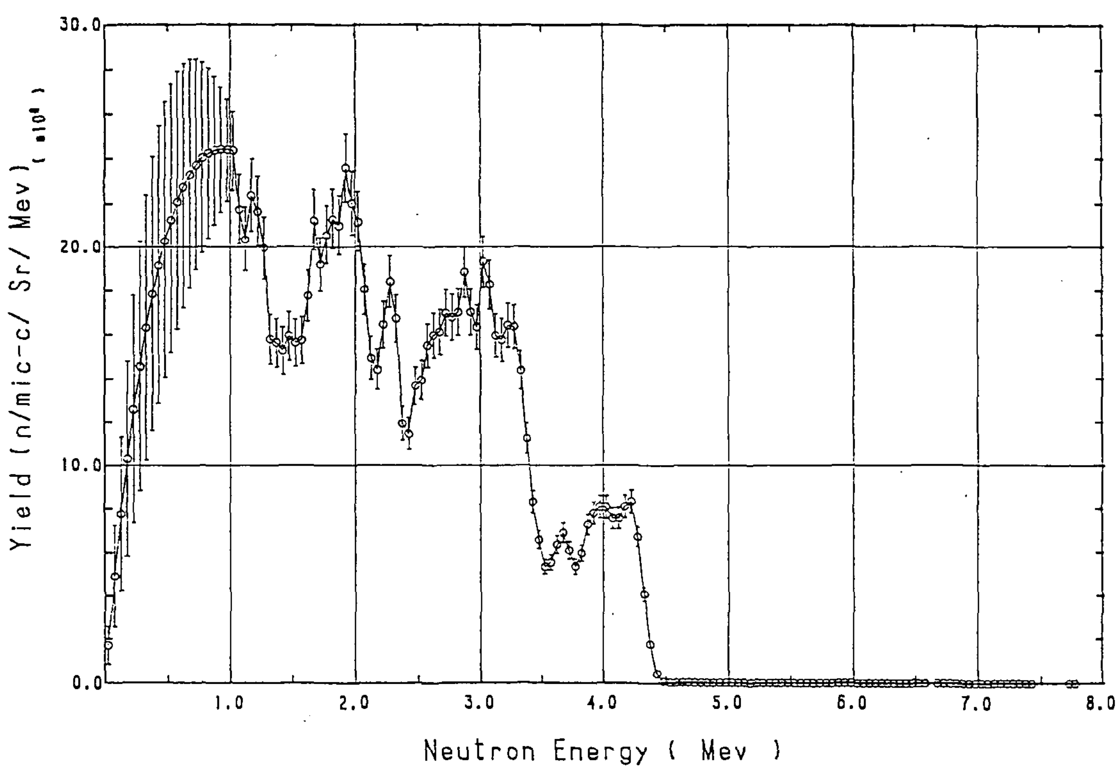

Fig. 2 Thick target (p,n) neutron spectrum from aluminum measured at 0 deg. with 10-MeV protons

II-D-10 Review of the Research and Application of KERMA Factor and DPA Cross Section

PKA spectra working group*

A paper on this subject was published as JAERI-M 91-043 with the following abstract:

The data for recoil atom spectra, KERMA factor and displacement cross sections from neutron-induced reactions are calling increasing interest for applications to the study of radiation damage, calculation of heat generation in reactor, neutron therapy and biological research. PKA spectra sub-working group was recently established in Japanese Nuclear Data Committee as part of developing JENDL Special Purpose Data Files. Current status of the data and various features of application of the KERMA-related problem were reviewed and discussed at the first meeting of the sub-working group. Present report is a compilation of the items presented at the meeting, covering a brief review of the existing research and the data, method of calculation, the KERMA factor data in neutron therapy, the deduction of KERMA factor of C-12 from Neutron reaction measurement and analysis, the data base for radiation damage, the damage simulation calculation, and the method of storaging the evaluated data in ENDF/B-VI format.

---

* Masayoshi KAWAI, Shungo IIJIMA(Toshiba Corporation), Takeo ARUGA, Tokio FUKAHORI, Keiichi SHIBATA, Teruo SUGI, Yoshimaro YAMANOUTI(JAERI), Kensuke KITAO(Nat. Int. of Radiological Sciences), Akito TAKAHASHI(Osaka Univ.), Naoki YAMANO(Sumitomo Atomic Energy Ind. Ltd.) and Kouichi Maki (Hitachi Ltd.)

III. Kinki University

III-A-1

An Improved Model for Fission Neutron Spectrum Calculation: Non–equitemperature Madland–Nix Model

Takaaki Ohsawa

A paper on this subject was published in the Proceedings of the 1990 Symposium on Nuclear Data, JAERI–M 91–032, pp.383–394, with the following abstract:

An attempt was made to improve the Madland–Nix model for the calculation of the fission neutron spectrum. In the original Madland–Nix model, statistical equilibrium was assumed between the two fission fragments at the scission point. This was the ground for using a single value of the nuclear temperature for both fragments. However, this assumption seems questionable, since the deformation energies of the fragments at the scission point, which are generally different for the nascent fragments, eventually converts into the internal excitation energy. The author tried to take into account the difference in the nuclear temperature of the light and heavy fragments in an empirical manner. This non–equitemperature model was applied to analyze the fission neutron spectra for neutron–induced fission of U–235 and Pu–239 and spontaneous fission of Cf–252. It was found that (i) consideration of the temperature difference had greater effects on the spectral shape than previous attempts, and (ii) this modification of the model gave better account of the experimental spectra for these nuclides.

B. Department of Reactor Engineering

III-B-1

Cross Sections of the Reaction $^{55}Mn(n,2n)^{54}Mn$, $^{58}Ni(n,2n)^{57}Ni$ and $^{58}Ni(n,np)^{57}Co$ Averaged Over the U-235 Fission Neutron Spectrum

O. Horibe and H. Chatani*

A paper on this subject has been submitted to the International Conference on Nuclear Data for Science and Technology held at Jülich, 1991, with the following abstract:

Cross sections of $^{55}Mn(n,2n)^{54}Mn$, $^{58}Ni(n,2n)^{57}Ni$ and ^{58}-Ni$(n,np)^{57}Co$ reactions are presented together with the 34 kinds of threshold reaction cross sections which have been measured earlier. The $^{55}Mn(n,2n)^{54}Mn$ reaction cross section values are also used to give specific variance-covariance matrix of the 35 kinds of cross sections. The $^{58}Ni(n,np)^{57}Co$ reaction includes the (n,pn) and (n,d) reactions. The obtained experimental values are compared with those of experimental values of other authors, or with the values calculated by the Horibe's formula, or with the integral values calculated with the cross section data in ENDF/B-V and JENDL-2, assuming the fission neutron spectrum shapes to be of Maxwell, or Madland-Nix, or Watt types.

*Research Reactor Institute, Kyoto University

IV. Kyoto University

A. Department of Nuclear Engineering

Faculty of Engineering

IV-A-1 Intermediate Energy *NN* Phase Shifts - I

Yoshio HIGUCHI, Norio HOSHIZAKI, Hiroaki MASUDA*) and Hiroomi NAKAO+)

A paper on this subject will be published in Prog. Theor. Phys. 86, No.1 (1991) with the following abstract. Tables of the summary of data kinds and data points used and of the obtained phase shift values are given there.

A *pp* phase shift analysis is reported incorporating the *pp* world data from 430-800MeV. The solutions show half-looping and anticlockwise motion for the $^1D_2$ and $^3F_3$ amplitudes. Similar structure is observed in the $^3P_2$ wave.

*) Present address: SLAC, Bin96, Stanford University, P.O.Box 4349, Stanford, CA94309, U.S.A.
+) Present address: Integrated Circuit CAD Department, Mitsubishi Electric Corporation, ASIC Design Engineering Center 401, Mizuhara, Itami City, Hyogo 664, Japan.

IV-A-2 Intermediate Energy *NN* Phase Shifts - II

Norio HOSHIZAKI and Takatoshi WATANABE*)

A paper on this subject will be published in Prog. Theor. Phys. 86, No.2 (1991) with the following abstract and figure. Tables of the summary of data kinds and data points used and of the obtained *I*-spin zero phase shift values are given there.

Neutron-proton phase-shift analyses with and without I=0 absorption are performed in the range from 430-800MeV with the I=1 phases being fixed to those values given previously. Solutions with I=0 absorption are better, in particular at 625 and 645 MeV, and reveal a narrow resonance in the $^1P_1$ wave.

*) Present address: Tokyo Electric Power Co. Ltd., Fukushima Nuclear Power Station No.1, Ohkuma-cho, Futaba-gun, Fukushima, Japan.

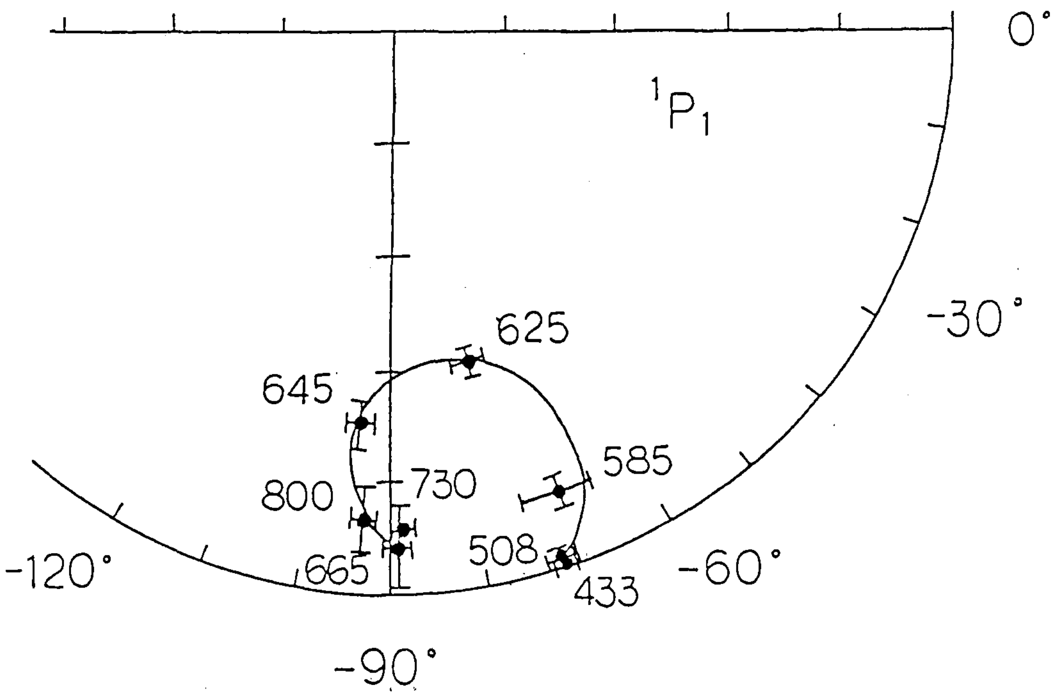

Fig. 1. Argand plots of $^1P_1$-partial wave amplitude. Numbers are T_{lab} in MeV. Breit-Wigner curve fitted to the phase shifts are also given. The parameters are M=2168MeV, Γ=25MeV, Γ_{el}/Γ=0.2.

IV-A-3

Narrow I-spin zero NN Resonance

Norio HOSHIZAKI and Takatoshi WATANABE*)

A paper on this subject will be published in Prog. Theor. Phys. 86, No.2 (1991) with the following abstract and figures. Resonance width and elasticity Γ_{el}/Γ are given there.

A narrow np inelastic resonance with I=0, $J^P=1^-$ and M=2168MeV/c^2 is reported on the basis of phase shift solutions given in the preceding paper. The np reaction cross section for I=0 state is predicted to have a sharp peak at 625 MeV in agreement with experiments by Dunaitsev and Prokoshkin.

*) Present address: Tokyo Electric Power Co. Ltd., Fukushima Nuclear Power Station No.1, Ohkuma-cho, Futaba-gun, Fukushima, Japan.

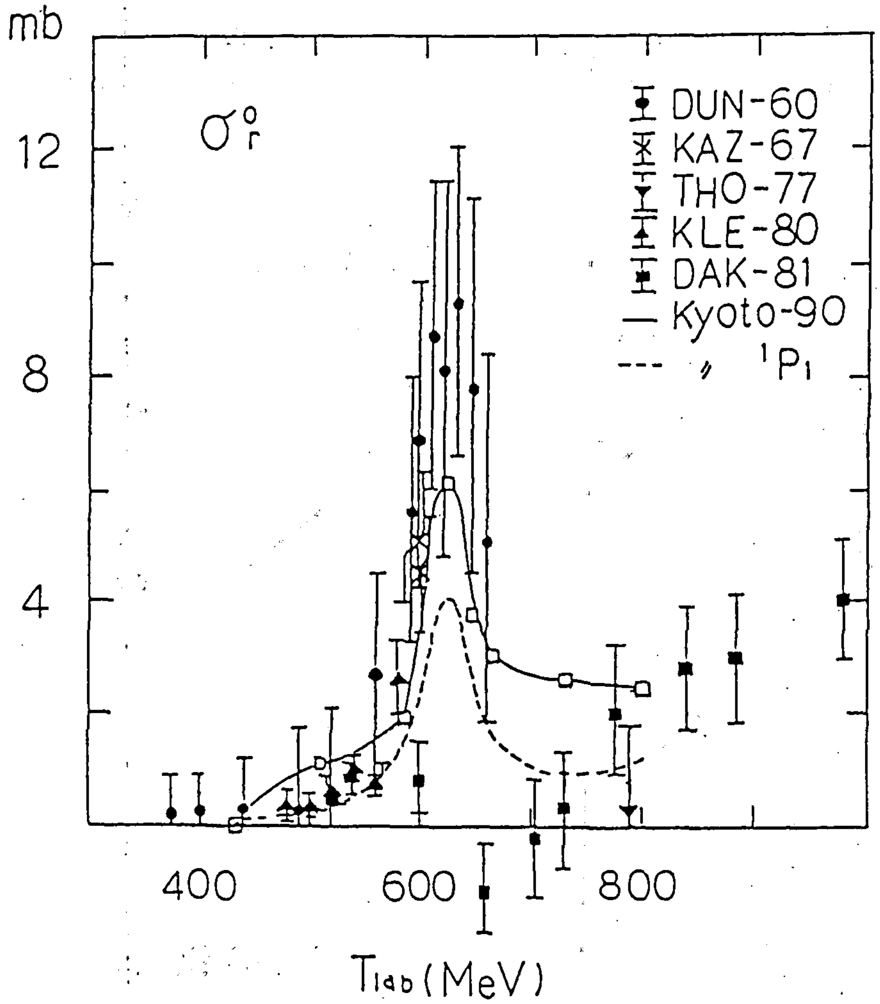

Fig. 1. Plots of σ_r^0 vs. T_{lab}. Solid curve connects the predictions by the absorptive I=0 solutions. Dashed one is the contribution from the $^1P_1$-wave. Experimental data are DUN-60, KAZ-67, THO-77, KLE-80 and DAK-81.

IV-B-3

Effects of Neutron Resonance Interference between Ta and Au

K. Kobayashi, A. Yamanaka+, I. Kimura+, S. Kanazawa+

and

R. Miki*

In the neutronic calculations for safety reactor design, it is of great importance to assess the neutron self-shielding[1,2] and mutual shielding effects[3-5] in fuels and reactor structural materials, especially for high conversion light water reactors with an intermediate neutron spectrum. In the high conversion reactors, fission product absorption is very important in the resonance energy region for burnup calculations, because the reactivity loss is caused predominantly by fission product absorption which is about 60 % of the total reactivity loss[5]. The mutual interference effects of resonance overlapping among major actinides and fission products are required for the estimation of the reactivity change and performing the burnup calculations. For that purpose, the resonance interference experiments between different nuclides are useful for the integral tests not only for the resonance parameters but also for the neutron resonance energy, because of its high sensitivity to the mutual

---

+ Dept. of Nucl. Eng., Fac. of Eng., Kyoto University
Yoshidahonmachi, Sakyo-ku, Kyoto 606

* Kinki University Atomic Energy Research Institute
3-4-1, Kowakae, Higashiosaka-shi, Osaka 577

interference in the resonance energy region.

In the present work, Au and Ta nuclei were selected for the mutual interference experiments at the resonances of 4.9 and 4.3 eV, respectively. Moreover, Cu sample was used to investigate the results without resonance interferences, because Cu can be one of the radioactive nuclides and has not a big resonance neutron cross section in the eV energy region. Tantalum cases whose outer and inner diameters were 45 and 15 mm, respectively, were prepared as seen in Fig. 1. A set of the Ta case and Au foil(50 μm thickness) or Cu foil(0.3 mm thickness), 12.7 mm in diameter each with Cd cover (0.5 mm thickness) was inserted at the central graphite cavity of the UTR-KINKI, where a good standard 1/E neutron spectrum field can be obtained in the energy region from about 1 eV to a few hundreds keV[6]. By changing the window thickness of the Ta case, the irradiations were performed at the reactor power of 1 W for 30 to 90 min. Induced activities of gold and/or copper were measured with a high purity Ge detector.

The mutual interference calculations were performed with a continuous slowing down Monte Carlo code VIM[7], using a nuclear data library generated by ENDF/B-IV. Figure 2 shows typical examples of the reaction rate spectrum at the Au and Ta resonances. Spectral changes due to the resonance interference can be seen as the Ta window thickness increases. Fractional distribution of the reaction rates are given in Table 1, where one can recognize that most of the reaction rates exist near the resonances. Figure 3 shows Au and Cu reaction rates from the Au-Ta and Cu-Ta combination sets depending upon the Ta window thickness. Uncertainties due to the experiment are within 2 to 3 % and several percent at most are from the VIM calculation. It can be seen that the reaction rate data of Au are rapidly decreasing with the Ta window thickness due to the mutual interference. Copper data, however, follow only neutron fluxes which penetrate the Ta windows, changing slowly without mutual interference between Ta and Cu.

For both cases with and without the interferences, a good agreement can be seen between the measurement and the calculation, as shown in Fig. 3. This implies that the existing nuclear data for Au and Ta are relatively well evaluated and established. It is also said that the present technique and/or procedure are applicable and useful for the integral tests of the neutron resonance energies and resonance parameters, which would be interested in neutronic calculations, especially for the high conversion light water reactors.

References:

1) R. C. Block, et al., Nucl. Sci. Eng., 80, 263 (1982).

2) Y. Fujita, et al., Proc. of Int'l Conf. on Neutron Phys., at Kiev, "Neutron Physics", No.2, p.195, Moscow (1988).

3) H. Takano, et al., Proc. of Int'l Conf. on Nuclear Cross Sections for Technology, p.244 (1979).

4) H. Mizuta, et al., Proc. of Thermal Reactor Benchmark Calculations, Techniques, Results and Applications, EPRI NP-2855 (1983).

5) H. Takano, et al., Nucl. Technol., 80, 250 (1988).

6) K. Kobayashi, et al., Annual Reports of Kinki University Atomic Energy Research Institute, Vol.25, 21 (1988).

7) D. K. Trubey and B. L. McGill, ORNL/RSIC-44 (1980).

Table 1 Fractional distributions of the reaction rates for the $^{197}Au(n,\gamma)^{198}Au$ reaction depending upon the window thickness of Ta cases.

Ta thickness	Fractional distribution of gold reaction rates		
	0 mm	1 mm	4 mm
Energy (eV)	(%)	(%)	(%)
1000 - 700	0.06	0.26	0.36
700 - 598	0.06	0.34	0.56
598 - 70	0.88	5.63	8.28
70 - 8	1.25	6.99	10.7
8 - 2	95.5	74.0	62.5
2 - 0.5	1.92	10.9	15.2
0.5 - 0.1	0.31	1.74	2.21
0.1 - 0.001	0.02	0.14	0.13

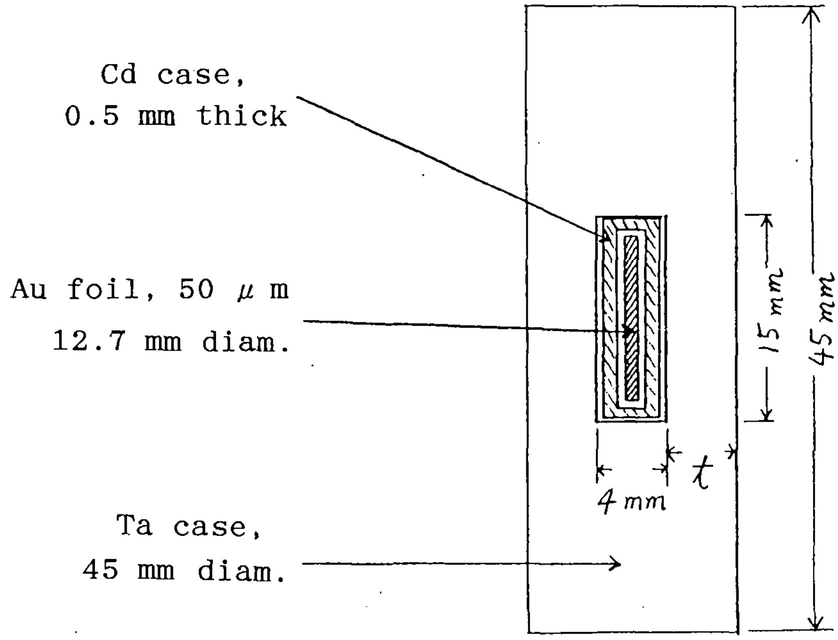

Fig. 1 Tantalum case for the present mutual experiment.
t = 0, 0.5, 1.0, 2.0, 4.0, 6.0, 9.0 mm .

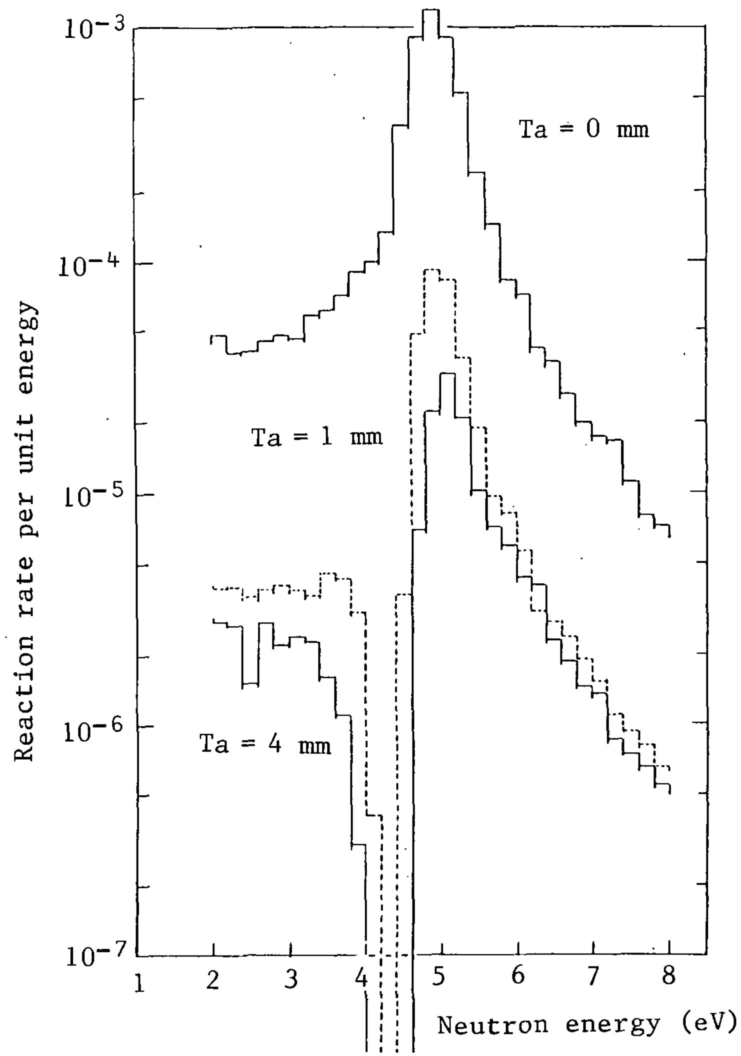

Fig. 2 Reaction rate spectra at Au and Ta resonances calculated with the MCNP code.

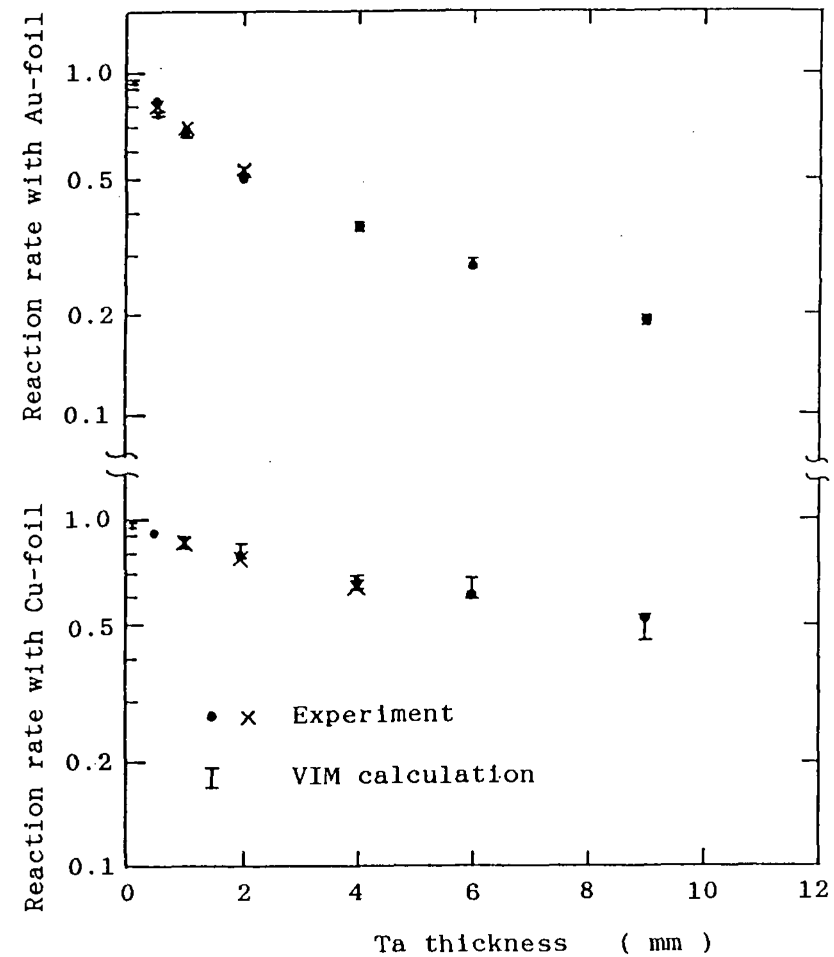

Fig. 3 Comparison of the measured and the calculated reaction rates by the mutual interference effects between Ta and Au and between Ta and Cu.

IV-B-4

Lead Slowing-Down Spectrometer Coupled to Electron Linac

--- Outline of the Spectrometer ---

Y. Nakagome, K. Kobayashi, S. Yamamoto, Y. Fujita,

A. Yamanaka+, S. Kanazawa+ and I. Kimura+

A lead slowing-down spectrometer has much higher neutron flux intensity by 3 to 4 orders of magnitude comparing with the widely applied normal neutron time-of-flight method[1,2], although the energy resolution is about 30 %. In spite of this disadvantage, by virtue of the intense neutron source, the spectrometer is though to be a valuable tool for cross section measurements for actinide nuclei, fission products and/or limited quantity of sample materials below several tens keV[2].

The Research Reactor Institute, Kyoto University, KURRI inherited the lead slowing-down spectrometer from the University of Tokyo, very recently. The spectrometer is a cube of 1.5x1.5x1.5 m^3 and about 40 tons, which is assembled with 1600 lead blocks (10x10x20 cm^3 each) of 99.99 % purity. The spectrometer was coupled to the 46 MeV electron linear accelerator (linac) at KURRI, as done for the Rensselaer Intense Neutron Source[2]. With this Kyoto University Lead slowing-down Spectrometer, KULS, we could expect to attain higher neutron source intensity than that using previous DT sources, by generating an

---

+ Dept. of Nucl. Eng., Fac. of Eng., Kyoto University
Yoshidahonmachi, Sakyo-ku Kyoto 606, Japan

order of 10^{11} photoneutrons per second at the center of the lead spectrometer.

A specific feature of the KULS is as follows:

1) The spectrometer was set on a platform car in the linac target room, as seen in Figs. 1 and 2. When the normal neutron time-of-flight measurements are made, the KULS is removed from the target room.
2) Each lead block was completely cleaned with alcohol or acetone and piled up to make a cube 1.5 m on a side without structural steel.
3) The photoneutron target is made of tantalum plates and cooled by compressed air. The target system is separated from the linac vacuum system to prevent troubles with the linac machine. The target was placed at the center of the spectrometer. For the multi-purpose and/or parallel measurements, eight experimental/irradiation holes were added to the originally designed spectrometer[3] which had removable lead stringers for the measuring positions.
4) One of the experimental holes was covered by Bi layers of 10 to 15 cm thickness to shield high energy (6-7 MeV) gamma-rays by the Pb(n, γ) reaction in the spectrometer.

We have just started the characteristic measurements with the KULS, and some of the recent results are shown in this progress report. In future we would like to apply this spectrometer to some nuclear data studies for actinide and/or fissile, fertile materials.

We would like to express our sincere thanks to Prof. M. Nakazawa, Prof. T. Kosako and people of Dept. of Nuclear Engineering, University of Tokyo for giving a ready consent to transferring the control of the lead slowing-down spectrometer to the Research Reactor Institute, Kyoto University and kindly making efforts and arrangements to set up the spectrometer there.

References:

1) A. A. Bergman, et al., Proc. of Int'l Conf. on Peaceful Uses of Atomic Energy, Vol.4, p.135, United Nations (1956).

2) R. E. Slovacek, et al., Nucl. Sci. Eng., 62, 455 (1977).

3) H. Wakabayashi, et al., J. Nucl. Sci. Technol., 7, 487 (1970).

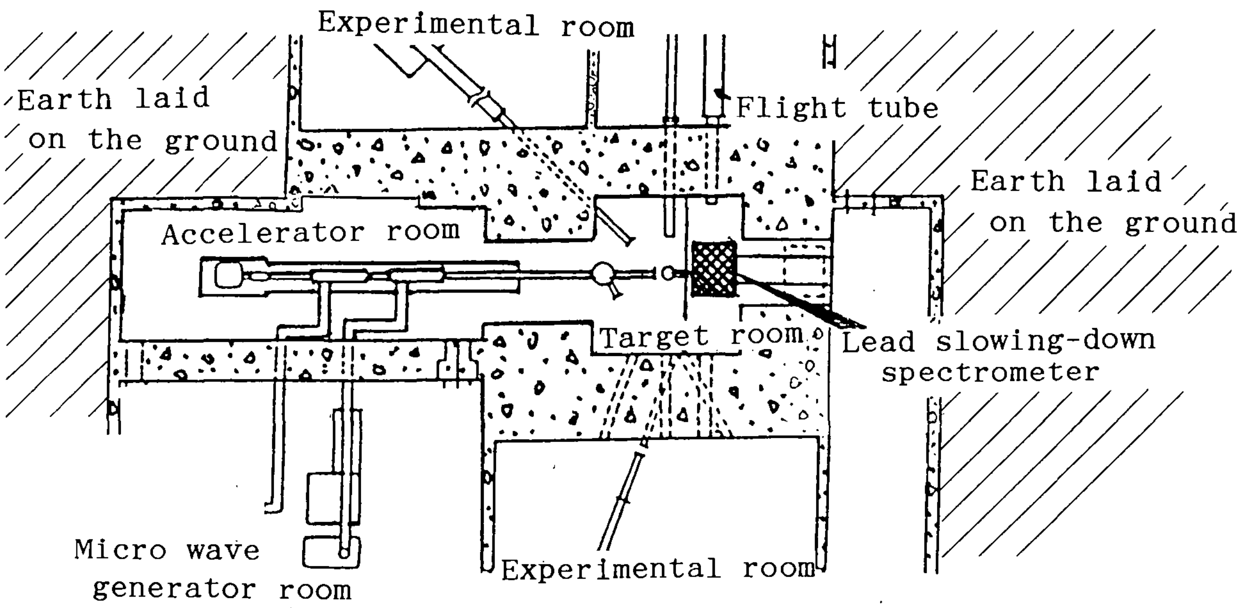

Fig. 1 Setting arrangement of the KULS at the KURRI linac.

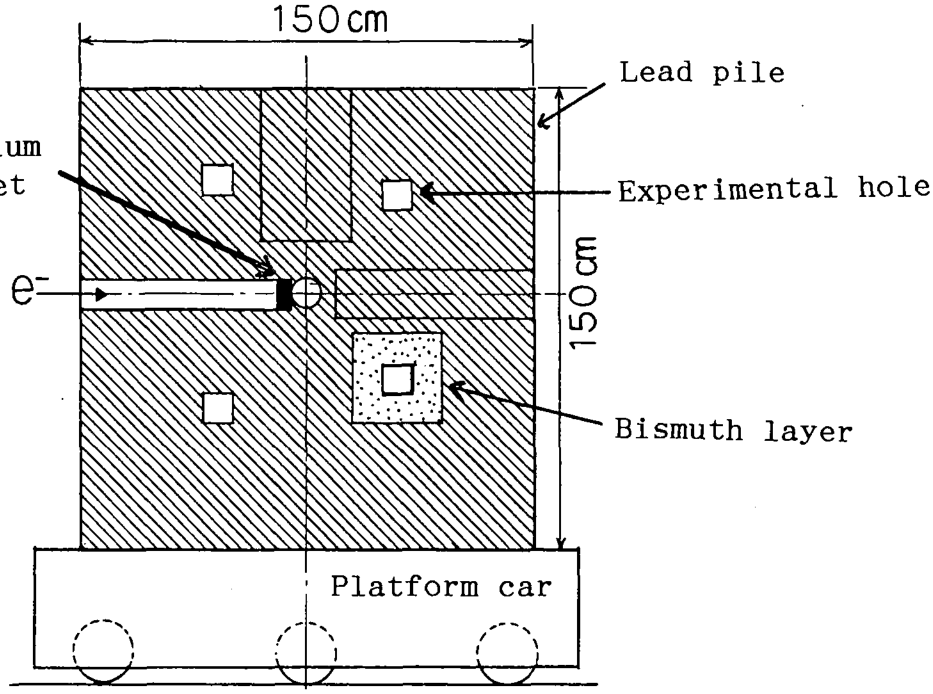

Fig. 2 The KULS on the platform car and the experimental holes, lead stringers and photoneutron target.

IV-B-5

Lead Slowing-Down Spectrometer Coupled to Electron Linac

--- Neutron Time Behavior in Lead ---

A. Yamanaka+, S. Kanazawa+, I. Kimura+,

K. Kobayashi, Y. Nakagome, S. Yamamoto and Y. Fujita

The lead slowing-down spectrometer, a cube of 1.5x1.5x1.5 m^3, has been installed by coupling to the 46 MeV electron linear accelerator at the Research Reactor Institute, Kyoto University, KURRI. The accelerator produces a short intense burst of photoneutrons at the center of the Kyoto University Lead slowing-down Spectrometer, KULS. The source neutrons are slowed down by elastic, inelastic or (n,2n) interactions with the lead nuclei. At energies from about 100 keV down to thermal neutrons, the inelastic, (n,2n) and neutron capture cross sections for lead are zero or negligibly small compared to the almost constant elastic scattering cross section of 11 barns. The neutron behavior in a lead spectrometer is represented adequately by the continuous slowing-down approximation, and the average neutron energy (in keV) is related to the expression[1)];

$$E = \frac{K}{(t_o + t)^2}$$

where t_o and K are the initial slowing-down correction time and the energy constant determined by the slowing-down time t (in

---

+ Dept. of Nucl. Eng., Fac. of Eng., Kyoto University
Yoshadahonmachi, Sakyo-ku, Kyoto 606, Japan

μ s), respectively.

In the present work, the constants K and t_o mentioned above and the energy resolving power of the KULS have been obtained by the resonance filter measurements. The Monte Carlo code MCNP[2] was also employed to calculate the slowing-down time and time dependent neutron behavior in the KULS.

The preliminary experiments to obtain the constants have been performed with BF_3 proportional counters covered with each of Mn, Co, Ta and Au neutron resonance filters. The spectral shape in neutron time-of-flight showed dips corresponding to the resonance peak energies, as seen in Fig. 1, as an example. The slowing-down time measured with the resonance filters showed a good linearity as a function of $1/\sqrt{E}$ (E is neutron energy in keV), as shown in Fig. 2. The energy constant K has been determined by the least squares fitting to these data. The result of the constant obtained is given in Table 1, comparing with those for other spectrometers.

The neutron behavior in the KULS has been also calculated with the MCNP code, and the relation between the average slowing-down time and the $1/\sqrt{E}$ function is close to that measured with the resonance filters, as shown in Fig. 2. The slowing-down time dependent neutron spectrum in the KULS is displayed in Fig. 3, and the time-integrated neutron spectrum is illustrated in Fig. 4.

The neutron energy resolving power of the KULS has been experimentally investigated by the resonance filter method. The deep dips derived from the filter measurements are broadened by the neutron energy spread and/or energy dispersion in the KULS.

The preliminary results of the energy resolution are 50 to 54 % from the measurement and 40 to 45 % from the calculation, as summarized in Table 2.

References:

1) R. E. Slovacek, et al., Nucl. Sci. Eng., 62, 455 (1977).

2) Los Alamos National Laboratory, "MCNP - A General Monte Carlo Code for Neutron and Photon Transport, Version 3A", LA-7396-M (1986).

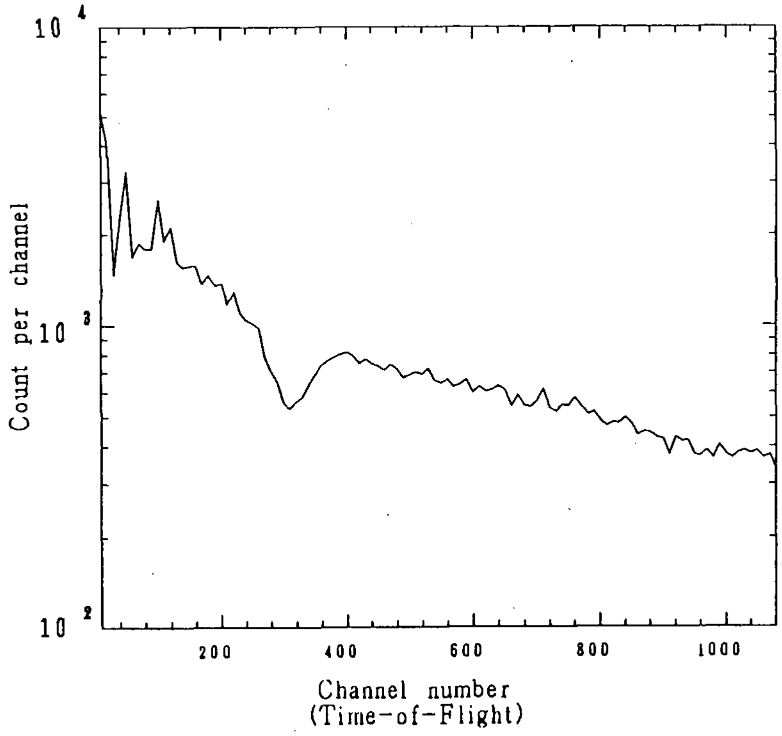

Fig.1 Slowing-down time measurement with resonance dips for Co sample.

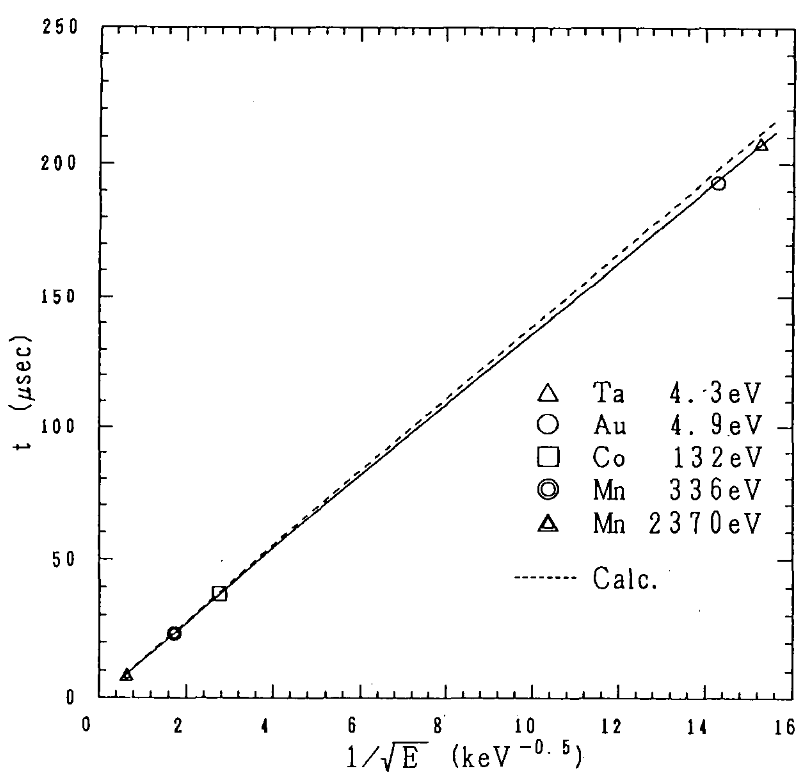

Fig.2 The calibration curve for the slowing-down times in the KULS.

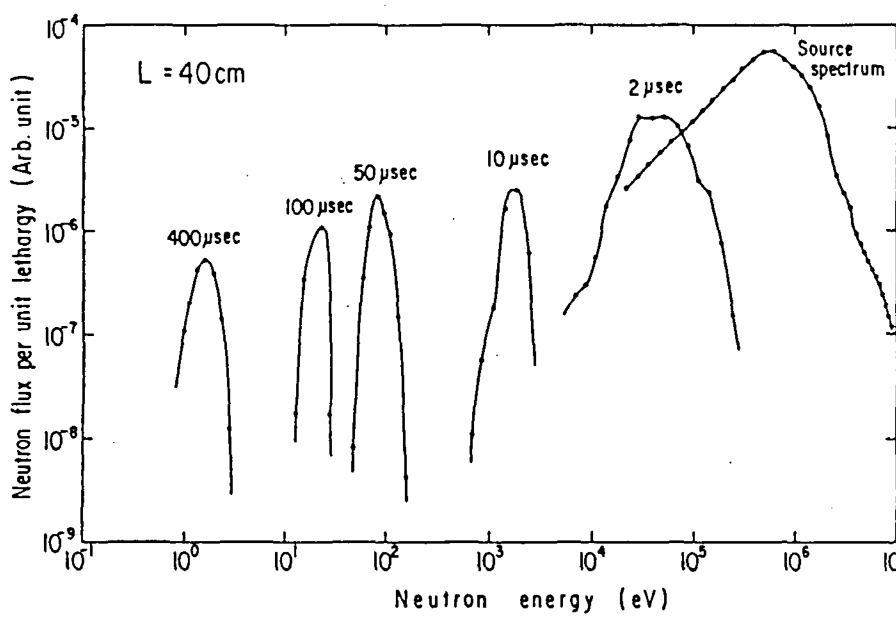

Fig.3 The slowing-down time dependent neutron spectrum in the KULS calculated by the MCNP code.

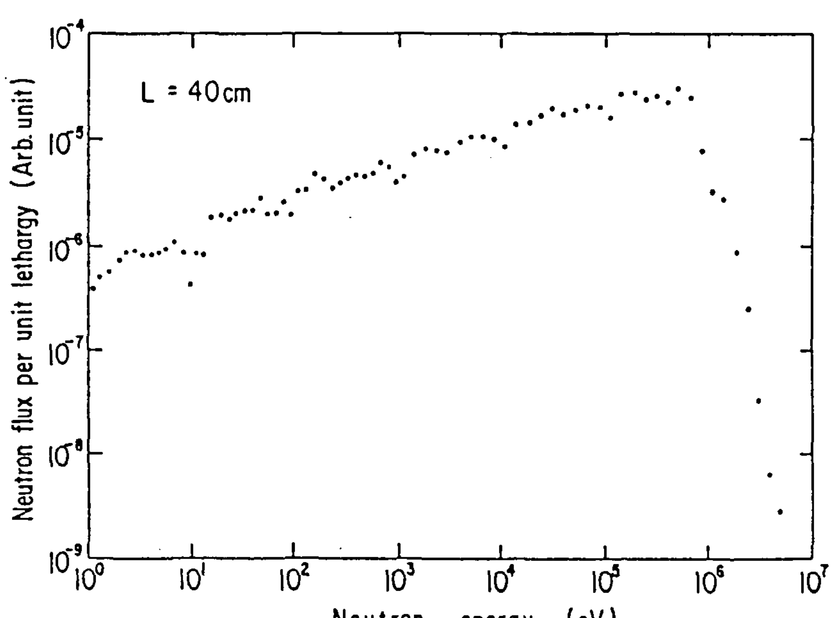

Fig.4 The time-integrated neutron spectrum in the KULS calculated by the MCNP code.

Table 1 Values of the energy constant K from several laboratories.

	Lead assembly	K(keV·μsec^2)
Present	1.5-m cube	184 ± 2
Present	MCNP Calc.	192
LESP	1.5-m cube	155
YAYOI	2.5-m octagon	74.7
RINS	1.8-m cube	165 ± 3
Bergmann	2 × 2 × 2.3 m^3	183

Table 2 Energy resolution (at FWHM) in the KULS.

Energy (eV)	Measurement(%)	Calculation(%)
4.9	54	40
132	50	44
336	52	44
2370	53	45

IV-B-6

Lead Slowing-Down Spectrometer Coupled to Electron Linac
--- Neutron Spectrum ---

K. Kobayashi, Li Zhaohuan*, Y. Fujita, S. Yamamoto, Y. Nakagome
A. Yamanaka+, I. Kimura+ and S. Kanazawa+

The Kyoto University Lead slowing-down Spectrometer, KULS was set up at the Research Reactor Institute, Kyoto University, KURRI and coupled to the 46 MeV KURRI electron linear accelerator. It is expected that the spectrometer can attain a strong neutron source intensity so that even a small cross section value and/or cross section with a small amount of sample material can be measured[1). We would like to apply this KULS to some minute cross section measurements as a spectrometer which gives a reference neutron spectrum field.

In the present work, as a part of the characteristics experimental series of the KULS, neutron spectrum in the KULS has been obtained by adjusting multi-foil activation data using the SAND-II type code, NEUSPEC[2). This code has a sub-program which generates uncertainties in the neutron flux spectrum with the Monte Carlo method. As seen in Table 1, 14 kinds of activation reactions were employed to obtain the neutron spectrum, which was

---

* Visiting scientist from Institute of Atomic Energy, Beijing, China.
+ Dept. of Nucl. Eng., Fac. of Eng., Kyoto University, Yoshidahonmachi, Sakyo-ku, Kyoto 606, Japan

measured at the irradiation position distant 15 cm from the photoneutron target at the center of the KULS. The cross section data for the NEUSPEC calculations were taken from JENDL-3 dosimetry file, which was generated as 642 groups cross sections, similar to the IRDF-85 data library. The initial neutron spectrum used for the present analysis was obtained by using the Monte Carlo code MCNP.

The neutron spectrum obtained is shown in Fig. 1, together with the uncertainty width, which was produced by the standard deviation of the foil activation data and by the variance of the cross section data used. By the Cd ratio measurements using Au and Mn foils, it was found that there exist scarcely thermal neutrons in the KULS, as observed in Fig. 1.

References:

1) R. E. Slovacek, et al., Nucl. Sci. Eng., 62, 455 (1979).

2) Li Zhaohuan, et al., Proc. of the 7-th ASTM-Euratom Symp. on Reactor Dosimetry held on 27-31 Aug. 1990, at Strasbourg, France.

Table 1 Nuclear Reactions and activation data used for the present work.

No	Reaction Type	$T_{1/2}$	Reaction Rate*10^{20}	Uncertainty (%)
1	$^{197}Au(n,\gamma)^{198}Au$	2.696d	45882.2	3.11
2	$^{55}Mn(n,\gamma)^{56}Mn$	2.676h	2299.75	3.06
3	$^{59}Co(n,\gamma)^{60}Co$	5.27 y	6302.87	3.30
4	$^{187}W(n,\gamma)^{187}W$	23.85h	20299.1	3.30
5	$^{24}Mg(n,p)^{24}Na$	15.02h	10.9195	4.91
6	$^{27}Al(n,p)^{27}Mg$	9.46m	26.9827	5.98
7	$^{27}Al(n,\alpha)^{24}Na$	15.02h	5.3125	3.63
8	$^{46}Ti(n,p)^{46}Sc$	83.80d	75.6741	9.86
9	$^{47}Ti(n,p)^{47}Sc$	3.422d	243.426	4.57
10	$^{48}Ti(n,p)^{48}SC$	43.67h	2.8025	7.50
11	$^{58}Ni(n,p)^{58}Co$	70.787d	721.384	3.26
12	$^{54}Fe(n,p)^{54}Mn$	312.2d	534.498	8.56
13	$^{64}Zn(n,p)^{64}Cu$	12.70h	417.486	3.45
14	$^{115}In(n,p)^{115m}In$	4.486h	2429.76	5.61

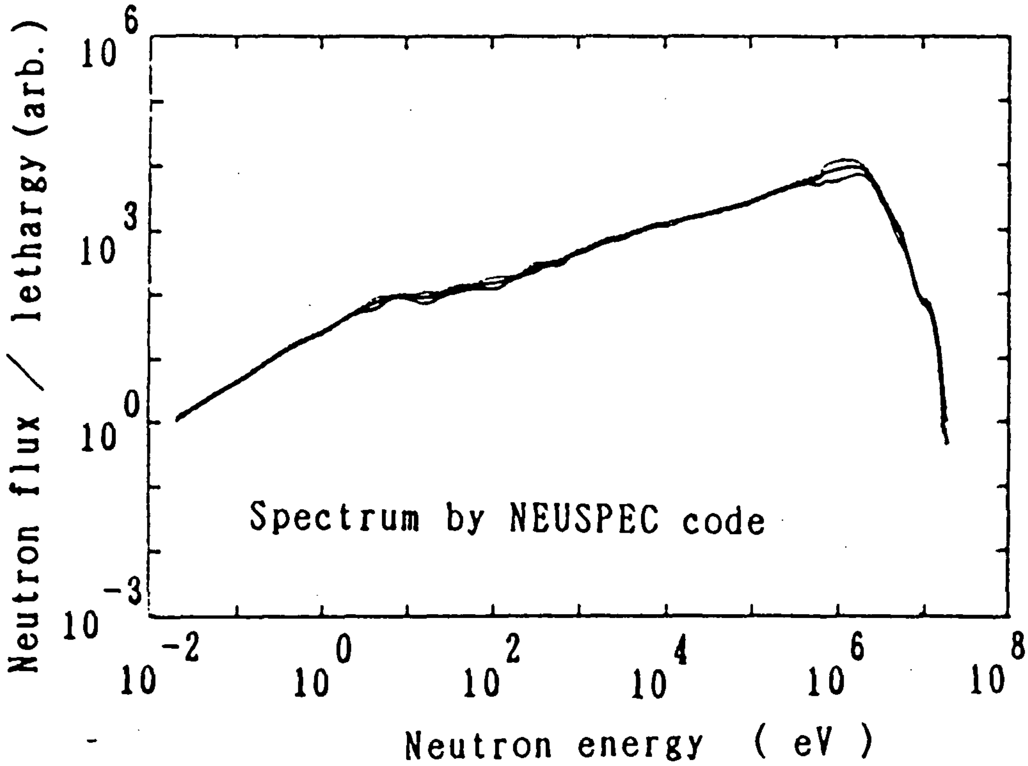

Fig. 1 Neutron spectrum unfolded with multi-foil activation data using NEUSPEC code.

V. Kyushu University

A. Department of Energy Conversion Engineering

Interdisciplinary Graduate School of Engineering Sciences

V-A-1 NEW PERSPECTIVE IN COVARIANCE EVALUATION FOR NUCLEAR DATA

Y. Kanda

A paper on this subject will be presented in the Proceedings of the International Conference on Nuclear Data for Science and Thechnology (13–17, May, 1991 at Jülich, Federal Republic of Germany), with the following abstract :

Methods of nuclear data evaluation have been highly developed during the past decade, especially after introducing the concept of covariance. This makes it utmost important how to evaluate covariance matrices for nuclear data. It can be said that covariance evaluation is just the nuclear data evaluation, because the covariance matrix has quantitatively decisive function in current evaluation methods. The covariance primarily represents experimental uncertainties. However, correlation of individual uncertainties between different data must be taken into account and it can not be conducted without detailed physical considerations on experimental conditions. This procedure depends on the evaluator and the estimated covariance does also. The mathematical properties of the covariance have been intensively discussed. Their physical properties should be studied to apply it to the nuclear data evaluation, and then, in this report, are reviewed to give the base for further development of the covariance application.

V-A-2 Application of Bayes Method to Optical Model Parameter Estimation for ^{209}Bi in Low Energy Region

T. Kawano and Y. Kanda

A paper on this subject was presented in J. Nucl. Sci. Tech. **28** (1991) 156.

A new application technique of the Bayes method is developed to estimate optical model parameters and to investigate energy dependence of the optical model parameters. A demonstration is made for ^{209}Bi, with the angular distribution of elastic scattering and an evaluated total cross section. Because, ^{209}Bi is generally treated as a spherical nucleus and has relatively high level density near the neutron binding energy.

The estimated real and imaginary potential parameters are expressed as volume integrals par nucleon (J_v, J_w), and below 3.5 MeV, their energy dependencies are different with ones deduced in higher energy region. The potential strengths for both real and imaginary part decrease when neutron energy approaches to zero.

V-A-3 Estimation of Optical Model Parameters at Few-MeV Energy Region

Toshihiko Kawano, Hiroya Tanaka, Kohta Kamitsubo

and Yukinori Kanda

A paper on this subject was presented at the 1990 Seminar on Nuclear Data, and published in JAERI-M 91-032, p.355, with the following abstract :

Optical model parameters for ^{59}Co, ^{58}Ni, and ^{60}Ni have been estimated by statistical method based on the Bayes' theorem, and energy dependencies of the parameters have been investivated at few-MeV energy region. A successful reproduction of differential elastic scattering cross section and total cross section has been achieved by energy dependent potential.

The tendencies of estimated parameters are similar to those reported for the global parameters in high energy region, however, the parameters show large energy dependencies in low energy region.

V-A-4 Estimation of Nuclear Reaction Model Parameters for ^{59}Co, ^{58}Ni, and ^{60}Ni

Toshihiko Kawano, Hiroya Tanaka, Kohta Kamitsubo and Yukinori Kanda

A paper on this subject will be presented in the Proceedings of the International Conference on Nuclear Data for Science and Thechnology (13–17, May, 1991 at Jülich, Federal Republic of Germany), with the following abstract :

Optical model parameters for ^{59}Co, ^{58}Ni, and ^{60}Ni have been estimated by a statistical method based on the Bayes' theorem, and energy dependencies of the parameters have been investivated at few-MeV energy region. A successful reproduction of differential elastic scattering cross section and total cross section has been achieved by energy dependent potential. The tendencies of the estimated parameters are similar to those reported for the global parameters in high energy region, however, the parameters show large energy dependencies in low energy region.

The estimated optical model parameters were used to Hauser-Feshbach calculation, and level density parameters were estimated by the statistical method in order to inspect consistency among the reaction model the parameters, and the measurements.

V-A-5 Systematic Measurement of Continuum (p,p') Spectra for Medium-Heavy Nuclei in the 12-18 MeV Region

Y. Watanabe, N. Koori*, M. Hyakutake** and I. Kumabe+

A paper on this subject was submitted to the International Symposium on Nuclear Physics, Nuclear Reaction Mechanism, Gaussig, Germany, November 12-16, 1990, with the following abstract:

Continuum (p,p') spectra were measured systematically for medium-heavy nuclei in the incident energy range from 12 to 18 MeV in order to investigate shell and odd-even effects of the target nucleus on preequilibrium proton emission and mass number and incident energy dependence. Some results of the exciton model analysis are reviewed.

* Present Address: College of General Education, The University of Tokushima, Tokushima 770

** Present Address: Sasebo Technical College, Sasebo

+ Professor Emeritus, Kyushu University

V-A-6 **Measurement of Double Differential Cross Sections of 25.6 MeV (p,xp) and (p,xd) Reactions on ^{98}Mo**

Yukinobu WATANABE, Akira AOTO and Hiroki HANE

A paper on this subject was submitted to Tandem ANNUAL REPORT 1990, Japan Atomic Energy Research Institute.

We have measured double differential cross sections of 25.6 MeV (p,xp) and (p,xd) reactions on ^{98}Mo in order to investigate preequilibrium process in nucleon-induced reactions. This work is an extension of investigation on the preequilibrium process in proton-induced reactions at incident energies of 10 to 20 MeV that have so far been made in Kyushu University[1]. Our interest is simultaneous analysis of (p,xp), (p,xd), and (p,xn) spectra for the same target nucleus and incident energy using the preequilibrium model such as the exciton model and the SMD/SMC model[2]. Note that the ^{98}Mo(p,xn) spectra for 25.6 MeV have already been measured by the other group[3]

The experiment was performed using a 25.6 MeV proton beam from the JAERI tandem accelerator. The proton beam was transported in a scattering chamber 50 cm ϕ which was newly installed in N1 beam line. The beam intensity was monitored by means of a current integrator connected to a Faraday cup: the beam current was from about 50 nA to 150 nA. A target of ^{98}Mo was a self-supporting metallic foil whose thickness and enrichment were 0.45 mg/cm^2 and 97.1%, respectively.

A charged particle detecting system consists of a ΔE-E counter telescope of two silicon surface barrier detectors having thickness of 200 μm and 5000 μm, respectively. A defining aperture 2.5 mm in diameter was placed just in front of the ΔE detector and was located 147 mm from the target. The electronic equipments used were standard commercially available

NIM modules. Energy spectra of emitted protons and deuterons were measured at six angles of 30°, 40°, 60°, 90°, 120°, and 150°.

Measured double differential proton emission cross sections are shown for 40°, 90°, and 120° in Fig.1. The angular distributions are peaked forward in the continuum region between 10 and 20 MeV. This result suggests that the preequilibrium process or the direct process is dominant in this energy region. Figure 2 shows experimental energy spectra of deuterons emitted into 30°, 60°, and 120°. Compared with the proton spectra, stronger forward-peaked angular distributions are observed at outgoing energies of 10 to 18 MeV. Bump structure are also exhibited around 15 MeV at the forward angle.

The (p,xp) spectra were analyzed preliminarily on the basis of the exciton model in which isospin conservation was taken into account. The same model parameters as in our previous analysis[4] were employed and a modified version[5] of Kalbach -Mann systematics was applied to calculations of angle-dependent energy spectra. The calculated result is shown by solid lines in Fig.1. The calculated spectra underestimate the experimental ones for 40° and 90°. Simultaneous analysis of proton, deuteron and neutron spectra is now in progress.

References

1) Y. Watanabe et al., *Proceedings of the 1989 Seminar on Nuclear Data*, JAERI-M 90-025, p 216.

2) H. Kalka, Phys. Rev. C **40**, 1619 (1989).

3) E. Mordhorst et al., Phys. Rev. C **34**, 103 (1986).

4) Y. Watanabe et al., Z. Phys. A **336**, 63 (1990).

5) I. Kumabe et al., Nucl. Scie. and Eng. **104**, 280 (1990).

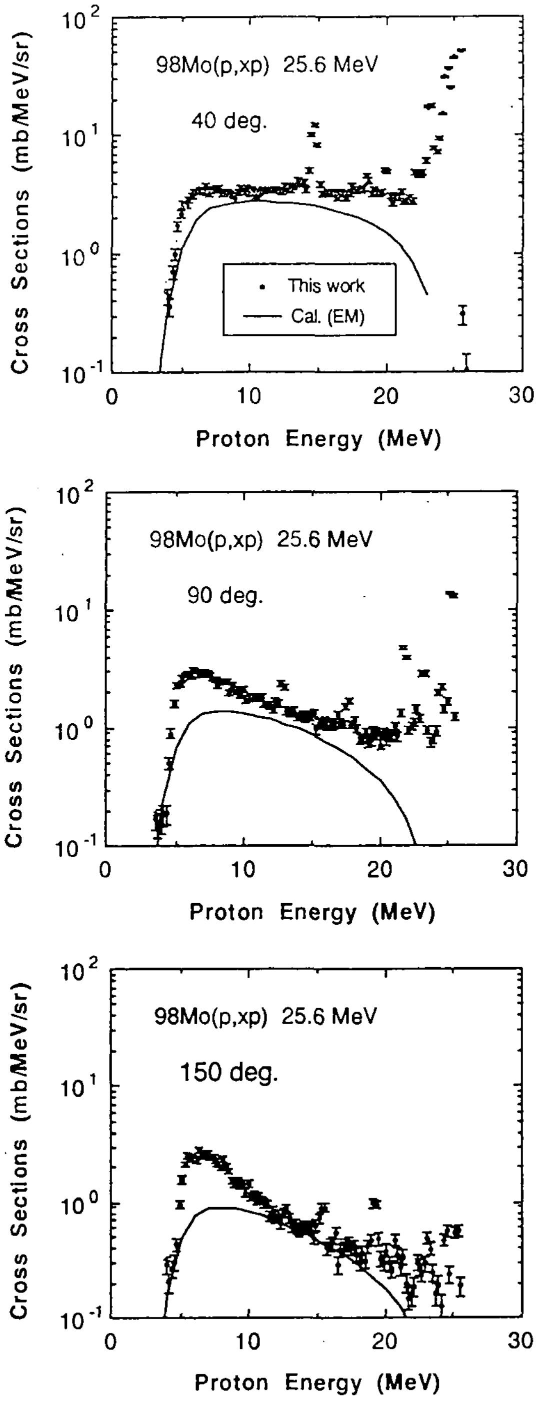

Fig.1 Comparisons of measured double differential proton emission cross sections for ^{98}Mo at 25.6 MeV and those calculated on the basis of the exciton model.

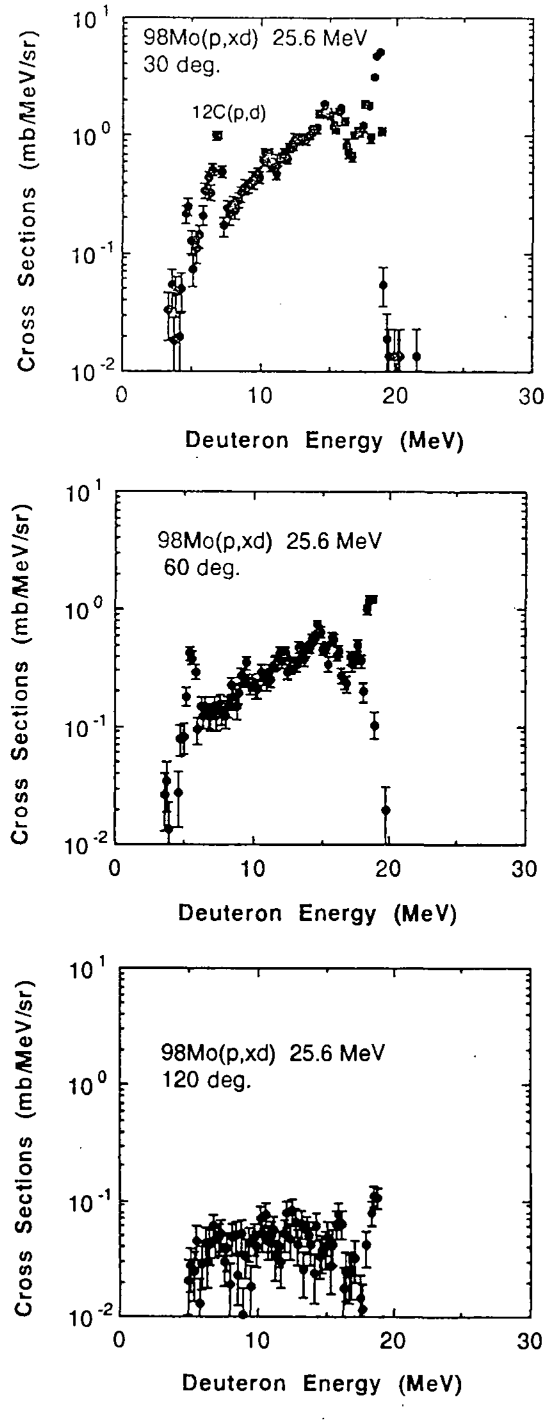

Fig.2 Measured double differential deuteron emission cross sections for ^{98}Mo at 25.6 MeV

B. Department of Nuclear Engineering

Faculty of Engineering

V-B-1 Evaluation of Neutron-Emission Cross Section for Spallation Reactions

K. Ishibashi, K. Higo, S. Sakaguchi, Y. Wakuta

H. Takada*, T. Nishida*, Y. Nakahara* and Y. Kaneko*

A study on this subject was presented at the International Conference on Nuclear data for Science and Technology, May 13-17, 1991, Julich, Federal Republic of Germany. The title and abstract are as follow:

Title

Systematic Evaluation of Neutron-Emission Cross Section for the Reactions Induced by Protons of 80-800 MeV.

Abstract

A moving source model uses a relatively small number of parameters. The neutron data for the spallation reactions induced by protons of 600 to 800 MeV are well reproduced by the moving source model. At incident energies below 400 MeV, however, the use of this model leads to an unsuccessful result. A new idea of a double moving source model is introduced in the lower energy region. The combination of the two models enables us to parameterize the double differential cross sections of neutron emission for incident protons of 80 to 800 MeV.

---

* Japan Atomic Energy Research Institute

V-B-2 Spallation Neutron Measurement

K. Ishibashi, K. Maehata, Y. Wakuta, Y. Watanabe, Y.Matsumoto*,
Y. Yoshimura**, M. Numajiri**, H. Takada*** and I. Kanno***

For the nuclear data in the spallation region, an incident energy around 1 GeV is of particular interest in the nuclear engineering. It is desirable to make use of the KEK 12-GeV proton synchrotron. The accelerator is capable of supplying protons of this energy at a secondary beam line coming from its internal target.

It is not clear how this beam line is suited for neutron measurement for the nuclear data or what is the best experimental method with regard to neutron background appearing in the experimental hall. The authors carried out a preliminary measurement of the neutron-emission cross section by the use of protons of 1.5 GeV at KEK. Figure 1 shows a typical result of TOF spectrum at 30 deg. The data analysis is to be made to seek the method suitable for performing a complete measurement.

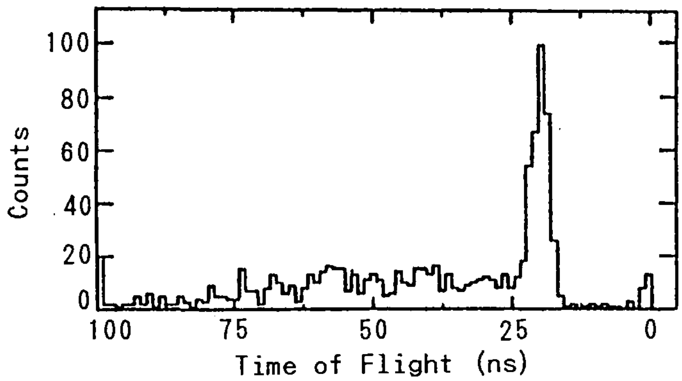

Fig. 1 Neutron TOF spectrum including γ ray flash.

* Kyushu Teikyo Junior College

** National Laboratory for High Energy Physics (KEK)

*** Japan Atomic Energy Research Institute

VI. Nagoya University

A. Department of Nuclear Engineering

Faculty of Engineering

VI-A-1 Measurement of Half-lives of Short-lived Nuclei

H. Yamamoto, K. Kawade, T. Katoh, A. Hosoya,
M. Shibata, A. Osa, T. Iida* and A. Takahashi*

A paper on this subject was submitted to The International Conference on Nuclear Data for Science and Technology held at Jülich on May 13-17. 1991 with the following abstract.

In case of half-life measurement of short-lived nuclei, the counting rate changes remarkably during the measuring time. The purpose of the present study is to establish a proper method of correction for the dead time and pile-up by using a pulser method(signals from a pulser are counted simultaneously at the measurement) and a standard radiation source method(gamma-rays from a standard source are counted at the time of measurement), and to measure the half-lives of short-lived nuclei($T_{1/2}$ = 1 - 15 m) produced by thermal or 14 MeV neutron irradiation precisely. The 14 MeV neutron source is the Intense 14 MeV Neutron Source(OKTAVIAN) of Osaka University. The TRIGA type reactor of Rikkyo University was used for the thermal neutron irradiation. Pneumatic tubes were used for the sample transfer at the 14 MeV Neutron Facility. Gamma-rays from produced short-lived nuclei were measured by Ge detectors. The decay of gamma-ray intensities were recorded by the multi-scaling method. Half-lives of short-lived nuclei, ^{51}Ti, ^{60m}Co, ^{89m}Zr, ^{91m}Mo, ^{97m}Nb, ^{104m}Rh, ^{108}Ag, ^{109m}Pd, ^{53g}Fe, ^{62m}Co and ^{91g}Mo were determined experimentally within 0.1 percent accuracy.

* Osaka University

VI-A-2 Measurement of Formation Cross Section of Short-lived Nuclei by 14 MeV Neutrons

K. Kawade, H. Yamamoto, T. Katoh, A. Taniguchi,
T. Ikuta, Y. Kasugai, T. Iida* and A. Takahashi*

A paper on this subject was submitted to The International Conference on Nuclear Data for Science and Technology held at Jülich on May 13-17, 1991, with the following abstract.

Acivation cross sections for the reactions leading to short-lived nuclei with half-lives between 0.5 and 20 m have been measured systematically to provide more reliable data required for fusion reactor technology by the acivation method. Up to now, 52 cross sections for the (n,2n), (n,p), (n,n'p), (n,t) and (n,α) reactions have been obtained relative to the standard cross section of $^{27}Al(n,\alpha)^{24}Na$ in the energy range of 13.4 to 14.9 MeV for N, Mg, Al, Si, P, S, Cl, Ti, V, Cr, Mn, Fe, Ni, Cu, Zn, Ga, Rb, Sr, Y, Zr, Mo, Ag and In. The D-T neutrons were generated by an intense 14 MeV neutron source facility (OKTAVIAN) at Osaka University. Some attention was paid to measure gamma-rays efficiently in a short time and positron emitters. The correction were made for contribution of low energy neutrons below 10 MeV, time fluctuation of neutron flux, thickness of sample, self-absorption of gamma-ray, sum peak effect of gamma-ray and contribution of interfering reactions. The total errors were within 3.6 %

* Osaka University

when good counting statistcs were acieved. A discussion of the systematic trends of the cross sections of short-lived nuclei at around 14 Mev neutron energy is given in comparison with those of long-lived nuclei.

VII. Nuclear Energy Data Center

A. Computer Code Development Section I

VII-A-1

On Application of the S-Matrix Two-Point Function to Nuclear Data Evaluation

S. Igarasi

A paper on this subject was submitted to the International Conference on Nuclear Data for Science and Technology, held at Jülich, 13 - 17 May, 1991.

Abstract: Statistical model calculation using S-matrix two-point function (STF) was tried. The results were compared with those calculated with the Hauser-Feshbach formula (HF) with and without resonance level-width fluctuation corrections (WFC). The STF gave almost the same cross sections as calculated using Moldauer's degrees of freedom for the χ^2-distributions (MCD). The effect of the WFC to the final states in continuum was also studied using the HF with WFC of the MCD and of Porter-Thomas distribution (PTD). The HF with the MCD is recommended for practical calculation of the cross sections.

VIII. Rikkyo (St. Paul's) University

A. Department of Physics, Faculty of Science

VIII-A-1

Measurements of the Neutron Emission Cross Sections of ^{nat}C and ^{nat}Fe for 14.1 MeV Incident Neutrons

S. Shirato, K. Hata* and Y. Ando

Double differential cross sections (DDX) for elastic and inelastic neutron scattering from ^{nat}C and ^{nat}Fe at 14.1 MeV, which were measured at forward angles from 10^{o} to 50^{o} in 10^{o} increments using the neutron time-of-flight (TOF) facility of the 300 kV Cockcroft-Walton accelerator of Rikkyo University, have been preliminarily analysed[1].

Neutron TOF spectra were obtained from the signals of scattered neutrons and the associated α-particles produced in the $^{3}H(d,n)^{4}He$ reaction at 165 keV, using an NE213 liquid scintillator of 2 in ϕ x 2 in for the neutron detector and a thin (50 μm) NE102A plastic scintillator for the α-particle detector[2]. The cylindrical scattering samples of 3 cm ϕ x 3 cm were made of natural graphite and iron of 99.9 % purity. We are still performing the measurement of neutron TOF spectra with a large NE213 scintillator of 10 cm ϕ x 30 cm in order to improve the statistical errors and to obtain cross sections relative to the absolute ones measured with the 2 in ϕ x 2 in detector[1,3].

---

* Present address: Hitachi Seisakusho Co.

The measured energy spectra of scattered neutrons for ^{nat}C and ^{nat}Fe should be reported in the near future in comparison with the theoretical curves[4] based on JENDL-3T, for example, as shown in figs. 1-a and 1-b.

Measured angular distributions for elastic scattering are in good agreement with optical model calculations, as seen in figs. 4 and 6 of ref. 1.

The results of the preliminary analyses of measured differential cross sections for inelastic neutron scattering from the first excited states of ^{12}C and ^{56}Fe using the exact finite-range DWBA have been shown in figs. 5 and 7 of ref. 1. The result of the DWBA reanalysis for the reaction $^{12}C(n,n')^{12}C^{*}$(1st) is in agreement with experimental data[1,5,6,7,8] as shown in fig. 2, indicating the deformation parameter β_2 = 0.65 in agreement with the value of Olsson et al.[9] Consequently, fig. 5 of ref. 1 should be replaced by fig. 2 of this paper. It is noted that the optical potential parameters of the exit channel in this reaction for ^{12}C, as given in table 1, are somewhat different from those[5] of the entrance channel. The DWBA calculation for the reaction $^{56}Fe(n,n')^{56}Fe^{*}$(1st) shows the deformation parameter β_2 = 0.23 using the potential parameters[1] of Hyakutake et al.[10] without changing those of the exit channel.

References:

1) K. Hata, S. Shirato and Y. Ando, JAERI-M 91-032, 328 (1991).

2) S. Shirato, S. Shibuya, Y. Ando, T. Kokubu and K. Hata, Nucl. Instr. Methods A278, 477 (1989).

3) K. Hata, S. Shirato and Y. Ando, JAERI-memo 02-308 (1990).

4) T. Fukahori and I. Tazaki, JAERI-memo 62-453 (JAERI, 1988).

5) K. Gul, M. Anwar, M. Ahmad, S. M. Saleem and N. A. Khan, Phys. Rev. C24, 2458 (1981).

6) R. Bouchez, J. Duclos and P. Perrin, Nucl. Phys. 43, 628 (1963).

7) D. W. Glasgow et al., Nucl. Sci. Eng. 61, 521 (1978).

8) G. Haouat et al., Nucl. Sci. Eng. 65, 331 (1978).

9) N. Olsson, B. Trostell and E. Ramstrom, Nucl. Phys. A496, 505 (1989).

10) M. Hyakutake et al., J. Phys. Soc. Japan 38, 606 (1975).

Table 1 Optical potential parameters for the reaction $^{12}C(n,n')^{12}C^*(1st)$. $[U_C(r) = 0]$

	V (MeV)	W_s (MeV)	V_{so} (MeV)	r_0 (fm)	r_0' (fm)	a (fm)	b (fm)	Ref.
Entrance channel:								
	46.5	8.88*	4.39+	1.28	0.86	0.39	0.39	5)
Exit channel:								
	55.0	2.60*	4.39+	1.20	0.86	0.39	0.39	

V: Real volume Woods-Saxon potentials with range parameters r_0 and a.

W_s: Imaginary surface Woods-Saxon potential with range parameters r_0' and b.

* Note $W_s = V_I/4$ using the DWUCK4 notation.

\+ Note $V_{so} = V_{LS}/4$ in the $\underline{l}$-$\underline{\sigma}$ form using the DWUCK4 notation.

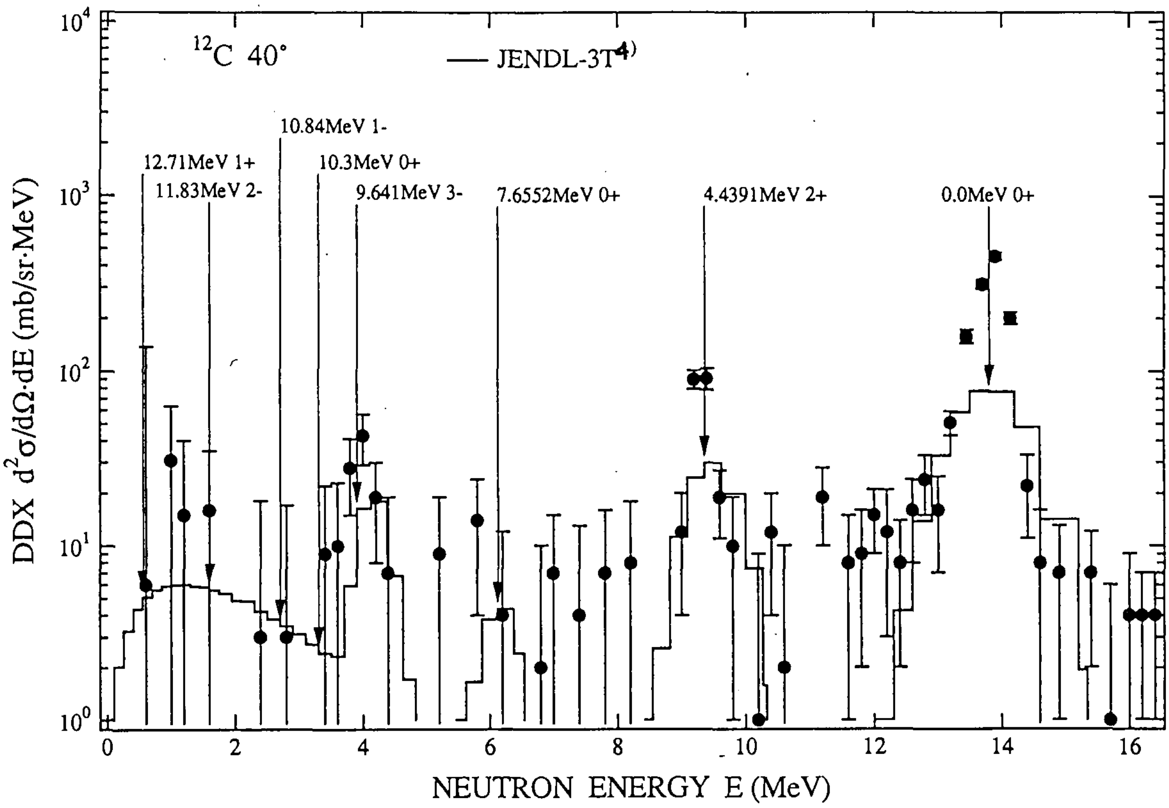

Fig. 1-a Measured and calculated[4)] double differential cross sections for 14.1 MeV neutron scattering from ^{12}C at 40°.

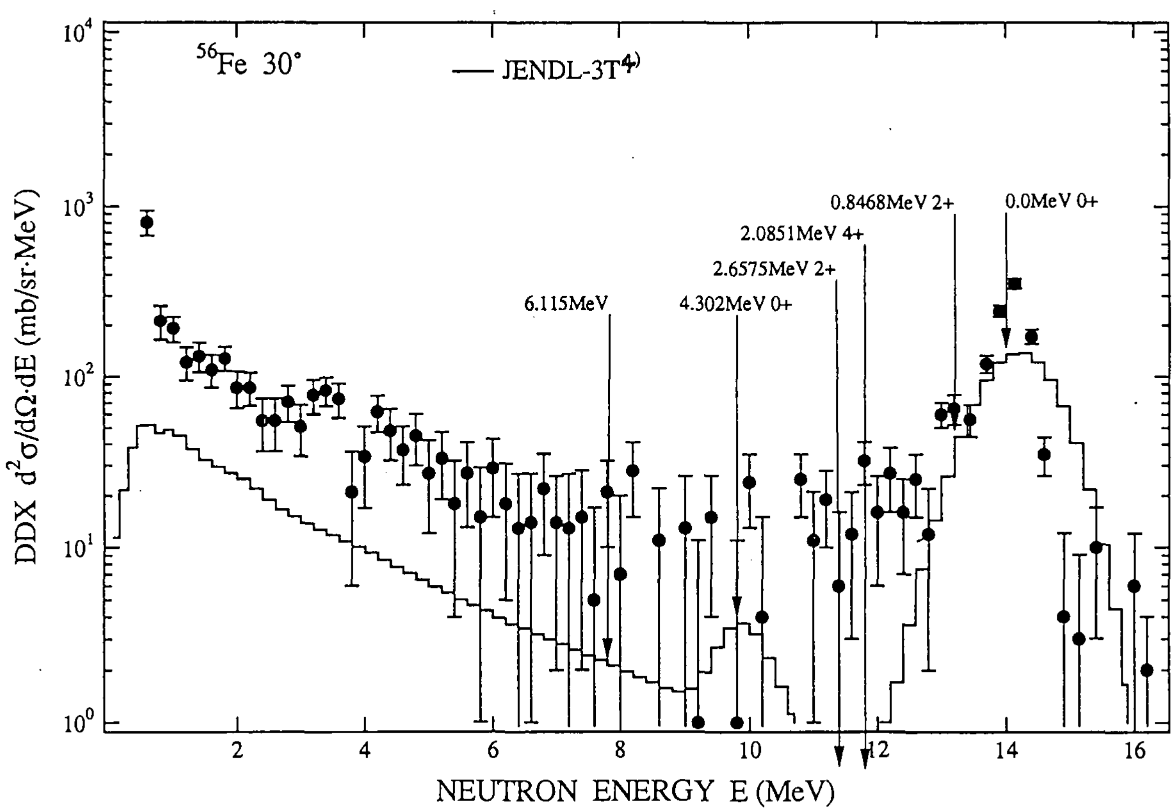

Fig. 1-b Measured and calculated[4)] double differential cross sections for 14.1 MeV neutron scattering from ^{56}Fe at 30°.

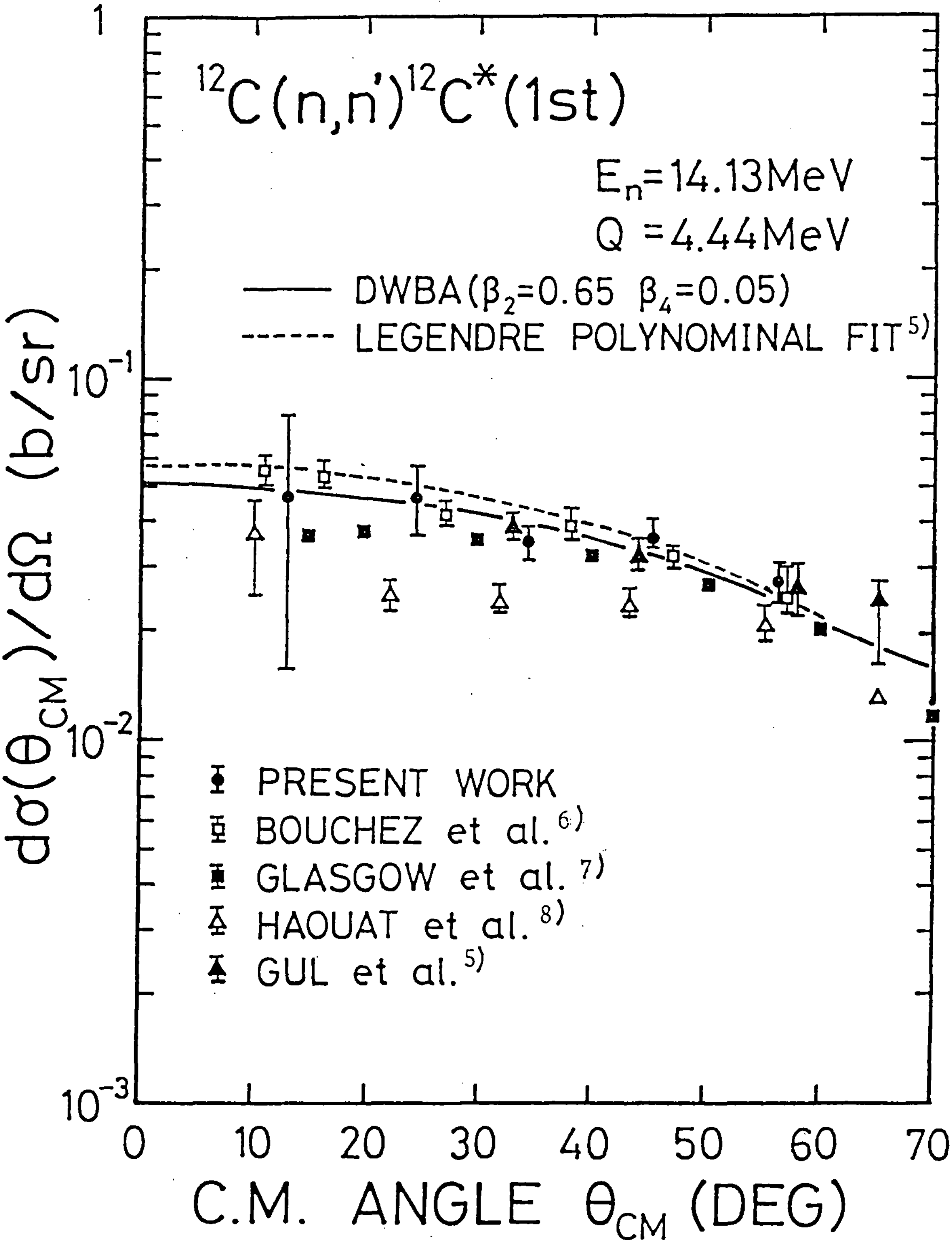

Fig. 2 Measured and calculated angular distributions for inelastic neutron scattering from $^{12}C^*$(1st).

IX. Tohoku University

IX-A-1

RECENT AND PLANNED EXPERIMENTS ON NEUTRON TRANSMISSION AND CROSS SECTIONS USING p-Li MONOENERGETIC NEUTRONS

Takashi Nakamura, Toshio Ishikawa and Yukio Miyama

and

Susumu Tanaka*, Shun-ichi Tanaka** and Ryuichi Tanaka*

ABSTRACT

The neutron transmission experiment through iron and concrete which are commonly used as shielding materials has been performed using monoenergetic neutron beams of 33 and 22 MeV which are produced from 2 mm thick Li target bombarded by 35 and 25 MeV protons extracted from the AVF cyclotron (K=50). The neutron energy spectra penetrated through materials were measured with NE-213 scintillator, proton-recoil proportional counter and multi-moderator ^{3}He spectrometer. The attenuation profiles of monoenergetic peak neutrons can be used as the integral check of the cross section data above 20 MeV.

The further experiments on neutron transmission and reaction cross sections are planned by our research group in the AVF cyclotron (K=110) facility. The monoenergetic neutrons in the energy range of 20 to 90 MeV can be obtained by ^{7}Li(p,n) reaction.

---

* Japan Atomic Energy Research Institute
Takasaki Establishment, Watanuki-cho, Takasaki, Gunma 370-12
** Japan Atomic Energy Research Institute
Tokai Establishment, Tokai-mura, Naka-gun, Ibaraki 319-11

1. Introduction

In recent years, high intensity and energy accelerators are being built and planned with the rapidly growing radiation application. This accompanies the increasing importance of radiation shielding design of the accelerator facility, especially for high energy neutrons having strong penetrability. The shielding calculation requires a comprehensive knowledge of nuclear data related to neutron and photon production by charged particles, neutron and photon transmission through matter, neutron scattering and activation and so on. These data above 20 MeV are scarce and no evaluated data library on neutron cross sections presently exists.

As for the shielding study on neutrons above 20 MeV, a few experiments have been reported using continuous energy(white) neutron sources [1,2]. We measured the neutron penetration through iron and concrete shielding materials with the 33 MeV and 22 MeV monoenergetic neutron beams. Neutrons were produced from 2-mm thick ^{7}Li target bombarded by 35 and 25 MeV protons extracted from the AVF cyclotron (k=50) at the Cyclotron and Radioisotope Center(CYRIC), Tohoku University.

We have made a research plan of the further experiment on neutron transmission and reaction cross sections in the AVF cyclotron (k=110) at theTIARA(Takasaki Ion Accelerator for Advanced Radiation Application) facility, Japan Atomic Energy Research Institute. Monoenergetic neutrons in the energy range of 20 to 90 MeV can also be obtained by the ^{7}Li(p,n) reaction. Differently from other monoenergetic p-Li neutron facilities [3-6], our neutron facility is put on stress for taking the experimental data to be incorporated in nuclear data base necessary for shielding study.

2. Neutron Transmission Experiment at CYRIC

2-1 Experimental Procedure

Figure 1 shows the cross sectional view of the experimental arrangement along the neutron beam line. A 35-MeV or 25-MeV proton beam extracted from the AVF cyclotron was stopped on the Li target(103 mg/cm^2 thickness) in the No.5 target room. Through two collimators, neutrons were incident to the shield which was set at the hole(50 cm height, 100 cm width and 283 cm length) in the concrete wall between the No. 5 target room and the TOF room. As seen in Fig. 1, we injected a proton beam to the Li target at an angle of 10 deg to the horizontal axis by the beam swing magnet, in order to prevent neutrons produced at the Faraday cup(proton beam stop) from the direct incidence into the collimator. We repeated the same measurements without the Li target to estimate the background components due to neutrons scattered on the concrete wall of the No.5 target room.

The source neutron energy spectrum produced from the Li target without the shield was measured with the 5.1-cm diam. by 5.1-cm long NE-213 scintillator by the TOF method. Shielding materials used in the experiment were iron(10, 20, 30 and 40 cm thickness) and concrete(25, 50, 75 and 100 cm thickness). The neutrons penetrated through the shield were measured with the same NE-213 scintillator, the 7.0-cm diam. spherical proton recoil proportional counter(hydrogen 4.5 atm and methan 0.5 atm) and the multi-moderator spectrometer with a 10-atm ^{3}He counter, i.e., Bonner Ball [7].

The neutron energy spectra penetrated through the shield were obtained by subtracting the background and unfolding the measured data with the FERDOU code [8] for the NE-213, the FERDOR code [9] for the proportional counter and the SAND-II code [10] for the Bonner Ball.

2-2 Results and Discussion

The source neutron spectra for 35 MeV and 25 MeV protons are shown in Figs. 2 and 3, respectively. The spectra have a monoenergy peak whose energy is 32.6 MeV and 21.8 MeV and FWHM is 1.4 MeV and 1.7 MeV, respectively. They have low energy continuum and a small peak of energy 4.6MeV lower than the peak energy which corresponds to the neutron emission from the second excited state of ^{7}Be.

The neutron spectra measured behind 30 cm thick iron and 75 cm thick concrete are shown in Figs. 4 and 5, respectively. The initial guess spectra of the SAND-II unfolding for the Bonner Ball were obtained from the calculation with the MORSE-CG code [11]. In the figures, the measured neutron energy ranges were above 2 MeV for the NE-213, from 200 keV to 2 MeV for the proportional counter and above 0.4 MeV for the Bonner Ball. The spectra obtained with these three detectors agree pretty well one another. There can be seen a peak of direct neutrons energy-undegraded through the shield. Figure 4 clearly gives a broad peak around several hundreds keV which is reduced to the valley of the iron elastic scattering cross section near 600 keV. In Fig. 5, the neutron spectrum below 100 keV is nearly constant, namely, the 1/E slowing down spectrum due to the multiple scattering of light elements in concrete.

Figures 6 and 7 show the attenuation curves of the energy-undegraded neutrons in the peak area of 32.6 MeV and 21.8 MeV as a function of the thickness of iron and concrete, respectively. In the figures, the exponential function curves are shown whose attenuation coefficients are macroscopic total cross sections in the 35-30 MeV and 25-20 MeV energy groups in the cross section data library DLC-87 [12]. The curves calculated by the MORSE-CG Monte Carlo code with the DLC-87 are also shown. The figures revealed that the MORCE-CG calculation for 32.6 MeV neutrons gave the lower values than the experimental results both for iron and concrete, while on the contrary, for 21.8 MeV neutrons they were much higher than the experimental results. This big discrepancy may come from the inaccurate neutron cross section data above 20 MeV in the DLC-87 library. This experiment will be used as benchmark data for integral check of neutron cross section data above 20 MeV.

3. Research Plan on Neutron Experiment at TIARA

Using a monoenergetic neutron beam, the following experiments are planned; 1) measurement of neutron total and double differential scattering cross sections, 2) measurement of neutron activation cross section, 3)measurement of neutron and secondary photon penetration through matter, 4)measurement of photon and charged particle production cross sections.

3-1 Outline of Monoenergetic Neutron Source

The monoenergetic neutron source in the energy range of 20 to 90 MeV is located in the switching magnet vault(SMV) and in the wall(3.4 m thickness) between the SMV and the experimantal room, as seen in Fig. 8.

Figure 9 shows the detail of the monoenergetic neutron beam line. A proton beam extracted from the cyclotron is focused on ^{7}Li enriched target in a target changer by a quadrupole magnet. The thickness of ^{7}Li target is selected such that the proton energy loss in the target is about 2 MeV, which means the target thickness of 2 mm for 20 MeV proton, 4 mm for 50 MeV proton and 7 mm for 90 MeV proton. The target changer can set the Li targets of six different thicknesses and quartz for beam profile monitor. The monoenergetic neutrons produced in the forward direction by the ^{7}Li(p,n) reaction are transported to the experimental room through a rotary shutter. The shutter consists of 1200 mm thick steel backed by 300 mm thick polyethylene which includes annular duct of 100 mm inside diameter for neutron beam transport, and it rotates at close position to shut off neutrons when this beam line is not in use. In the shielding wall just behind the shutter, there is an experimental hole for placing shielding materials, which is 120 cm x 120 cm x 120 cm in size. The proton beam passed through the target is deflected by a clearing magnet and absorbed in a beam dump. The beam current on a dump is measured by a Faraday cup.

3-2 Calculation of Source Neutron Energy Spectrum

The source neutron energy spectrum transported through the neutron beam collimator shown in Fig. 9 was estimated by the MORSE-CG calculation with the DLC-87 neutron cross section data library. The calculation was done for 50 MeV proton energy when the rotary shutter is opened and closed. The three sources to produce neutrons by proton beam loss were considered in the calculation, ^{7}Li target, copper Faraday cup and aluminum vaccum duct.

The neutron energy spectrum from thin ^{7}Li target by the ^{7}Li(p,n) reaction at 0 deg for E_p = 50 MeV is cited from the data by Batty et al.[13]. The neutrons are assumed to be emitted in a solid angle subtended by the entrance of the neutron beam collimator.

The energy spectra of neutrons produced from Faraday cup are cited from the data on thick copper target for E_p = 52 MeV by Nakamura et al.[14]. The neutrons are emitted in the whole solid angle.

The neutrons may also be produced from the aluminum duct inside the clearing magnet bombarded by protons scattered at an angle larger than 1 deg through the Li target. The fraction of this scattered protons to the total is estimated to be about 0.037 from the Monte Carlo simulation. The neutrons are also assumed to be emitted in the forward direction as in the ^{7}Li(p,n) reaction. The neutron spectrum was approximated to be equal to that at 45 deg from thick aluminum target for E_p = 52 MeV given by Shin et al.[15]. The calculation was performed with the ACOS S 2000 computer of the Computer Center, Tohoku University. The history numbers were from 5,000 to 30,000.

Figure 10 shows the neutron spectra at the collimator exit when the rotary shutter is opened. In Fig. 10, Li(direct) means the direct neutrons from the Li target without collision, Li(scattered) the neutrons scattered in the collimator. Al corresponds to neutrons from the vaccum beam duct. Cu(penetrated) means the neutrons penetrated through shielding wall from the Faraday cup and Cu(reflected) the neutrons which are produced at the Faraday cup, reflected by the clearing magnet and passed through the collimator. Figure 10 clearly reveals that the direct monoenergetic neutron component overwhelms the other components. From the comparison of neutron spectra for open and closed rotary shutters, the rotary shutter was found to decrease the direct neutrons to the order of 10^{-4} or more.

These calculations showed that this neutron beam line is well designed to produce monoenergetic neutrons. The experiment using this neutron beam line will start from the next year.

References

1) Shin,K., Uwamino,Y., Yoshida,M., Hyodo,T. and Nakamura,T.: Nucl. Sci. Eng. 71 (1979) 294
2) Uwamino,Y, Nakamura,T. and Shin,K.: Nucl. Sci. Eng. 80 (1982) 360
3) Brady,F.P.: Can. J. Phys. 65 (1987) 578.
4) Helmer,R.: Can. J. Phys. 65 (1987) 588.
5) Pocanic,D., Wang,K., Martoff,C.J., Hanna,S.S., Byrd,R.C., Foster,C.C., Friesel,D.L. and Rapaport,J.: Can. J. Phys. 65 (1987) 687.
6) Conde,H. et al.: Nucl. Instr. and Meth. A292 (1990) 121
7) Uwamino,Y., Nakamura,T. and Hara,A.: Nucl. Instr. and Meth. A239 (1985) 299.
8) Shin,K., Uwamino,Y. and Hyodo,T.: Nucl. Technol. 53 (1981) 78
9) Burrus,W.R., Verbinski,V.V.: Nucl. Instr. and Meth. 67 (1969) 181
10) McElroy,W.N., Berg,S., Crockett,T. and Hawkins,R.G.: AFWL-TR 67-41, Air Force Weapons Laboratory (1967)
11) Emmett,M.B.: ORNL-4972, Oak Ridge National Laboratory (1975)
12) Alsmiller,R.G.,Jr. and Barish,J.: ORNL/TM-7818, Oak Ridge National Laboratory (1981)
13) Batty,C.J., Bonner,B.E., Kilvington,A.I., Tschalar,C., Williams,L.E. and Clough,A.S.: Nucl. Instr. and Meth. 68 (1969) 273
14) Nakamura,T., Fujii,M. and Shin,K.: Nucl. Sci. Eng. 83 (1983) 444
15) Shin,K., Saito,T., Fujii,M. and Nakamura,T.: Nucl. Instr. and Meth. 187 (1981) 587

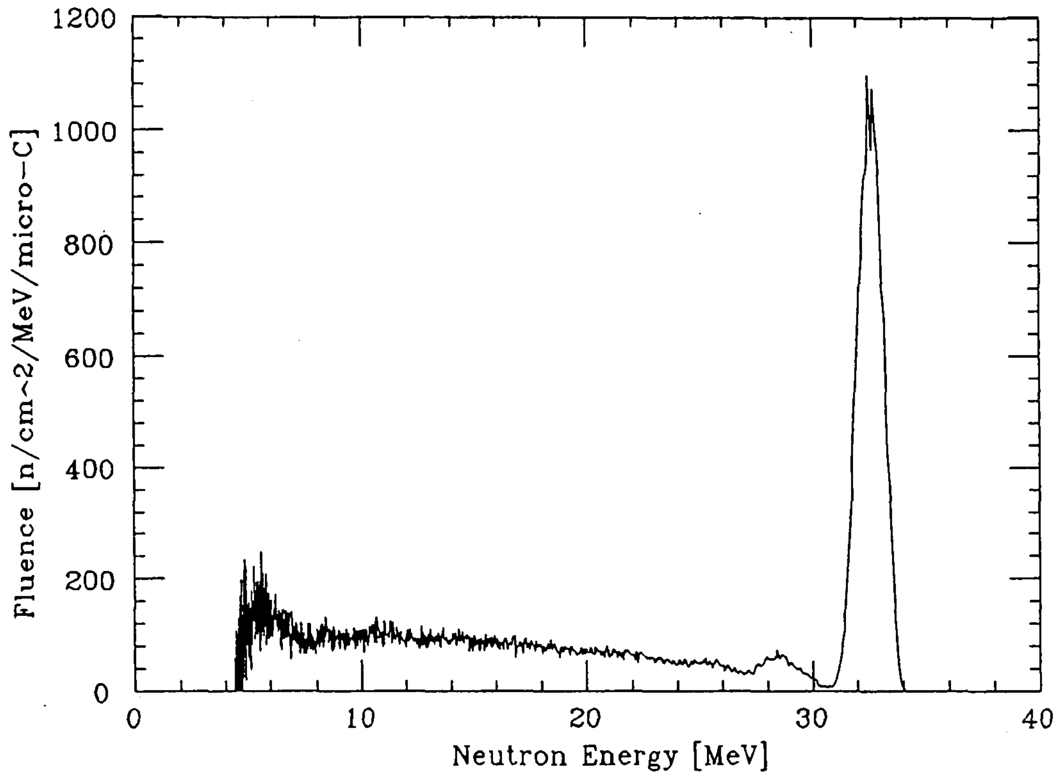

Fig. 2 Source neutron energy spectrum of ^{7}Li(p,n) reaction for 35 MeV proton

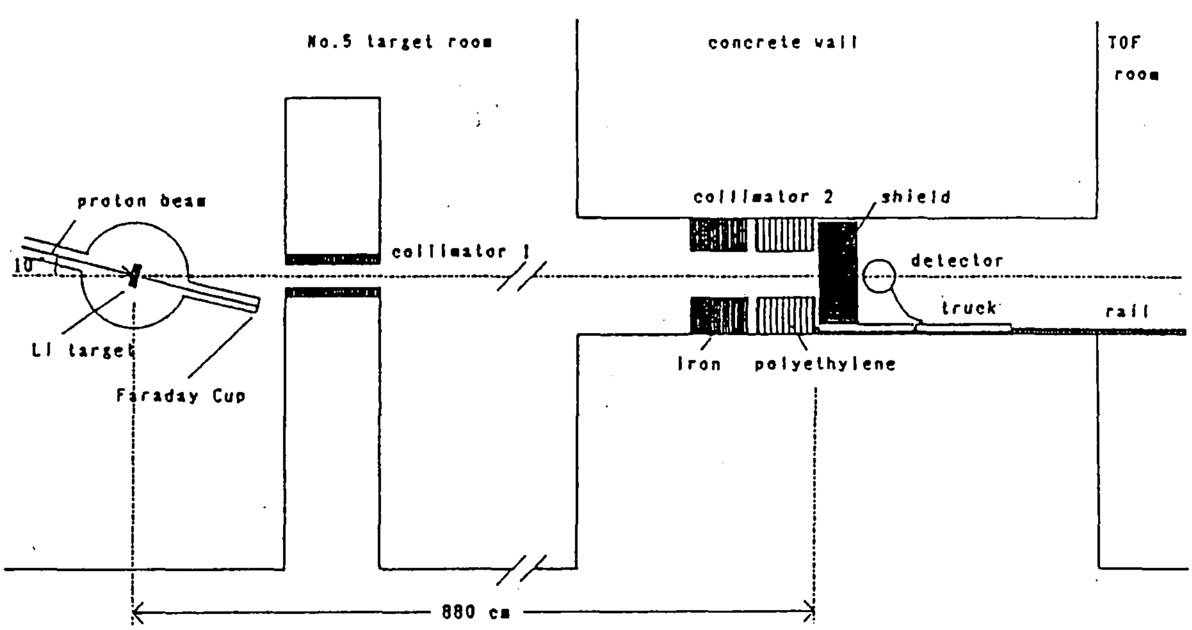

Fig. 1 Cross sectional view of experimental arrangement along neutron beam line

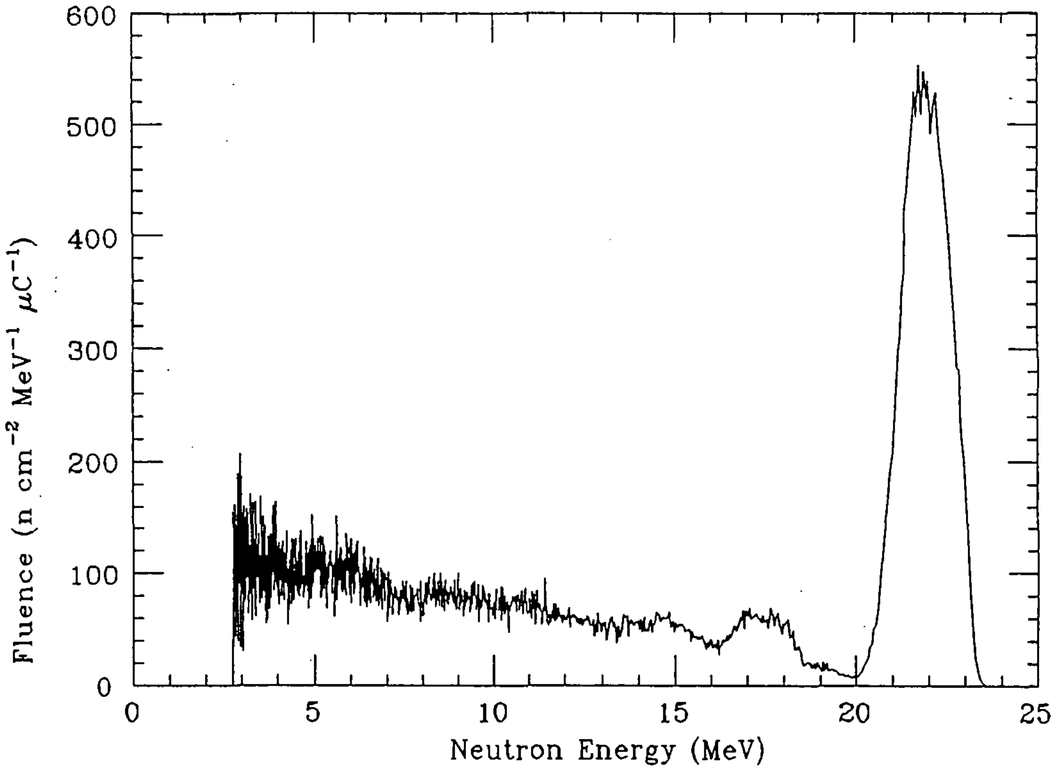

Fig. 3 Source neutron energy spectrum of ^{7}Li(p,n) reaction for 25 MeV proton

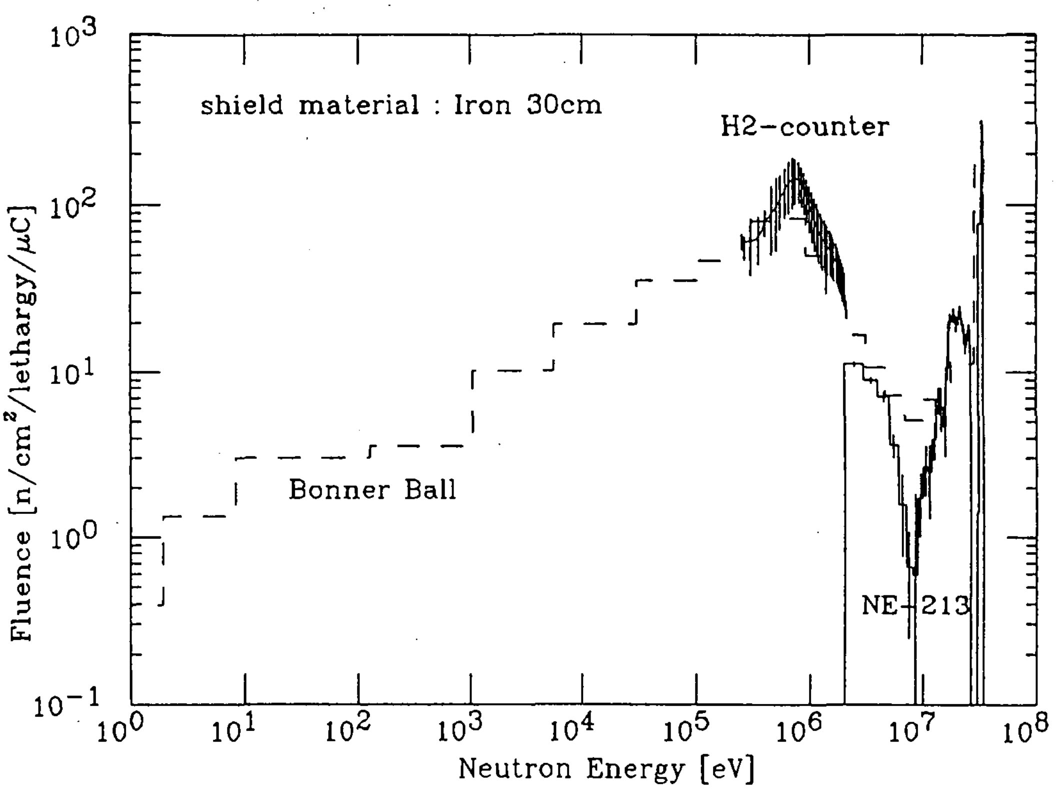

Fig. 4 Neutron energy spectrum transmitted through 30 cm thick iron

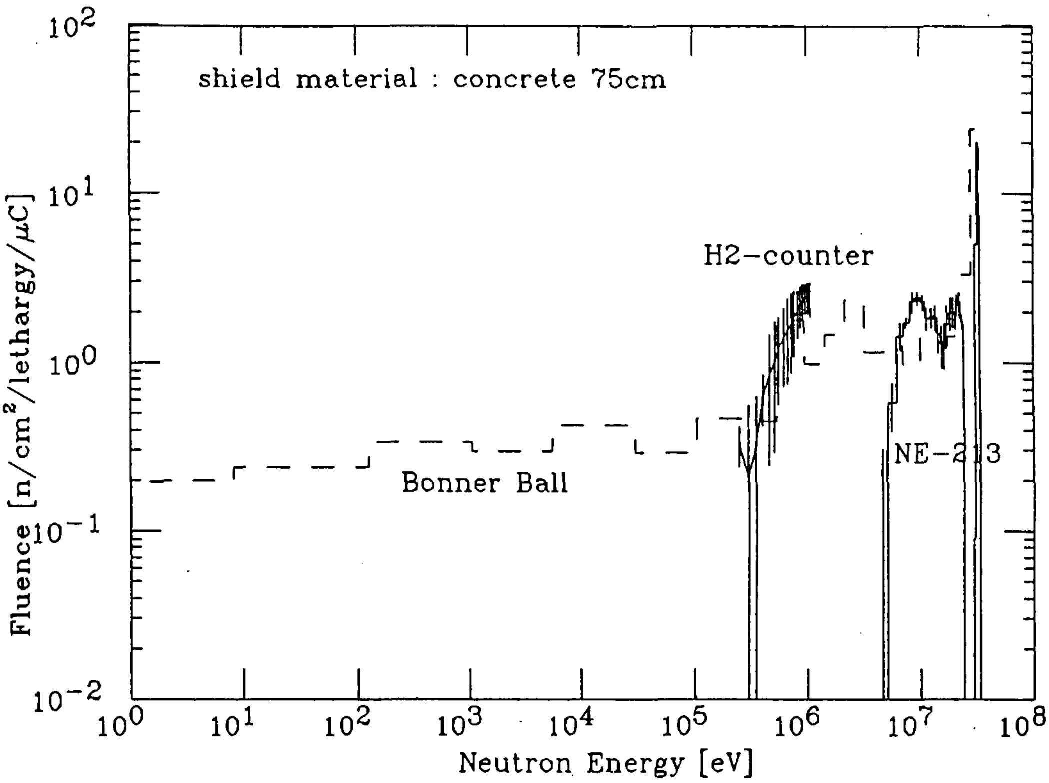

Fig. 5 Neutron energy spectrum transmitted through 75 cm thick concrete

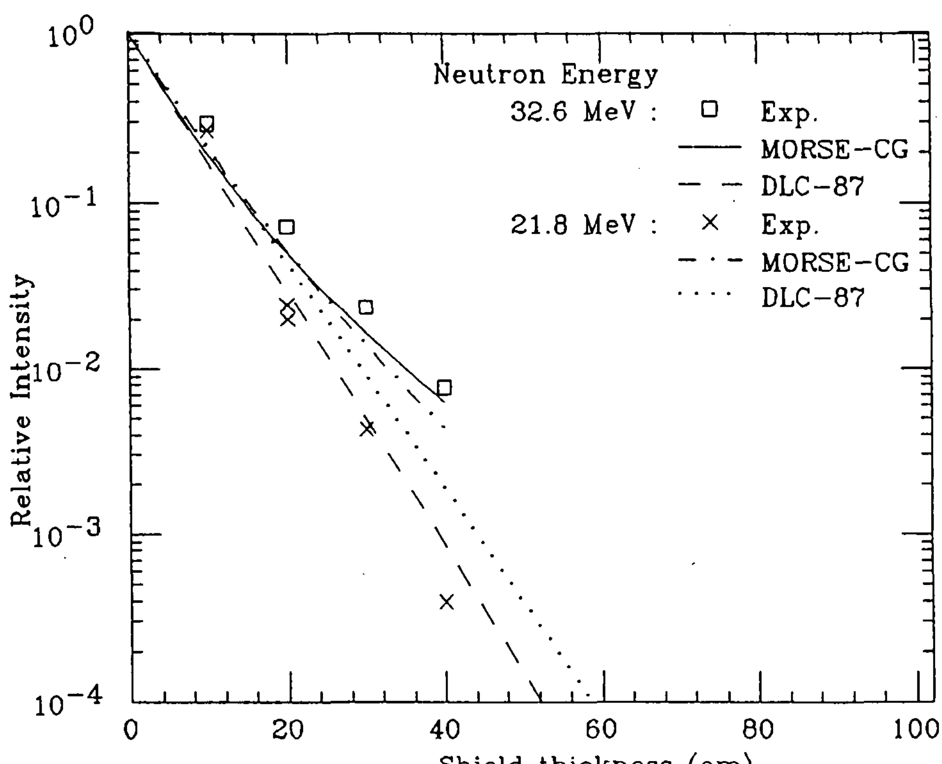

Fig. 6 Attenuation profiles of neutrons in a monoenergy peak regionas a function of iron thickness

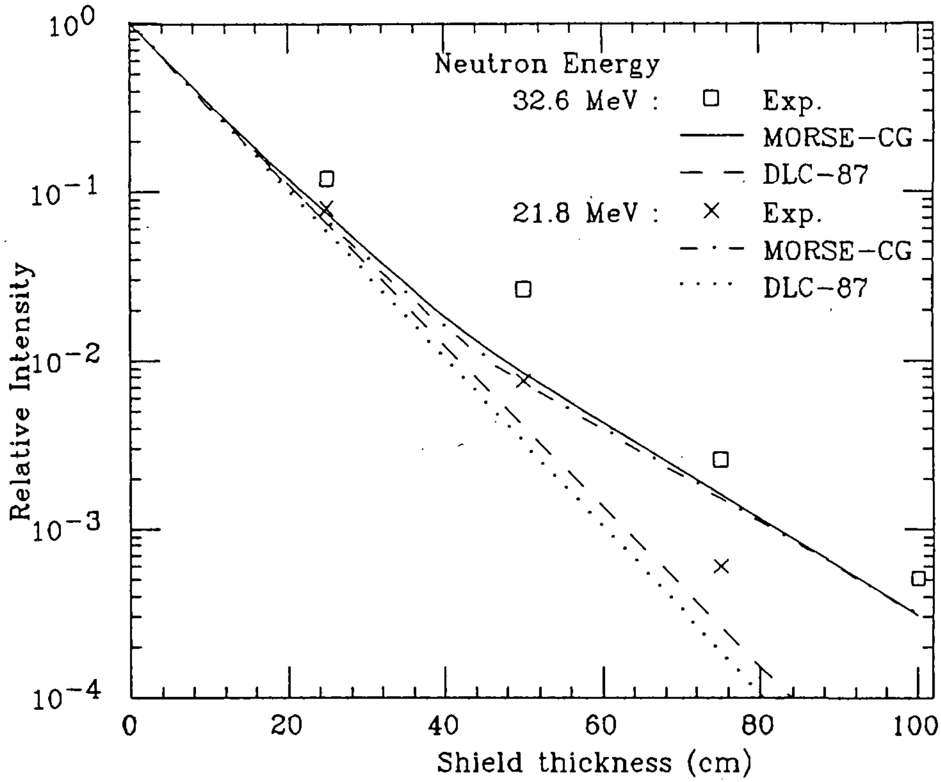

Fig. 7 Attenuation profiles of neutrons in a monoenergy peak regionas a function of concrete thickness

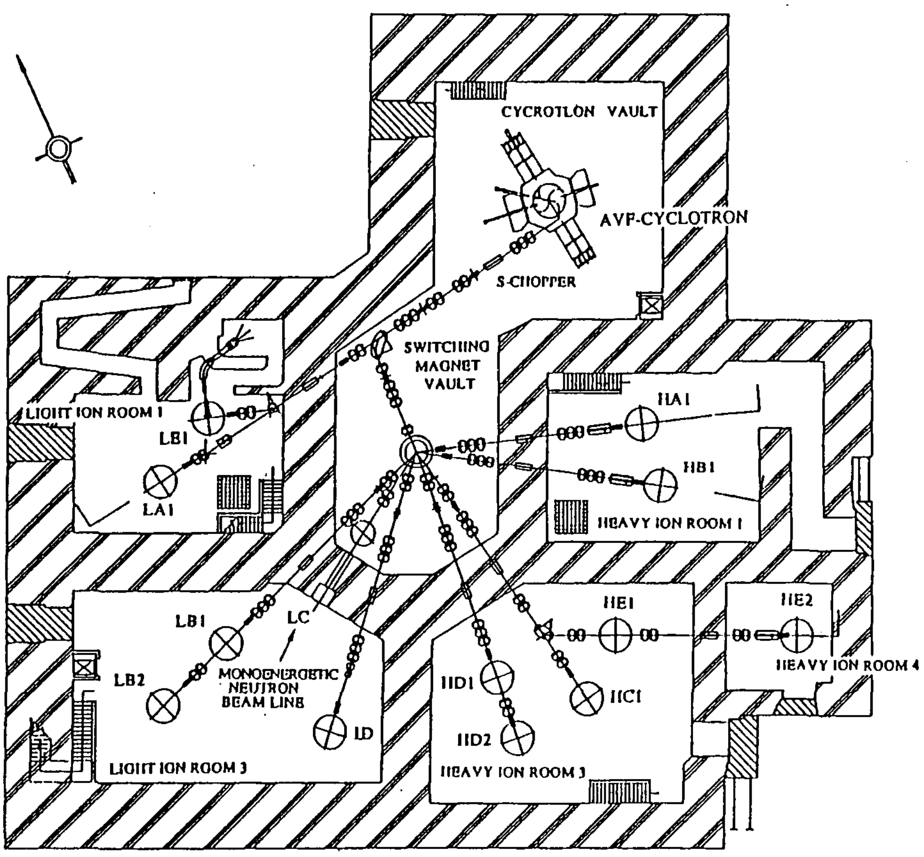

Fig. 8 Cross sectional view of the AVF cyclotron building together withthe layout of the beam lines at the TIARA facility

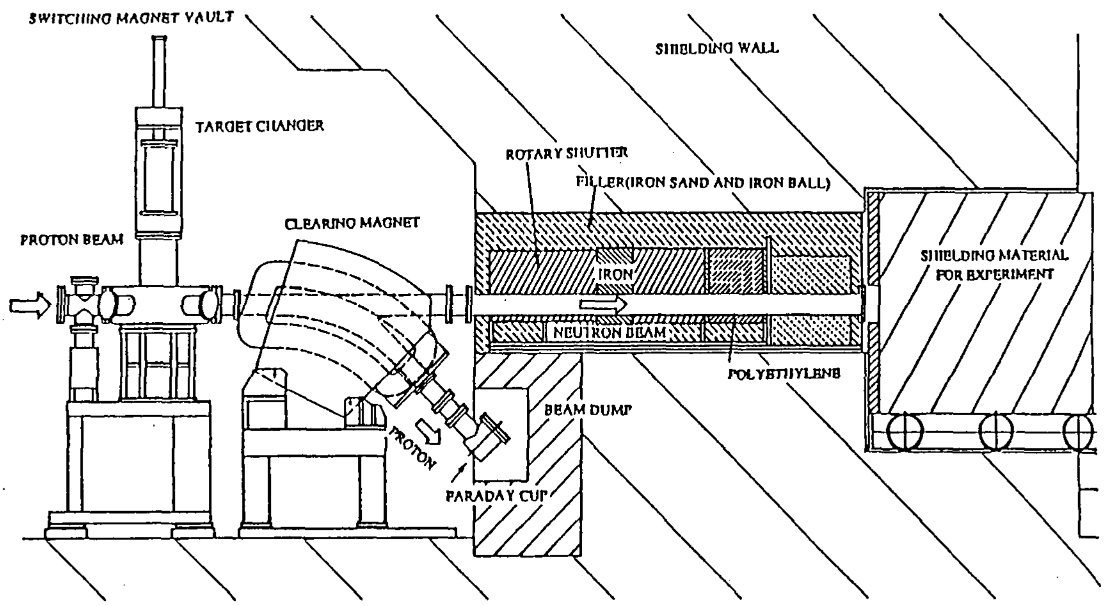

Fig. 9 Schematic view of the monoenergetic neutron beam line

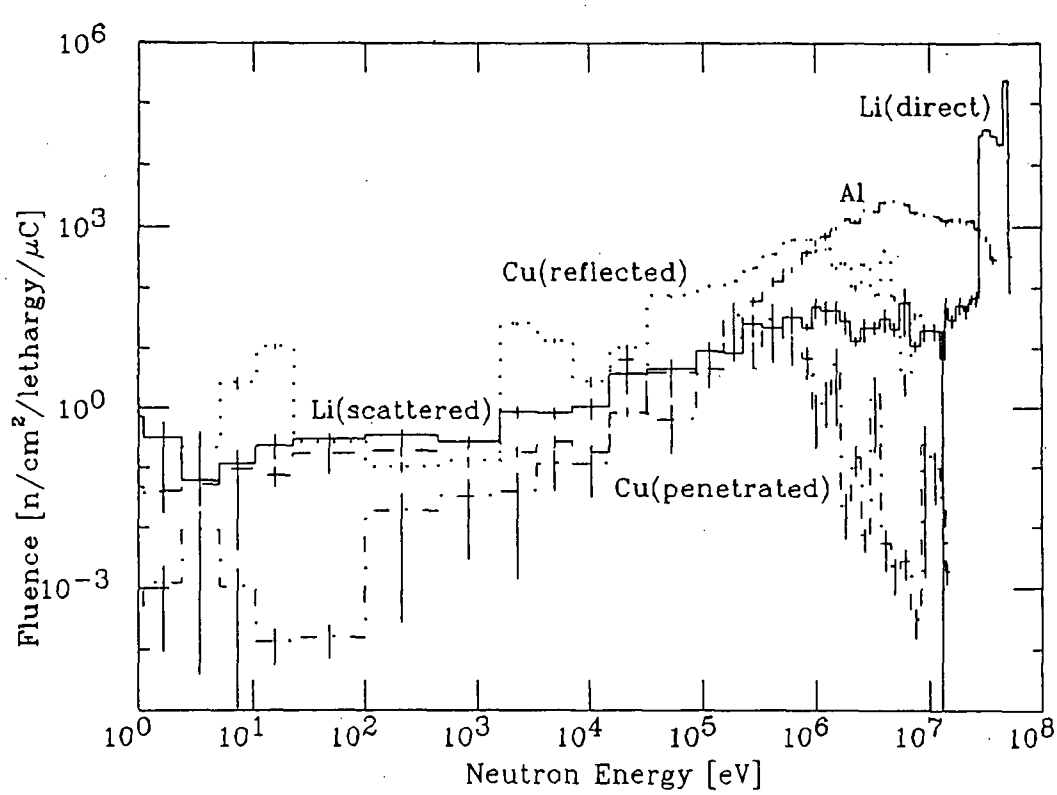

Fig. 10 Neutron energy spectra from several sources at the collimator exitfor 50 MeV proton when the rotary shutter is opened

B. Department of Nuclear Engineering

Faculty of Engineering

IX-B-1 Measurement of Double-differential Neutron Emission Cross Sections of ^{238}U, ^{232}Th and ^{12}C for 18 MeV Neutrons

M.Baba, S.Matsuyama, T. Ito, N. Ito, K. Maeda and N.Hirakawa

The paper of the title has been published in JAERI-M 91-059 with the following abstract:

Double-differential neutron emission cross sections of ^{238}U, ^{232}Th and ^{12}C have been measured for 18-MeV incident neutrons using the neutron time-of-flight technique and Tohoku University 4.5MV Dynamitron accelerator as a pulsed neutron generator. In the experiment, energy resolution of the spectrometer was improved by employing a newly developed post-acceleration beam-chopper and by adjustment of timing property of the neutron detector.

Measurements were made at laboratory angles between 30- and 145-deg., and data were obtained for secondary neutrons between 0.8 and 18 MeV. In the data processing, a care was taken for the data correction for the effects of parasitic neutrons associated with primary neutrons; the correction proved to be of special importance in the present measurement.

We compared the data obtained in the present experiment with the evaluated data, JENDL-3 and ENDF/B-IV (B-V for ^{12}C), and discussed the origin of the discrepancies. The anisotropy observed for secondary neutrons from ^{238}U and ^{232}Th was found to be reproduced by Kalbach-Mann systematics on the assumption of isotropy of fission neutrons. The experimental results for

^{12}C showed marked discrepancies concerning the scattering cross sections and neutron spectrum in the continuum region.

The results on ^{238}U and ^{232}Th have been presented also at the international conference on Nuclear Data for Science and Technology held at Jeulich, Germany May 13-17, 1991.

IX-B-2

High Efficiency Charged-particle Spectrometer using Gridded Ionization Chamber for Fast-Neutron Induced Reactions

M.Baba, N.Ito, S.Matsuyama and N.Hirakawa

A high efficiency charged particle spectrometer for fast neutron induced reactions has been developed using a gridded-ionization chamber taking advantage of its large solid angle and capability of energy-angle determination and of particle selection.

The present spectrometer is characterized by high stopping-power and low background to be applicable for alpha-particles up to 18 MeV emitted by 14 MeV neutrons and for protons up to around 6.5 MeV. The basic characteristics and proper performance of the spectrometer have been confirmed using the ^{6}Li(n,t) and H(n,p) reactions whose energy-angle distributions are well established.

The spectrometer has been applied successfully for (n,alpha) and (n,p) reactions on Ni and Cu. Test experiments revealed that the present spectrometer has much larger counting efficiency compared with conventional spectrometers based on counter-telescope geometry. Therefore, this spectrometer is a useful means for studies of energy-angular distributions of secondary charged particles especially for alpha-particles.

For further Improvement, however, technical developments are required for long term stability and for reduction of backgrounds due to neutron interaction with counter-gas which mask low energy parts of emission spectrum.

This work was presented at the international conference on Nuclear Data for Science and Technology held at Jeulich May 13-17, 1991.

IX-B-3

A Post-Acceleration Beam Chopper for 4.5 MV Dynamitron Pulsed Neutron Generator

S.Matsuyama, M.Fujisawa, M.Baba, T.Iwasaki, S.Iwasaki
R.Sakamoto, N.Hirakawa and K.Sugiyama

A post-acceleration beam chopper has been installed for Tohoku University 4.5MV Dynamitron pulsed neutron generator to improve the energy resolution in fast neutron time-of-flight experiment by reducing the pulse-width, and applied successfully for various experiments.

The post-chopper sweeps again the pulsed beam accelerated by Dynamitron with a pair of deflector plates around a chopping slit to eliminate the tail components in the original beam. It has been performing as expected and proved very useful for improving the overall resolution in time-of-flight experiments especially in neutron scattering experiments which require shorter duration of pulsed beam.

Since the installation, the post-chopper has been applied effectively for measurement of neutron scattering and emission cross sections of various elements.

This work was presented at the international conference on Nuclear Data for Science and Technology held at Jeulich May 13-17, 1991, with the experimental results on double-differential neutron emission cross sections of ^{6}Li and C.

IX-B-4 A New method for Measurement of (n,2n) Cross Section

T.Iwasaki, H.Kimiyama, S.Meigo, S.Matsuyama, M.Baba and N.Hirakawa

A new method has been developed for measurement of (n,2n) cross section on the basis of measurement of time intervals between detected neutron signals in a large ^{3}He-counter banked detector. The detector consists of thirty ^{3}He proportional counters appropriately distributed in a large polyethylene moderator assembly, about 60 cm cube. The events by (n,2n) reaction are distinguished from those by scattering processes on a measured time interval spectrum since two neutrons from (n,2n) reactions produce correlated time interval while those from scattering distribute randomly. This method is advantageous than activation method owing to applicability to every nuclide.

For the purpose, a ^{3}He-counter banked detector was developed to have high efficiency and appropriate neutron capture-time, and tested under various experimental conditions. Expected time interval spectra were confirmed in the experiments. The efficiency and the neutron capture-time of the detector were measured using a Cf-252 source; these values agreed very well with those calculated using the code Multi-KENO. A neutron fluence monitor suitable for the present detector was also developed.

This technique has applied for (n,2n) cross section measurement of structural elements.

This work was presented at the international conference on Nuclear Data for Science and Technology held at Jeulich May 13-17, 1991.

C. Laboratory of Nuclear Science

IX-C-1 Examination of the Giant Dipole Resonances of ^{11}Be in the (e,π^+) Reaction on ^{11}Be

T. Yamaya*, M. Saito*, H. Yamazaki, T. Taniuchi, K. Shoda and H. Tsubota†

Mass radii of some neutron-rich light nuclei like ^{11}Li, and ^{11}Be extend beyond the usual nuclear radius[1]. Such the large nuclear radii are responsible to the loosely bound single-particle wave function. These neutrons do not couple strongly to the motion of the core, thus it is expected that the dipole response of the nucleus be enhanced at low excitation. These strength distributions and energies have been calculated in the theoretical investigations by many authors[2]. However, experimental observations of the such giant resonances have hardly ever been done directly. In this report, the giant dipole resonances and energies were experimentally studied with the reaction $^{11}Be(e,\pi^+)^{11}Be$ at the electron energy of 200 MeV. In the (e,π^+) reactions near the photopion threshold energies, the transitions are sensitive only to the spin-part of magnetization densities, and the multipolarity of the transition can be determined from the dependence in the angular distribution. The energy spectra of positive pions and the deferential cross sections from the (e,π^+) reaction on ^{11}B were measured at five angles. The electron beam was provided from the Tohoku University linear accelerator. The energy spectra of pions to the levels of ^{11}Be are shown in Fig. 1. The spin-dipole transition strength to the ground, $1/2^+$ state of ^{11}Be is weak, however the transition strength to the ground, the 6.8 MeV, $(3/2^+)$ state is about three times of that of the ground state. On the other hand, the 1.78 MeV, $(3/2, 5/2)^+$ state was not observed. The strong resonances were observed at E_x=9.4 and 17.4 MeV. Hoshino et al.[3] have suggested that the charge exchange spin-flip dipole strengths from the ground state of ^{11}Be to the excited state are mainly distributed between E_x=5

*Department of Physics, Tohoku University
†College of General Education, Tohoku University

and 13 MeV, and the peak is lowered to 9 MeV form 11 MeV because of the angular distributions of the observed resonances are doing now and the charge exchange spin-dipole strengths will be deduced.

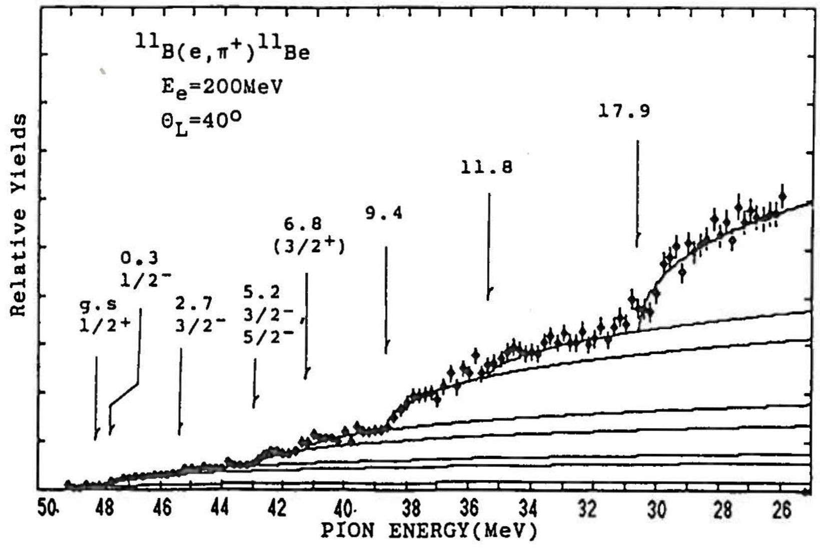

Fig. 1 π^+ energy spectrum in the $^{11}B(e,\pi^+)^{11}Be$ reaction.

References

1) I. Tanihata et al., Phys. Rev. Lett. **55** (1985) 2676.

2) Y. Suzuki et al., Prog. Theor. Phys. **83** (1990) 180;

G. Bertsch and J. Foxwell, Phys. Rev. **C 41** (1990) 1330.

3) T. Hoshino et al., Nucll. Phys. **A523** (1991) 228.

IX-C-2 (e,e'p) and (e,e't) coincidence on ^{6}Li

M. Nomura, T. Tamae, K. Takahisa, E. Tanaka, M. Sugawara, H. Miyase* and T. Suda*

The (e,e'p) and (e,e't) coincidence cross sections were measured on ^{6}Li at energy and momentum transfer of ω=37 MeV and q=63 MeV/c. Momentum distributions of p-shell and s-shell protons in ^{6}Li were reduced form the (e,e'p) cross section. In Fig. 1, they are compared with a PWIA calculation and other experimental results. Final sate interactions are excluded form the results of the present experiment and the tagged photon experiment[1]. The momentum distribution of p-shell proton deduced from our data is described well with the PWIA calculation. On the other hand, the experimental values dominate the calculation for the momentum distribution of the s-shell proton. It shows tat reaction mechanisms besides a direct knockout are important for experiments with low momentum transfer such as our experiment and the tagged photon experiment. Large longitudinal-transverse components of the cross sections can not be described by the direct knockout process both for the p-shell and s-shell protons.

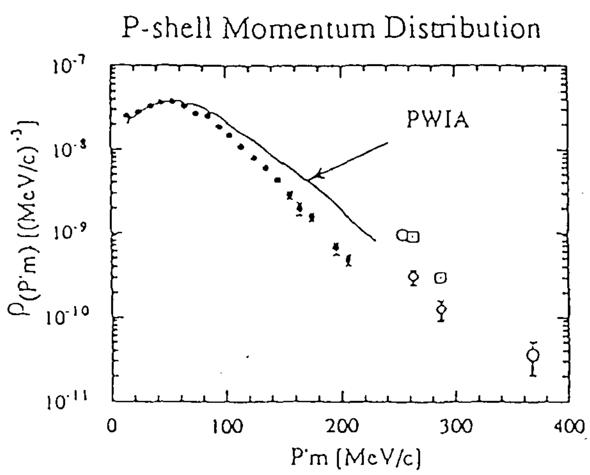

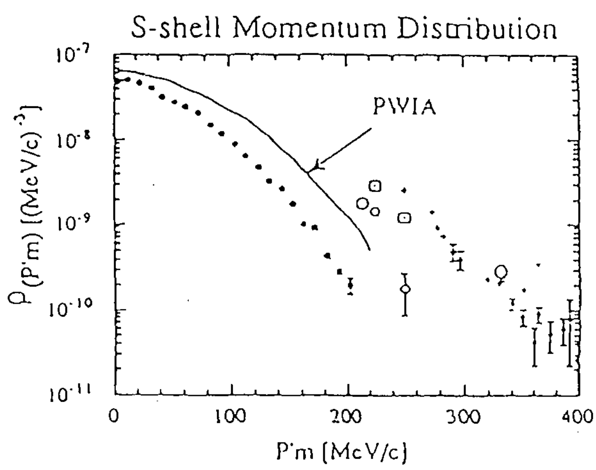

Fig. 1 Momemtum distributions of p-shell and s-shell protons in^{6}Li.

○□◇, present results; ●, quasi-elastic experiment[1].

Final state interactions are not excluded.; ◆, tagged photon experiment[2].

*College of General Education, Tohoku University

Fig. 2 shows the angular distribution of triton measured in the $^{6}Li(e,e't)$ coincidence experiment. It is fitted well with C1 and E1 components, and the reduced Legendre parameter a_2=-0.86±0.35 is in agreement with that given from the photo reaction.

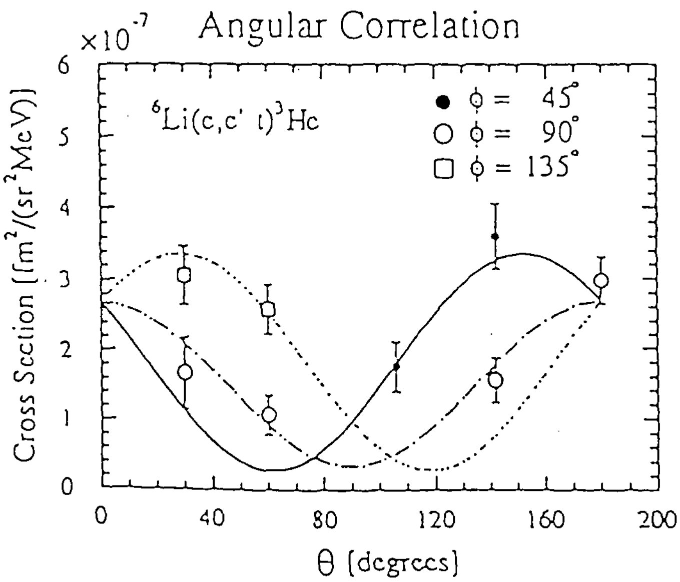

Fig. 2 Triton angular distributrion.
Curves: Calculated results with C1 and E1 components.

References

1) J.B.J.M. Lanen et al., Phys. Rev. Lett. **62** (1989) 2925.

2) I. Nomura, Doctor thesis.

IX-C-3

$^{13}C(e,e'n)^{12}C$ and $^{40}Ca(e,e'n)^{39}Ca$ reactions in the giant resonance region

S. Suzuki, C. Takakuwa, T. Saito, K. Takahisa, T. Tohei*, T. Nakagawa* and K. Abe†

Angular distributions of the $^{13}C(e,e'n)^{12}C$ and $^{40}Ca(e,e'n)^{39}Ca$ reactions in the giant resonance region have been measured at the momentum transfer q=0.33 fm^{-1}. The experimental cross section was expanded with the Legendre polynomials which are related with nuclear response functions W_L, W_T and W_{LT}. Fig. 1 shows the parameters fitted

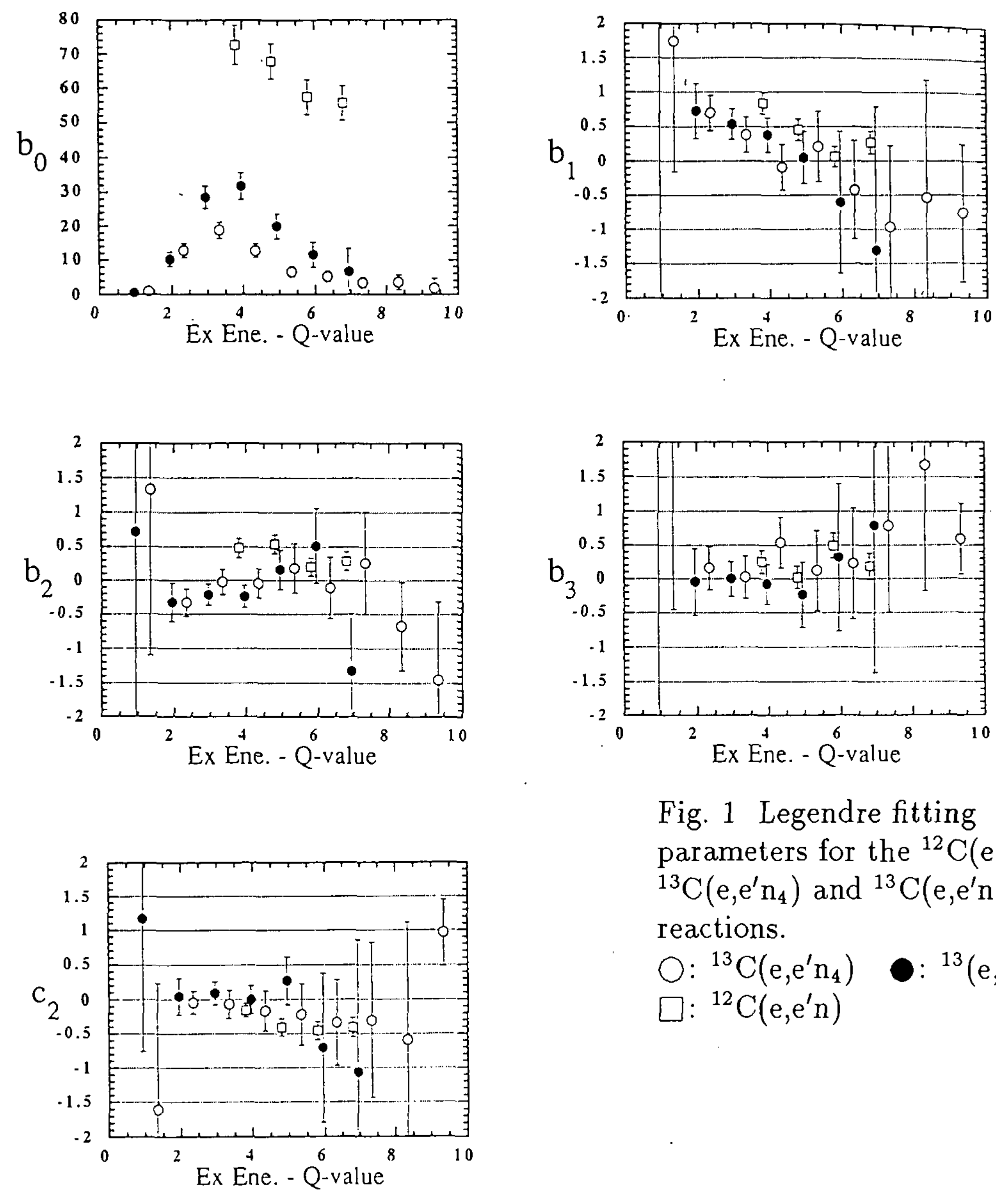

Fig. 1 Legendre fitting parameters for the $^{12}C(e,e'n)$, $^{13}C(e,e'n_4)$ and $^{13}C(e,e'n_5)$ reactions.
○: $^{13}C(e,e'n_4)$ ●: $^{13}(e,e'n_5)$
□: $^{12}C(e,e'n)$

*Department of Physics, Tohoku University
†College of General Education, Tohoku University

with the Legendre polynomials for the decay neutrons to the 12.7 MeV, T=0 state (open circles) and the 15.1 MeV, T=1 state (black circles) in ^{12}C from the giant resonance in ^{13}C. Also shown on the same graph are the parameters for the decay neutrons in the $^{12}C(e,e'n_0)^{11}C$ reaction (squares).

The parameter b_0 indicates that the sum of $T_<$ and $T_>$ cross sections in ^{13}C equal the cross section in ^{12}C. The other parameters $b_1 \sim b_3$, and c_2 are consistent in both ^{13}C and ^{12}C. From these the giant resonance in ^{13}C may be interpreted as excitation of the core of ^{13}C. Fig. 2 shows the parameters for the $^{40}Ca(e,e'n_0)$ reaction compared with $^{40}Ca(e,e'p_0)$ reaction[1]. The parameters b_1 and b_3 agree well in both reactions, but b_2 shows remarkable difference.

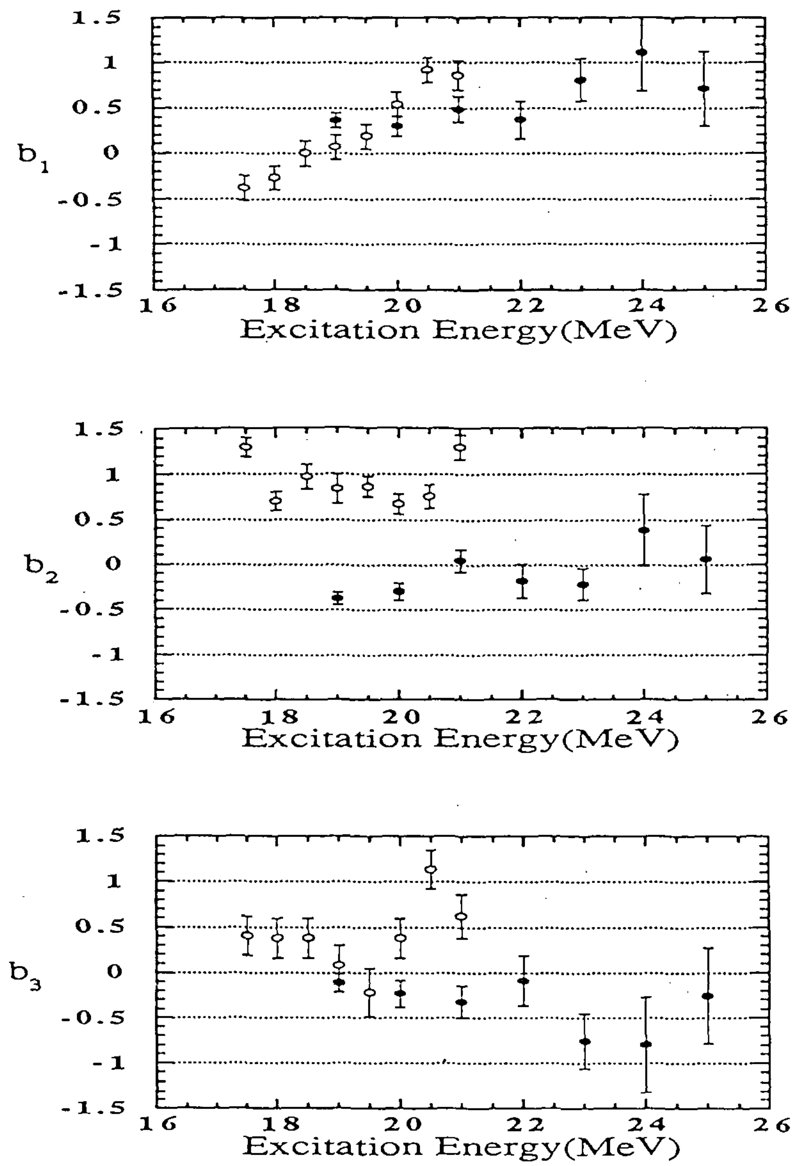

Fig. 2 Legendre fitting parameters for the $^{40}Ca(e,e'n_0)$ and $^{40}Ca(e,e'p_0)$ reactions.
●: $^{40}Ca(e,e'n_0)$ ○: $(e,e'p_0)$

References

1) A. Tanaka et al., Nucl. Phys. **A489** (1989) 381.

IX-C-4

Measurements of ^{9}Be(γ, pp) reactions at $80 < E_\gamma < 100$ MeV

T. Suda*, K. Maeda* , S. Ito, O. Konno, H. Matsuyama, I. Nomura†, Y. Sugawara T. Terasawa, A. Bates‡ , J. Eden‡, D. McLean‡ and M. Thompson‡

The measurements of ^{9}Be(γ, pp) reactions were carried out at Tohoku University using tagged photons produced by the continuous electron beam from the pulsed beam stretcher. The photon tagging system provides monochromatic photons in the energy range from 30 MeV to 100 MeV in a 2.6 MeV step. The photon energies above 70 MeV were used in this experiment, however, due to a large Q-value and a high proton detection threshold. A natural beryllium sheet of 200 mg/cm^2 thickness was used as the target. A total of 18 segmented plastic scintillators and a long plastic scintillator were arranged in order to cover a wide range of opening angles of two outgoing protons. The total solid angle of the proton detectors was about 1sr.

The angular correlations of two nucleons from ^{9}Be(γ, pn) and ^{9}Be(γ, pp) reactions are shown in Fig. 1. The emitted nucleons from both reactions show similar back-to-back correlations. The ratio of the (γ, pp) to (γ, pn) cross sections was obtained as R=(γ, pp)/(γ, pn)=0.044 ± 0.011. An inter-nuclear cascade model calculation, in which a (γ, pn) reaction is followed by a n-p collision inside the nucleus and changes to a (γ, pp) reaction, successfully reproduces the shape of the experimental angular correlations and gives R=0.07.

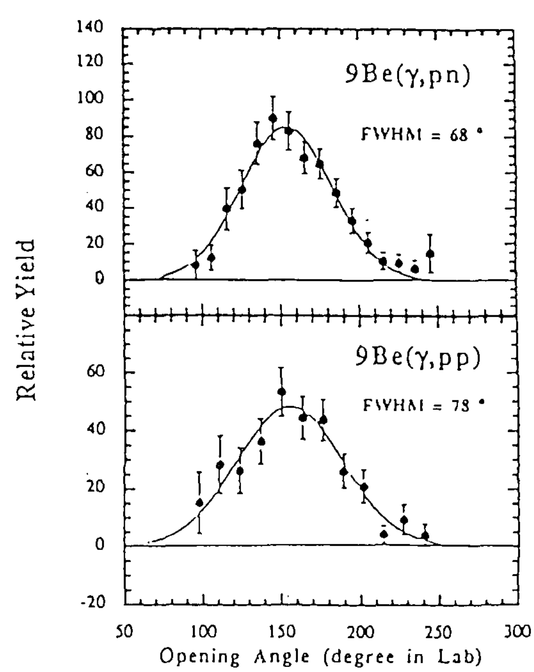

Fig. 1 Angular correlations of photo-nuclear pairs.

*College of General Education, Tohoku University
†Institute of Physics and Chemical Research
‡School of Physics, The University of Melbourne

The missing energy spectrum of two protons from the $^9Be(\gamma, pp)$ reaction at photon energies from 80 to 100 MeV is shown in Fig. 2. A narrow peak is observed at around two proton threshold from ^9Be. This peak can not be explained by any effect of the final state interaction simulated by the cascade model. It may suggest the existence of the direct (γ, pp) reactions.

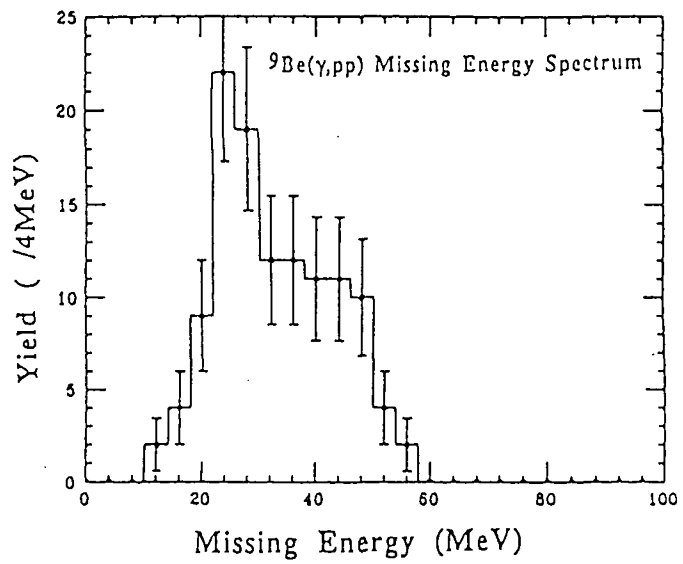

Fig. 2 Missing energy spectrum of the $^9Be(\gamma,pp)$ reaction.

X. Tokyo Institute of Technology

A. Research Laboratory for Nuclear Reactors

X-A-1 Fusion cross sections for $^{16}O,^{19}F+^{54,56}Fe$ near the Coulomb barrier

H. Funaki, M. Shimizu* and E. Arai

The enhancement in the sub-barrier fusion cross sections is one of the interesting subjects in heavy-ion reaction studies. We have started a series of light heavy-ion fusion measurements at energies around the Coulomb barrier. A time-of-flight mass spectrometer is used to separate evaporation residues from particles scattered by the target. The projectiles are ^{16}O and ^{19}F from the Heavy Ion Accelerate System at Tokyo Institute of Technology, and the target nuclei are ^{54}Fe and ^{56}Fe. We expect to observe the effect of proton transfer on the fusion cross section of the ^{19}F + $^{54,56}Fe$ systems, which have large positive Q_{gg} values (+3.99, +2.66 MeV) for the one proton pick-up. The ^{16}O fusion reactions have negative Q_{gg} values and are regarded as bench marks.

Figure 1 shows the angular distributions for the four systems at two incident energies. The absolute differential cross sections were obtained by normalizing the evaporation residue yield to the elastic scattering cross sections. The solid curves represent the Gaussian fits. Integration of the Gaussian distributions over the whole solid angle gave the total fusion cross sections, which were used to convert the single-angle excitation functions into the total fusion one.

Figure 2 shows measured cross sections as a function of center-of-mass energy for (a) the ^{19}F + $^{54,56}Fe$ and (b) the ^{16}O + $^{54,56}Fe$ systems.

---

*Present Address: Mitubishi Material Co.,

Theoretical values are calculated by using the constant coupling model code CCFUS [1]. Barrier parameters V_b and R_b were deduced by fitting the data at energies above the barrier. These values were listed in Table I with the systematics by Vaz et al. [2].

The solid curves have no coupling mode and correspond to the one-dimensional tunneling model. It is clear that the experimental data cannot be reproduced at energies below the Coulomb barrier for all four systems. The dash-dotted curves include the coupling to low-lying existed states in the projectile and target nuclei. The results still underestimate the cross sections for the ^{19}F + $^{54,56}Fe$ systems. The dotted curves include, in addition to the inelastic channels, the one-nucleon-transfer channels where the coupling strength F is 1 MeV. The discrepancy between the calculation and experiment was fairly reduced.

Recently we have accomplished a ^{15}N + $^{54,56}Fe$ measurement. The analysis of the experiment is now going on.

References:

[1] C.H. Dasso and S. Landowne, Comput. Phys. Commun. 46 (1987) 187.

[2] L.C. Vaz, M. Alexander and G.R. Satchler, Phys. Rep. 69 (1981) 373.

Table I. Barrier parameters extracted from our data and from the systematics of ref. [2].

	This work			Vaz et al.	
System	V_b (MeV)	R_b (fm)	$\hbar\omega$ (MeV)	V_b (MeV)	R_b (fm)
$^{16}O+^{54}Fe$	30.3	9.15	3.80	29.6	9.34
$^{16}O+^{56}Fe$	30.0	9.27	3.76	29.4	9.41
$^{19}F+^{54}Fe$	33.2	9.43	3.70	32.8	9.48
$^{19}F+^{56}Fe$	33.0	9.48	3.66	32.6	9.54

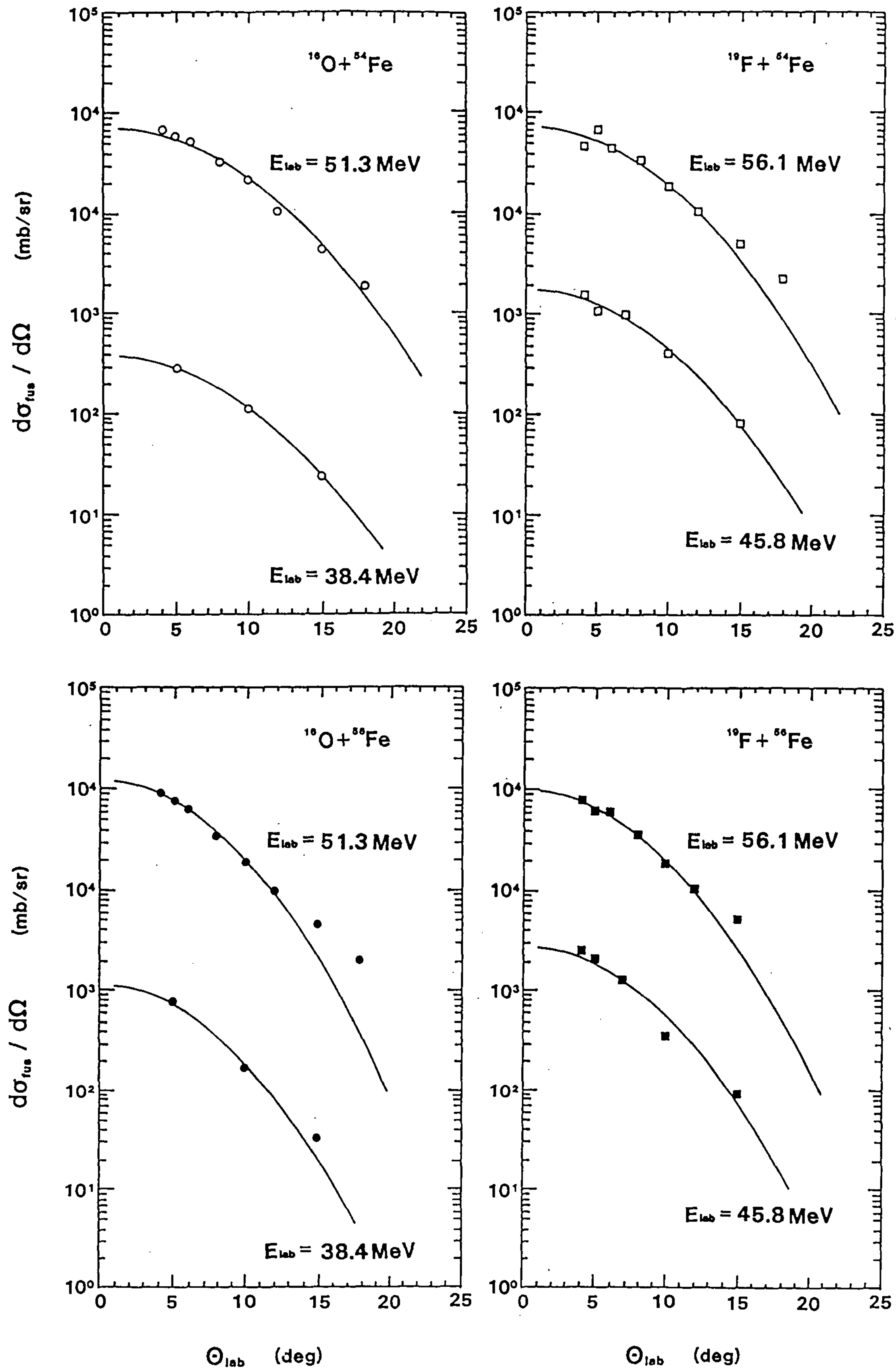

Fig. 1. Angular distributions obtained for four systems. The curves are the Gaussian fits.

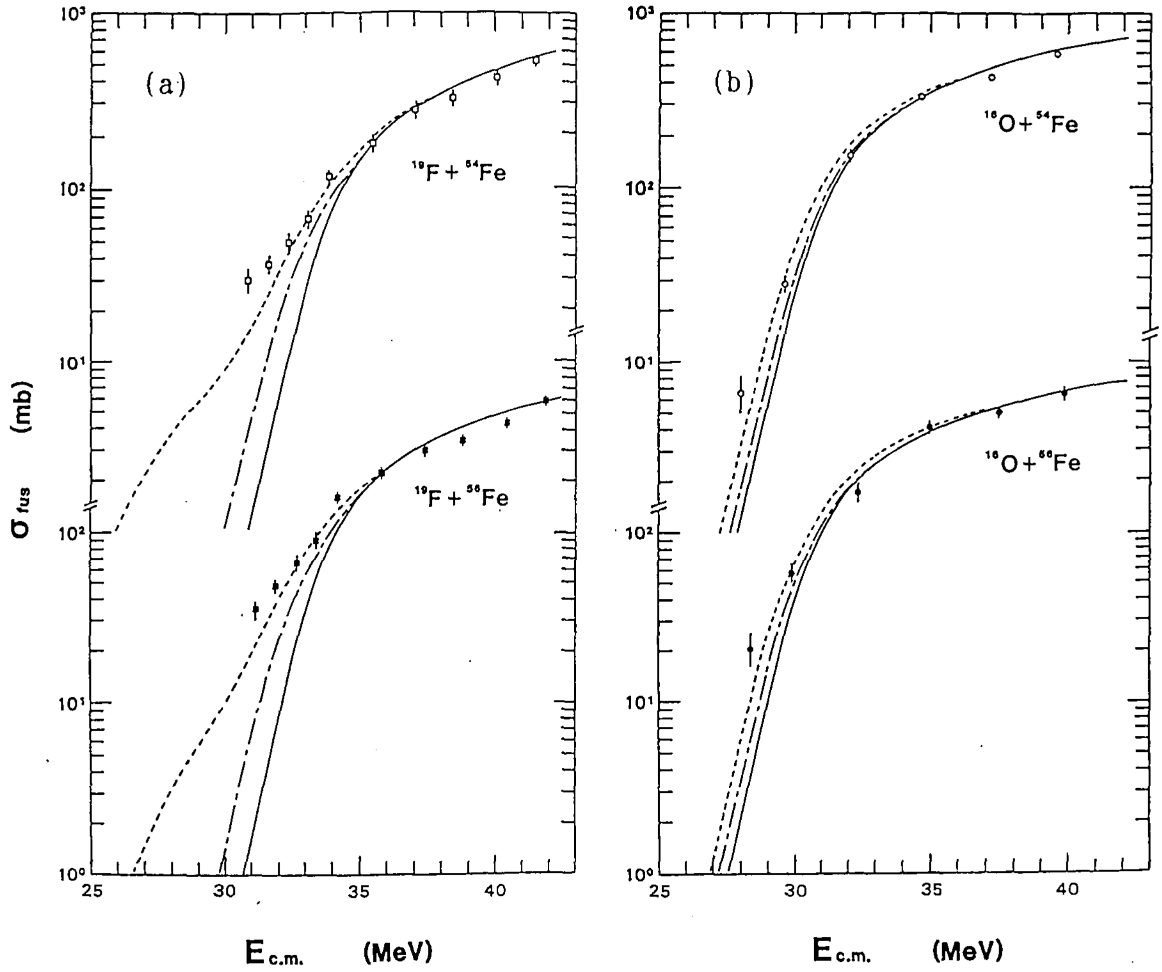

Fig. 2. The fusion cross sections as a function of center-of-mass energy for (a) the ^{19}F + $^{54,56}Fe$ and (b) the ^{16}O + $^{54,56}Fe$ systems. The curves represent theoretical predictions: The solid curves include no coupling. The dash-dotted curves have the coupling to low-lying existed states in the projectile and target nuclei. The dotted curves include the coupling to the one-nucleon-transfer channels in addition to the inelastic channels.

X-A-2
Channel-Capture Mechanism in Low-Energy Neutron Capture by ^{12}C

Yu-Kun Ho, H. Kitazawa and M. Igashira

This paper shows that, at least, in the neutron energy region from thermal to 30 keV, the measured neutron radiative capture cross sections of ^{12}C feeding the first four states in ^{13}C can be well understood in the framework of a channel-capture model for El transition. The characteristics for each kind of transitions are investigated.

A paper on this subject will be published in Physical Review C.

X-A-3
Core Polarization in the 203 keV $p_{1/2}$-Wave Neutron Resonance Capture by ^{32}S

H. Kitazawa, M. Igashira, Y. Achiha, N. Mukai, F. Uesawa, T. Andoh and S. Shibata

We have observed gamma-ray spectra from neutron capture in the 203 keV $p_{1/2}$-wave resonance of ^{32}S with an anti-Compton NaI(Tl) detector, employing a neutron time-of-flight technique. Partial radiative widths were measured from the strong El transitions to the ground $(\frac{3}{2}^{+})$ and 840 keV $(\frac{1}{2}^{+})$ states, and for the weak Ml transition to the 3220 keV $(\frac{3}{2}^{-})$ state. The observed El transitions are in a marked discrepancy with predictions of the Lane-Mughabghab valence-capture model. However, those transitions are well explained by a particle-vibrator coupling model, in which an explicit account is taken of the core polarization due to quadrupole and octupole one-phonon excitation in the resonance state. In particular we emphasize that the $(2^+ \otimes f_{5/2})$ configuration component in a model wave function of the resonance state plays an important role for the El transitions. A brief discussion is also presented on the Ml transition.

A paper on this subject has been submitted to Nuclear Physics A.

X-A-4 Valence-Neutron Capture in the 434-keV $p_{3/2}$-Wave Resonance of ^{16}O

M. Igashira, H. Kitazawa, and K. Takaura

We have measured γ-ray spectra from the 434-keV $p_{3/2}$-wave neutron resonance capture and from the off-resonance capture at 280 keV with an anti-Compton NaI(Tl) detector, employing a time-of-flight technique. Partial radiative widths and partial off-resonance capture cross sections were obtained for the transitions to the ground $(5/2^+)$ and 871 keV $(1/2^+)$ states in ^{17}O. The radiative widths are well predicted by the valence capture formula of Lane and Mughabghab, although the ground-state transition seems to be slightly retarded. Moreover, we found that the potential-capture theory substantially reproduces the partial off-resonance capture cross sections.

A paper on this subject has been submitted to Nuclear Phyaics A.

X-A-5

Measurements of keV-Neutron Capture Gamma Rays From Some Structural and Shielding Materials

M. Igashira, Y. Dozono, F. Uesawa, M. Shimizu and H. Kitazawa

We have measured capture gamma rays from the structural and shielding materials, Mg, Al, Si, Ca, Cr, Co and Zr, with an anti-Compton NaI(Tl) detector, at several neutron energies between 10 and 600 keV, employing a time-of-flight technique. Observed pulse-height spectra were unfolded using a response matrix of the detector in order to obtain capture gamma-ray spectra. Those spectra from Al, Si, Ca and Cr were compared with statistical model calculations. In general the calculations reproduce fairly well the observed spectra at neutron energies of several hundreds keV.

A paper on this subject will be published in Proc. Int. Conf. on Nuclear Data for Science and Technology, Jülich (1991).

X-A-6

Neutron Capture Cross Sections of Light Nuclei in Primordial Nucleosynthesis

Y. Nagai, K. Takeda, S. Motoyama, T. Ohsaki, M. Igashira, N. Mukai, F. Uesawa, T. Ando, H. Kitazawa and T. Fukuda

Neutron radiative capture sections of ^{7}Li and ^{12}C were measured at a neutron energy of 30 keV to study the production rate of intermediate-mass nuclei in primordial nucleosynthesis. The reaction cross sections were obtained by using pulsed neutrons and by observing prompt γ-rays from the captured state. The present results favor the nucleosynthesis of intermediate-mass nuclei in the early universe.

A paper on this subject has been published in Nuclear Instruments and Methods in Physics Research B56/57(1991)492.

X-A-7

Measurement of The Neutron Capture Rate of the $^{12}C(n,\gamma)^{13}C$ Reaction at Stellar Energy

Y. Nagai, M. Igashira, K. Takeda, N. Mukai, S. Motoyama, F. Uesawa,H. Kitazawa and T. Fukuda

The reaction $^{12}C(n,\gamma)^{13}C$ at stellar energy plays important roles in the nucleosynthesis of intermediate-mass nuclei in inhomogeneous big bang models and in that of heavy elements during stellar evolution. In the present study the reaction rate was measured by detecting γ-rays emitted from a capture state; 16.8 ± 2.1 μbarn was obtained, about 5 tims larger than the estimated value from the thermal-neutron capture cross section. The present result favors the nucleosynthesis of intermediate-mass nuclei in inhomogeneous big bang models and also of heavy elements in exploding supernovae.

A paper on this subject has been published in The Astrophysical Journal 372(1991)683.

X-A-8

Neutron Optical Potential of ^{28}Si Derived From the Dispersion Relation

H. Kitazawa, S. Igarasi, D. Katsuragi and Y. Harima

According to Feshbach's generalized optical potential model, the nucleon mean field is described as the sum of a Hartree-Fock component and a diapersive component. The Hartree-Fock component is theoretically approximated by a local potential whose strength decreases linearly with increasing incident particle energy. While, the dispersive component is represented by a dispersion relation that connects the real part of an optical potential with the imaginary part including surface and volume absorption terms.

In the present study, we determined and optical potential for the ^{28}Si + n system in the neutron energy region from the Fermi energy to to 20 MeV, extrapolating an empirical optical potential for sd-shell nuclei at $E \geqq 11.0$ MeV by using the dispersion relation. In order to remove an overestimation of the averaged total cross section for low energy neutrons, which is made by a simple extrapolation of the empirical optical potential, we increased linearly the radius parameter of the central potential at $E \leq 11.0$ MeV with decreasing neutron energy in the domain 1.18 - 1.27 fm, and also decreased linearly the diffuseness parameter with decreasing neutron energy in the domain 0.58 - 0.64 fm.

A remarkable improvement for the calculation of total cross sections at low energies is made by adding the dispersion term for the surface absorption rather than for the volume absorption. It results from the fact that calculated total cross sections below 2.0 MeV are much sensitive to the radius parameter, different from calculations for high energy neutrons, and consequently the cross section decreases rapidly with an increase of the parameter. This effect seems to originate from the Ramsauer-like interference found by Hodgson in the analysis of the total cross section of ^{40}Ca. That is to say, in the low energy region where there is no essential contribution of partial waves with angular momentum $l > 0$, the effect is produced by a gradual approach to 180° of the s-wave nuclear phase shift with an increase of the radius parameter. Below 2.0 MeV, moreover, we found a possible Fermi-surface anomaly in the real volume integral J_V/A for the full optical potential including two dispersive components.

The optical potential obtained above was also applied to the calculation of neutron single-particle states in ^{29}Si. The results were compared with the spectroscopic data observed in the $^{28}Si(d,p)^{29}Si$ reaction.

A paper on this subject will be published in Proc. Int. Conf. on Nuclear Science and Technology, Jülich (1991).

XI. THE UNIVERSITY OF TOKUSHIMA

A. College of General Education

XI-A-1 Breakup Reaction of ^{12}C by Polarized Protons

N. Koori, Y. Watanabe+, Kashimoto+, H. Hane+, A. Aoto+, A. Nohtomi++,

S. Widodo++, O. Iwamoto++, R. Yamaguchi++, K. Sagara+++,

H. Nakamura+++, K. Maeda+++ and T. Nakashima+++

In the interaction of fast neutrons with carbon, the contribution of the $^{12}C(n,n')3\alpha$ reaction to the nonelastic cross section becomes dominant at neutron energies above 10 MeV.[1) In order to investigate the details of the breakup reaction mechanism, we have studied the $^{12}C(p,p')3\alpha$ reaction, which is analogous to the $^{12}C(n,n')3\alpha$ reaction. Double differential cross sections and analyzing powers were measured with a ΔE-E silicon counter telescope at incident polarized-proton energies of 14 and 16 MeV.

The continuum portion formed by the $^{12}C(p,p')3\alpha$ breakup reaction was observed in the measured proton and alpha spectra. For the (p,p') spectra measured at 16 MeV, the integrated cross section of the continuum amounts to about 40 % of the total cross section. The proton energy spectra for 16 MeV were compared with the phase space distributions calculated

+ Department of Energy Conversion Engineering, Kyushu University.
++ Department of Nuclear Engineering, Kyushu University.
+++ Department of Physics, Kyushu University.

by assuming the following three-body and four-body simultaneous breakup (3BSB and 4BSB) processes:

(i) $^{12}C + p \rightarrow p' + \alpha + {}^{8}Be$, and (ii) $^{12}C + p \rightarrow p' + \alpha + \alpha + \alpha$.

For the sequential decay (i) from the ground and 2.9 MeV states of ^{8}Be, the α-α final state interaction was taken into account.[2)]

The measured proton and alpha spectra in the continuum regions can reasonably be reproduced by the calculation based on the 4BSB model. As shown in Fig.1, however, the difference between the calculated 3BSB and 4BSB spectra appears near the threshold of the breakup reaction. On the other hand, both calculated spectra have almost the same shape in the low outgoing energy region. From the analysis of the 3BSB process, it is also shown that the contribution of the sequential decay via ^{8}Be(g.s.) is smaller than that via ^{8}Be(2.9 MeV).

Although the calculated proton and alpha spectra showed rather good agreement with the continuum spectra in the low energy region, it will be necessary to clarify the dominant reaction mechanism for the 3α breakup of ^{12}C by analyses of the proton and alpha spectra on the basis of the same reaction model.

References

1) D.J. Brenner and R.E. Prael: *Atomic Data and Nuclear Tables* **41** (1989) 71.
B. Antolkovic et al: *Nucl. Sci. Eng.* **107** (1991) 1.
R.C. Haight et al: *Nucl. Sci. Eng.* **87** (1984) 41.
A. Takahashi et al: *J. Nucl. Sci. Technol.* **25** (1988) 215.

2) Y. Watanabe et al: Proc. 1990 Symp. on Nuclear Data, JAERI-M 91-032 (1991) p.336.

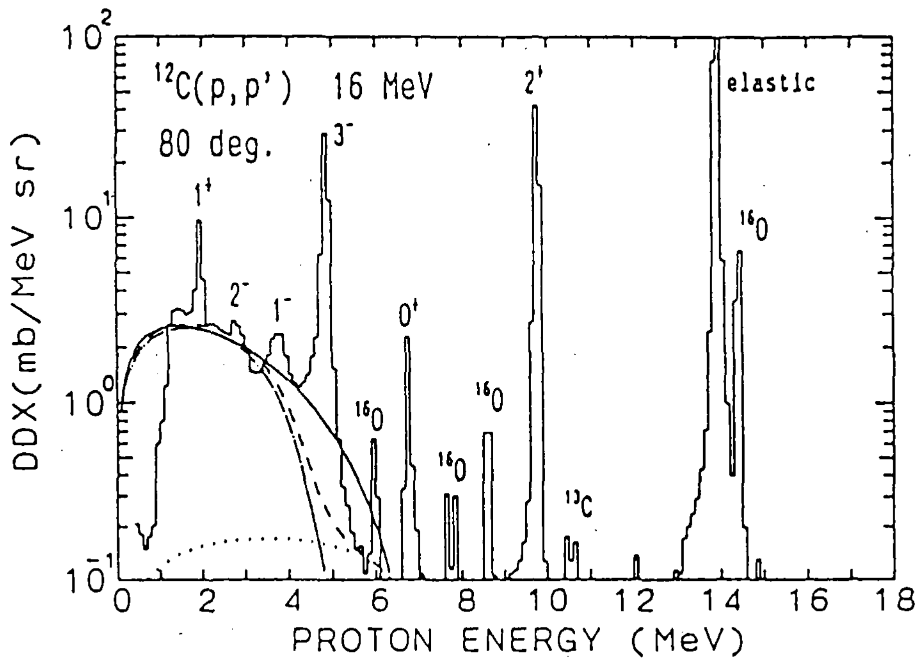

Fig.1. Double differential proton emission cross section of the $^{12}C(p,p')$ reaction at 16 MeV. Solid and dashed lines show the calculated 4BSB and 3BSB components, respectively. Dotted line is for the sequential decay of ^{8}Be(g.s.) and dot-dashed lines for that of ^{8}Be(2.9 MeV) in the 3BSB model.

XII. University of Tokyo

XII-A-1

Measurement of Activation Cross Sections of Energy up to 40 MeV

Y. Uwamino, H. Sugita*, Y. Kondo* and T. Nakamura*

Using a proton beam and a simple target system consisting of a Be disk and a water coolant, an intense semi-monoenergetic neutron field for activation experiment of energy up to 40 MeV was developed [1] at the SF cyclotron of the Institute for Nuclear Study. The activation samples were irradiated by turns for one hour at 20 cm from the Be target, and after that they were placed on a Ge detector for gamma-ray spectrometry. This irradiation was repeated for 9 proton energies.

The measured reaction rates were converted into excitation functions by the SAND-II and the NEUPAC unfolding codes with an aid of the guess excitation functions which were mostly derived from calculational results of the ALICE/ LIVERMORE82 code.[2] Excitation functions were also evaluated by the least square fitting. (L.S.F.)

The reactions of which cross sections were measured are listed in table 1 with their threshold energies. Since the fertile element consists of a single isotope, the $^{23}Na(n,2n)^{22}Na$ reaction is definitely identified as a unique reaction. Natural V consists of ^{50}V and ^{51}V isotopes, but the ^{51}Ti production can be considered as a single reaction of $^{51}V(n,p)^{51}Ti$, since the production of ^{51}Ti from ^{50}V is impossible. Because of a high threshold energy of the

*Cyclotron and Radioisotope Center, Tohoku University

$^{52}Cr(n,5n)^{48}Cr$ reaction, the $^{50}Cr(n,3n)^{48}Cr$ reaction is also clearly identified. From similar reasons, upper 17 reactions in table 1 could be identified.

The ^{24}Na can be produced by the $^{24}Mg(n,p)$, $^{25}Mg(n,d)$ and $^{26}Mg(n,t)$ reactions, and this production is noted as Mg(n,xnp) reaction. The lowest threshold energy among the possible reactions is listed with the corresponding reaction. The lower 15 reactions are treated in the similar way. Some Q values of the possible reactions are positive, for example $^{50}V(n,\alpha)^{47}Sc$. The cross sections for thermal neutrons, however, are negligibly small, and they are also treated as fast-neutron activation.

The obtained cross section curves are shown in the Figs. 1 through 6 for the reactions of $^{23}Na(n, 2n)^{22}Na$, $^{27}Al(n,\alpha)^{24}Na$, $^{51}V(n,\alpha)^{48}Sc$, V(n,xn2p) ^{46}Sc, $^{197}Au(n,4n)^{194}Au$, and $^{197}Au(n,2n)$ ^{196}Au. The results obtained by the unfolding processes performed by the SAND-II and the NEUPAC codes are shown in a thick zigzag solid line and a histogram, respectively. The vertical bars attached on the histogram show errors estimated by the NEUPAC code. Results of the least square method are shown in a thick dashed line. If some reference data are available, they are also drawn in the same figure in a thin solid line for ENDF-B/V, in a thin dotted line for ENDF-B/IV, in a thin dashed line for IAEA Tech. Rep. 273, in a thin dash and dot line for the data of Greenwood, [3] and in circles for experimental values compiled by McLane et al., [4] which is the 4th edition of the BNL-325 and referred as BNL-325.

A detailed report treating the upper 17 reactions of table 1 will be submitted to Nuclear Science and Engineering.

References

1] Y.Uwamino et al., Nucl. Instr. and Meth. **A271**, 546 (1988).

2] M.Blann and J. Bisplinghoff, "Code ALICE/ LIVERMORE 82", Lawrence Livermore National Laboratory Report No. UCID 19614 (1983).

3] L.R.Greenwood, "Extrapolated Neutron Activation Cross Sections for Dosimetry to 44 MeV", ANL/FPP/TM-115, Argonne National Laboratory (1978).

4] V.McLane et al., "Neutron Cross Sections", Vol. 2, "Neutron Cross Section Curves", Academic Press, Inc. (1988).

Table 1. Reactions of which cross sections were measured and their threshold energies.

Reaction	Threshold energy	of reaction
$^{23}Na(n,2n)^{22}Na$	13.0 MeV	
$^{27}Al(n,\alpha)^{24}Na$	3.2	
$^{51}V(n,\alpha)^{48}Sc$	2.1	
$^{51}V(n,p)^{51}Ti$	1.7	
$^{50}Cr(n,3n)^{48}Cr$	24.1	
$^{50}Cr(n,2n)^{49}Cr$	13.3	
$^{55}Mn(n,p\alpha)^{51}Ti$	9.2	
$^{55}Mn(n,4n)^{52}Mn$	31.8	
$^{55}Mn(n,2n)^{54}Mn$	10.4	
$^{63}Cu(n,3n)^{61}Cu$	20.1	
$^{63}Cu(n,2n)^{62}Cu$	11.0	
$^{65}Cu(n,p)^{65}Ni$	1.4	
$^{64}Zn(n,t)^{62}Cu$	10.2	
$^{64}Zn(n,3n)^{62}Zn$	21.3	
$^{64}Zn(n,2n)^{63}Zn$	12.0	
$^{197}Au(n,4n)^{194}Au$	23.2	
$^{197}Au(n,2n)^{196}Au$	8.1	
$Mg(n,xnp)^{24}Na$	4.4	$^{24}Mg(n,p)$
$Si(n,xnp)^{28}Al$	3.5	$^{28}Si(n,p)$
$Si(n,xnp)^{29}Al$	2.5	$^{29}Si(n,p)$
$Si(n,xn2p)^{27}Mg$	4.3	$^{30}Si(n,\alpha)$
$Ca(n,xnp)^{42}K$	2.3	$^{42}Ca(n,p)$
$Ca(n,xnp)^{43}K$	5.4	$^{43}Ca(n,p)$
$V(n,xn2p)^{46}Sc$	10.1	$^{50}V(n,n\alpha)$
$V(n,xn2p)^{47}Sc$	-	$^{50}V(n,\alpha)$
$Cr(n,xnp)^{52}V$	2.7	$^{52}Cr(n,p)$
$Cr(n,xnp)^{53}V$	2.2	$^{53}Cr(n,p)$
$Cu(n,xn2p)^{62m}Co$	0.1	$^{65}Cu(n,\alpha)$
$Zn(n,xn2p)^{65}Ni$	-	$^{68}Zn(n,\alpha)$
$Zn(n,xnp)^{64}Cu$	-	$^{64}Zn(n,p)$
$Zn(n,xnp)^{66}Cu$	1.4	$^{66}Zn(n,p)$
$Zn(n,xnp)^{68m}Cu$	3.4	$^{68}Zn(n,p)$

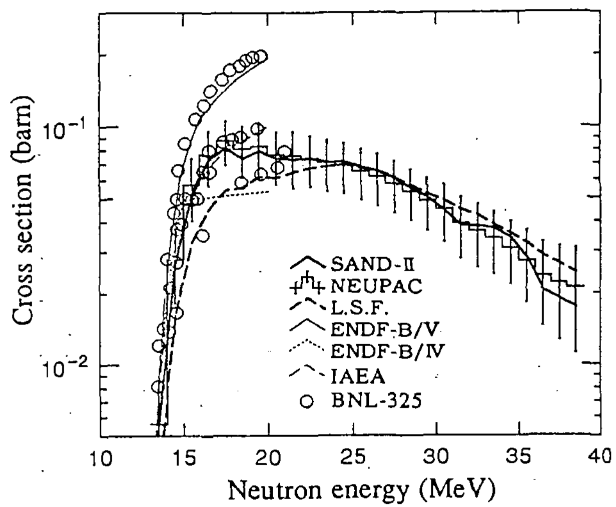

Fig. 1 Excitation function of $^{23}Na(n,2n)^{22}Na$.

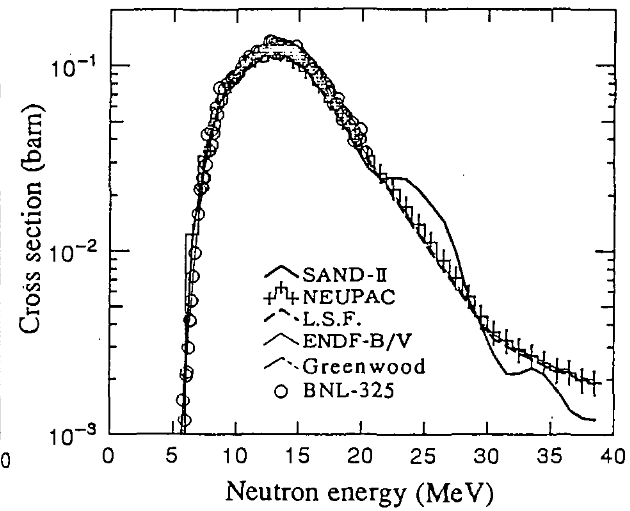

Fig. 2 Excitation function of $^{27}Al(n,\alpha)^{24}Na$.

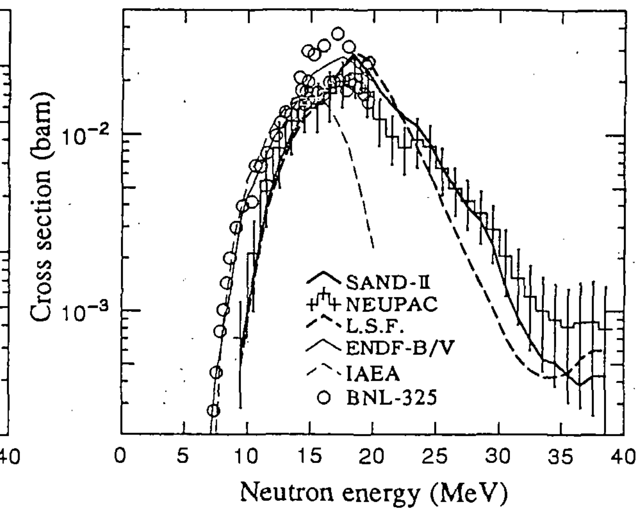

Fig. 3 Excitation function of $^{51}V(n,\alpha)^{48}Sc$.

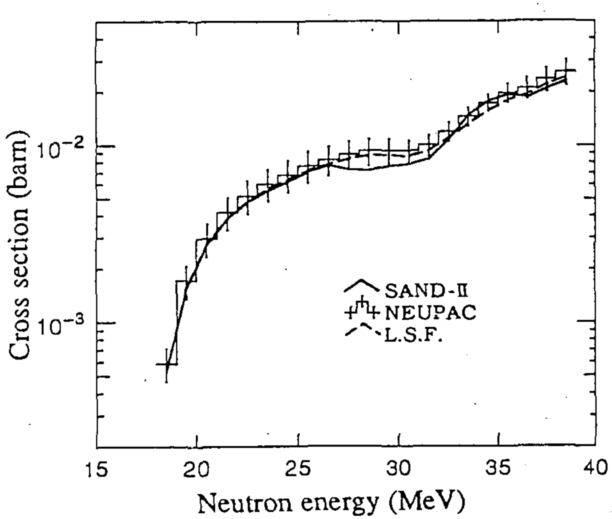

Fig. 4 Excitation function of $V(n,xn2p)^{46}Sc$.

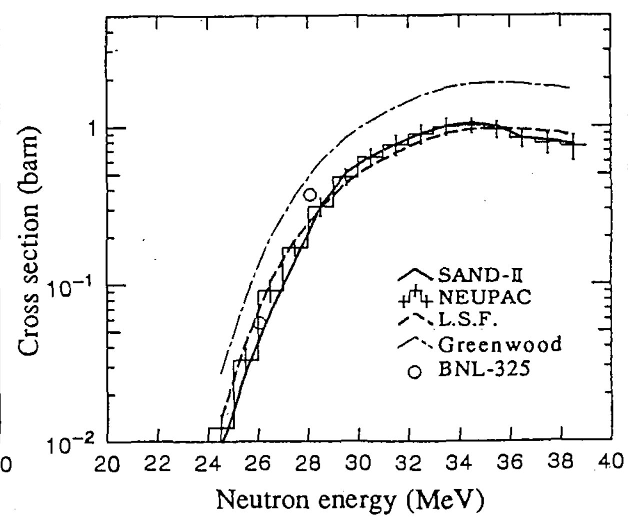

Fig. 5 Excitation function of $^{197}Au(n,4n)^{194}Au$.

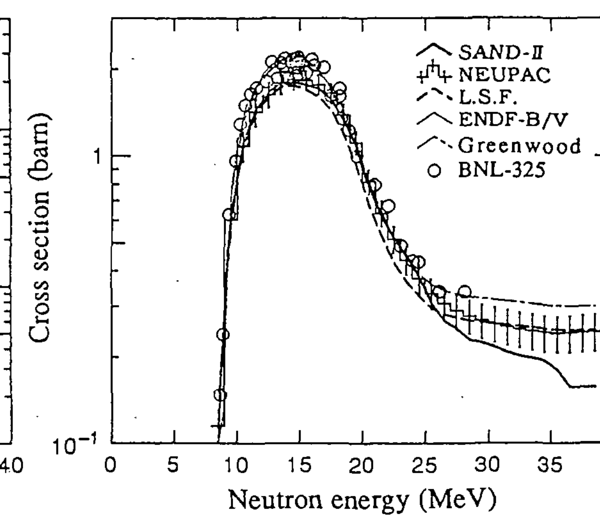

Fig. 6 Excitation function of $^{197}Au(n,2n)^{196}Au$.